1991

In vitro desmin assembly and in vivo changes in developing smooth muscle

Rong-Ghi Robert Chou
Iowa State University

INFORMATION TO USERS

This manuscript has been reproduced from the microfilm master. UMI films the text directly from the original or copy submitted. Thus, some thesis and dissertation copies are in typewriter face, while others may be from any type of computer printer.

The quality of this reproduction is dependent upon the quality of the copy submitted. Broken or indistinct print, colored or poor quality illustrations and photographs, print bleedthrough, substandard margins, and improper alignment can adversely affect reproduction.

In the unlikely event that the author did not send UMI a complete manuscript and there are missing pages, these will be noted. Also, if unauthorized copyright material had to be removed, a note will indicate the deletion.

Oversize materials (e.g., maps, drawings, charts) are reproduced by sectioning the original, beginning at the upper left-hand corner and continuing from left to right in equal sections with small overlaps. Each original is also photographed in one exposure and is included in reduced form at the back of the book.

Photographs included in the original manuscript have been reproduced xerographically in this copy. Higher quality 6" x 9" black and white photographic prints are available for any photographs or illustrations appearing in this copy for an additional charge. Contact UMI directly to order.

U·M·I

University Microfilms International
A Bell & Howell Information Company
300 North Zeeb Road, Ann Arbor, MI 48106-1346 USA
313/761-4700 800/521-0600

Order Number 9202343

In vitro desmin assembly and *in vivo* changes in developing smooth muscle

Chou, Rong-Ghi Robert, Ph.D.

Iowa State University, 1991

U·M·I
300 N. Zeeb Rd.
Ann Arbor, MI 48106

In vitro desmin assembly and in vivo changes in developing smooth muscle

Rong-Ghi Robert Chou

A Dissertation Submitted to the
Graduate Faculty in partial Fulfillment of the
requirements for the Degree of
DOCTOR OF PHILOSOPHY

Department: Food Science and Human Nutrition
Major: Food Technology

Approved:

Members of the Committee:

Signature was redacted for privacy.

In Charge of Major Work

Signature was redacted for privacy.

Signature was redacted for privacy.

For the Major Department

Signature was redacted for privacy.

For the Graduate College

Iowa State University
Ames, Iowa
1991

TABLE OF CONTENTS

GENERAL INTRODUCTION

Smooth Muscle Physiology and Structure

Smooth muscle is located principally in the walls of the digestive, respiratory and urogenital tracts, of arteries, veins and larger lymphatic vessels and in the skin. Both sympathetic and parasympathetic fibers of the autonomic nervous system exert control over smooth muscle contraction. It is generally recognized that, in addition to specific nerve impulses, smooth muscle contraction can also be caused by hormonal stimulation and by local membrane potential changes that originate in the smooth muscle cell. The membrane potential changes often occur when smooth muscle is stretched (Guyton, 1986).

Smooth muscle is usually composed of fusiform-shaped cells or fibers that range from 1-20 μm in diameter at the central nuclear region and from 25 to several 100 μm long (Burnstock, 1970). Some cells are irregular in shape and may fluctuate in size depending on the physiological state of the tissue. The single nucleus is nearly centrally located in the cell and typically has a cluster of 10-20 mitochondria at each end. The nucleus is linked directly to the cytoskeleton via desmin-containing intermediate filaments attached to the nuclear membrane (Stromer and Bendayan, 1990).
The plasma membrane of the smooth muscle cell is a trilaminar membrane about 7.5-8.0 nm thick. Rows of flask-shaped

invaginations or caveolae are prominent at the surface of the cell. Although the function of these caveolae is not known, it has been suggested that they may occupy about 30% of the surface area, and thus, would significantly increase the cell's surface area (Gabella, 1981; Garfield and Daniel, 1977). The caveolae seem to not participate in pinocytosis or endocytosis but are often seen near mitochondria and the sarcoplasmic reticulum (Gabella, 1971; Somlyo et al., 1969; Wootton and Goodford, 1975). The sarcoplasmic reticulum inside smooth muscle cells consists of a network of tubules and sacs that may occupy 2.0-7.5% of the cell volume (Devine et al., 1972; Somlyo et al., 1971). The relative prominence of the tubules versus sacs may vary among sources of smooth muscle. Smooth muscle sarcoplasmic reticulum is less regularly organized than its skeletal muscle counterpart, but may form surface couplings between junctional sarcoplasmic reticulum and the plasma membrane in arterial tissue (Somlyo, 1979). Electron probe X-ray microanalysis has shown that high concentrations of calcium are present in sarcoplasmic reticulum tubules in normal cells (Somlyo et al., 1978) and that caffeine and norepinephrine cause release of this calcium. These studies together with the findings that the free calcium concentration in normal smooth muscle is below 10^{-5} M and that the sarcoplasmic reticulum can continue to accumulate calcium down to 10^{-6} M free calcium, provide strong evidence that the sarcoplasmic reticulum participates in regulating smooth muscle contraction by accumulating and releasing intracellular calcium (Somlyo et al., 1982).

Smooth muscle cells contain three prominent types of protein filaments, thin or actin (6-8 nm diameter), thick or myosin (15-16 nm diameter) and intermediate composed of desmin or vimentin (10-12 nm diameter). Contraction of smooth muscle occurs via the interaction of thick and thin filaments. Regulation involves formation of a calcium-calmodulin complex which interacts with the myosin light chain kinase to phosphorylate the two 20 kd light chains of myosin. This phosphorylated myosin is able to interact with actin filaments to generate force. Reduction of free calcium inactivates the myosin light chain kinase, phosphatase dephosphorylates myosin and relaxation occurs (Hartshorne and Persechini, 1984; Trybus, 1989). The greater length of smooth muscle thick filaments (average about 2.2 μm) (Ashton et al., 1975) and perhaps also smooth muscle thin filaments (may average about 1.5 μm or more) (Bagby, 1983) presumably contributes to the ability of smooth muscle to shorten as much as 60% of rest length. Recent evidence suggests that smooth muscle thick filaments may be side polar (Cooke et al., 1989).

Thin filaments are attached to cytoplasmic dense bodies with a polarity analogous to that observed between striated muscle thin filaments and Z-lines (Bond and Somlyo, 1982; Tsukita et al., 1983) and also insert with analogous polarity into membrane-associated dense bodies (Somlyo and Franzini-Armstrong, 1985). In addition to their probable greater length, some smooth muscle thin filaments contain caldesmon instead of troponin as do their counterparts in striated muscle. The molar ratio of actin:tropomyosin:caldesmon in

sheep aorta thin filaments has been reported to be 28:4:1 based on the molecular weight of 120 kd for caldesmon which was estimated from SDS-PAGE analysis (Smith and Marston, 1985). The reported molecular weight of caldesmon, however, has been variable. Based on SDS-PAGE, the molecular weight of caldesmon from eleven bovine tissues is 149 kd, and that of chicken gizzard caldesmon is either 141 kd (Clark et al., 1986) or is between 135 and 140 kd (Bretsher, 1984). From sedimentation equilibrium measurements, the range of molecular weight is from 75 kd for turkey gizzard caldesmon (Malencik et al., 1989) to 93 kd for chicken gizzard caldesmon (Graceffa et al., 1988). The molar ratio of actin:tropomyosin: caldesmon in purified chicken gizzard thin filaments determined by gel densitometry and based on a caldesmon molecular weight of 93 kd is 26.7:3.8:1 (Lehman et al., 1989). Studies with antibodies suggest that both ends of caldesmon are closely associated with the thin filament backbone which may permit or encourage a specific parallel association or interaction with tropomyosin (Moody et al., 1990).

The third filament type in smooth muscle is the intermediate filament. Intermediate filaments were so named because their average diameter of 10 nm is not only between the diameter of actin filaments (6-8 nm) and microtubules (25 nm) in nonmuscle cells, but also between the diameter of actin filaments and thick filaments (15 nm) in muscle cells. Ishikawa et al. (1968), therefore, first described these 10-nm filaments in skeletal muscle as "intermediate-sized"

filaments. In addition to the difference in diameters, the major constituent of intermediate filaments can be distinguished from that of microtubules and actin filaments both biochemically and immunologically (Lazarides, 1982; Osborn et al., 1982).

Although there is no agreement about specific linkages or interactions between intermediate filaments and other structures, intermediate filaments are associated with cytoplasmic dense bodies. Campbell et al. (1971) observed that intermediate filaments are associated with the ends of cytoplasmic dense bodies and can be seen in the interior of and may form a backbone for assembly of cytoplasmic dense bodies. This is consistent with the high concentration of anti-desmin labeling observed by Small et al. (1986) at the ends of cytoplasmic dense bodies. Tangential contact with cytoplasmic dense bodies and an oblique orientation of intermediate filaments have been observed by Somlyo et al. (1984). More recently, Stromer and Bendayan (1988) used anti-desmin and protein A-colloidal gold labeling to show that intermediate filaments are concentrated in an axial bundle that extends the length of the cell, that intermediate filaments fray out from this bundle and extend toward cytoplasmic dense bodies, and that the label is concentrated at the ends of the dense bodies. Small and Sobieszek (1983) and Somlyo and Franzini-Armstrong (1985) have also shown that intermediate filaments are associated with or inserted into membrane-associated dense bodies located on the cytoplasmic side of the plasma membrane. Analysis of movement of dense bodies during contraction

of isolated smooth muscle cells suggests there are two populations of dense bodies. One group moves rapidly toward one another axially during contraction, suggesting that they are linked to filaments participating in the contractile process. The second group moves little during contraction, suggesting that they are linked to cytoskeletal components more involved with maintaining cell shape and/or geometry (Kargacin et al., 1989).

There is, at this time, no agreement either on the specific arrangement of the three filament types or on how they interact in smooth muscle. Bagby (1983, 1986), Cooke et al. (1987) and others have attempted to collate this information into three-dimensional models for the smooth muscle cell. Convincing evidence has been published for the existence of a contractile system that, at a minimum, consists of thick filaments, some thin filaments and some dense bodies. Much greater uncertainty exists about the organization and components of the non-contractile or cytoskeletal system. Based primarily on the absence of any detectable interactions between the proteins of intermediate filaments and the proteins of the contractile filaments, it has been proposed that intermediate filaments, microtubules, some dense bodies and perhaps some actin filaments, may constitute the smooth muscle cell cytoskeleton. For a recent review on this topic, see Bagby (1990).

It would be useful to define the smooth muscle cell cytoskeleton, but because our understanding of the function of various intracellular components is incomplete, a definition is problematic. One view of

the cytoskeleton is based on solubility and suggests that structures remaining after extraction with a particular solution (often an isotonic salt solution) are cytoskeletal components. A principal weakness of this view is that function of a component, even if known, is not considered in this classification. Another view that has been referred to by Bagby (1983) suggests that the cytoskeleton should include only those components that contribute to the intracellular framework that allows the smooth muscle cell to maintain both its shape and intracellular organization. Myosin filaments and actin filaments that interact with myosin filaments would not be considered as part of the cytoskeleton. This view is based primarily on studies by Cooke and his colleague who showed that, after removal of thick and thin filaments, a network of intermediate filaments, cytoplasmic dense bodies and membrane-associated dense bodies remain that would respond to stretch and that seems to be at least partly responsible for maintaining cell shape (Cooke and Fay 1972; Fay and Cooke, 1973; Cooke, 1976). It should also be pointed out that antibodies to filamin or to caldesmon have been used to isolate and identify two types of thin filaments from chicken gizzard. One type contains filamin and little caldesmon, and the other contains caldesmon and little filamin (Lehman et al., 1987). Filamin has been associated with filaments in the cytoskeletal domain (Malecki and Small, 1987; Small et al., 1986) and caldesmon has been found in the contractile domain (Fürst et al., 1986). Because there is no consensus on the definition of the smooth muscle cell cytoskeleton, I will include, for purposes of this

dissertation, microtubules, actin filaments and intermediate filaments in my definition of the cytoskeleton.

Classification of Intermediate Filaments

Intermediate filaments are present in various cell types. Lazarides (1980, 1982) grouped intermediate filaments into the following five distinct subclasses on the basis of their cell type of origin: (1) keratin filaments, found in epithelial cells; (2) neurofilaments, found in neurons; (3) glial filaments, found in astrocytes and glial cells; (4) vimentin filaments, found in mesenchymal cells and some vascular smooth muscle cells; and (5) desmin filaments, found in muscle cells. Recently, the nuclear lamins, which are located at the nuclear periphery during interphase, have been added as the sixth subclass of intermediate filaments (Franke, 1987). This system of classification becomes ambiguous when two subclasses of intermediate filaments coexist in a single cell type. For instance, HeLa cells and PtK_2 cells contain both keratin and vimentin (Franke et al., 1979; Osborn et al., 1980; Henderson and Weber, 1981). In addition, desmin and vimentin are coexpressed during skeletal muscle myogenesis (Gard et al., 1979; Bennett et al., 1979; Bilak et al., 1987) and co-exist in vascular smooth muscle (Berner et al., 1981a). On the basis of nucleic acid and protein sequences, Steinert and Roop (1988) therefore, reclassified intermediate filaments into the following five sequence types: Type I, acidic keratins (40-60 kd);

Type II, neutral/basic keratins (50-70 kd); Type III, desmin (53 kd), vimentin (54 kd) and glial fibrillary acidic protein (51 kd); Type IV, neurofilaments (NF-L 60-70 kd, NF-M 105-110 kd, NF-H 135-150 kd); and Type V, the nuclear lamins A, B and C (60-70 kd). In addition, peripherin, a 57 kd neural intermediate filament protein, which is located at the periphery of neurons (Parysek and Goldman, 1988; Leonard et al., 1988), has been added as a member of the Type III subclass (Goldman et al., 1990). Morphologically, Types I-IV are identical to native or reassembled intermediate filaments when studied with the electron microscope, despite the wide difference in molecular weight. On the other hand, Type V intermediate filament proteins do not form cytoplasmic filament structures but form a quasi-tetragonal meshlike lattice composed of fibers about 10 nm wide in interphase cells in vivo (Aebi et al., 1986) and paracrystalline arrays in vitro (Parry et al., 1987).

Possible Functions of Intermediate Filaments

Although a substantial amount of evidence related to the structure of intermediate filaments has been accumulated, the precise functions of intermediate filaments are still unclear (Bloemendal and Pieper, 1989). One of the possible functions of intermediate filaments is as a mechanical integrator or cytoskeletal scaffolding in intracellular space to organize cytoplasmic components (Lazarides, 1980; Osborn and Weber, 1982). Recent supporting evidence

demonstrated that connections exist between the nucleus and mitochondria and both vimentin filaments in nonmuscle cells (Traub, 1985; Goldman et al., 1986) and desmin filaments in smooth muscle cells (Stromer and Bendayan, 1988, 1989, 1990; Stromer, 1990). The plasma membrane is also linked to keratin filaments at cell-cell adherence junctions in epithelial cells (Traub, 1985), to vimentin filaments in red blood cells (Granger and Lazarides, 1982) through the binding of ankyrin, a membrane-associated protein, (Georgatos and Marchesi, 1985; Georgatos et al., 1985), and to desmin filaments in smooth muscle at membrane-associated dense bodies (Bagby, 1983; 1986; Stromer, 1990), as well as in striated muscle at Z-lines (Lazarides et al., 1982). Through these junctional connections, the system of intermediate filaments within each individual cell can be effectively linked. It was, therefore, proposed that, in cells containing spot desmosomes or hemidesmosomes and keratin intermediate filaments, these filaments play a role as a supracellular scaffold to protect cells from mechanical deformation (Klymkowsky et al., 1983; Klymkowsky et al., 1989). Furthermore, recent evidence indicates that the N-terminal head domain of vimentin and desmin attaches to the plasma membrane, while, the C-terminal end domain binds to the nuclear envelope (Georgatos and Blobel, 1987a; Georgatos et al., 1987). The attachment site for vimentin filaments at the nuclear envelope is composed of lamin B, a type V intermediate filament. (Georgatos and Blobel, 1987b). Lamin B is highly specialized for attachment of the lamina to the inside surface of the nuclear

membrane and is different from lamins A and C biochemically and immunologically (Burke and Gerace, 1986). Collectively, this evidence implies that intermediate filaments may serve as signal transducers between the nucleus and plasma membrane (Metuzals and Mushynski, 1974; Goldman et al.,1986). In addition, the assembly and reassembly of the nuclear lamina are related to the breakdown and reformation of the nuclear envelope during mitosis (Newport and Forbes, 1987). Experimental removal of the nuclear lamins after nuclear envelope breakdown during mitosis will block both reformation of the nuclear envelope (Burke and Gerace, 1986) and the subsequent change from telophase-like chromatin into interphase chromatin (Benavente and Krohne, 1986). On the other hand, it has been proposed that lamin B serves as a link between lamins A and/or C and the inner nuclear membrane, whereas lamins A and C interact with chromatin (Gerace and Blobel, 1980; Gerace, 1986). Thus, nuclear lamins, which are Type V intermediate filament proteins, may be involved in organization of the interphase nucleus.

Molecular Aspects of Intermediate Filaments

Isolation and purification of intermediate filament proteins

Solubility of intermediate filament proteins, in general, is very low compared to other cytoskeletal elements and cell structures. Most intermediate filament proteins require low pH (O'Shea et al.,

1981) or denaturing reagents such as urea (Huiatt et al., 1980; Steinert et al., 1982; Vorgias and Traub, 1983) or guanidine hydrochloride (Geisler and Weber, 1981a; Liem and Hutchison, 1982) for solubilization. Small and Sobieszek (1977) developed a procedure for purification of desmin (skeletin) that involved the solubilization of KCl- and KI-insoluble residues of smooth muscle with 1 M acetic acid followed by gel permeation chromatography in the presence of SDS. Because the method used by Small and Sobieszek (1977) produces desmin that is contaminated with actin, several other procedures have been developed for purification of desmin (Huiatt et al., 1980; Geisler and Weber, 1980; Vorgias and Traub, 1983). Huiatt et al. (1980) reported the first reproducible procedure for the purification of desmin from an avian source. Washed cell fragments are extracted with an ATP solution and a solution containing 0.6 M KCl to produce a crude native intermediate filament fraction. This fraction is extracted with 6 M urea solution to release desmin and other proteins. The urea extract is chromatographed on a hydroxyapatite column, and the desmin-rich fractions are further purified by ion exchange chromatography on a DEAE-Sepharose CL-6B column in the presence of 6 M urea. After removal of the urea by dialysis against 10 mM Tris-acetate buffer, pH 8.5, in the presence of a reducing reagent, purified desmin that is free of actin contamination remains in soluble form. This purification scheme also provided the basis for purification of vimentin from smooth muscle cells in porcine aortas (Hartzer, 1984).

Monomeric structure of intermediate filament protein

On the basis of abundant amino acid sequence information (see the list in Parry, 1990), intermediate filament protein chains are usually divided into three domains: a central rod domain, N-terminal (head) domain and C-terminal (tail) domain (Geisler et al., 1982; Steinert et al., 1983; Steinert and Parry, 1985; Geisler and Weber, 1986; Weber and Geisler, 1987; Steinert and Roop, 1988). The rod domain contains approximately 310 residues and is approximately 45 nm long in types I-IV intermediate filament proteins. The sequence of the rod domain reveals a high α-helical content (approximately 90%) with a heptad repeat pattern $(a\text{-}b\text{-}c\text{-}d\text{-}e\text{-}f\text{-}g)_n$ where residues in a and d are mainly hydrophobic amino acids. Such a pattern forms the basis of a coiled-coil structure (Crewther et al., 1978; Geisler et al., 1982; Geisler and Weber, 1982). A centrally located non-α-helical spacer (L12) clearly divides the rod domain into two major segments, each about 140 residues or 21-22 nm long. Segment 1 is separated by a spacer (L1) into 1A and 1B, and segment 2 is separated by another spacer (L2) into 2A and 2B with less precise boundaries (Geisler and Weber, 1982; Crewther et al., 1983; Hanukoglu and Fuchs, 1983; Steinert et al., 1983; Parry and Fraser, 1985; Geisler and Weber, 1986). The rod domain of type V subunits, however, may contain around 356 residues and is α-helical throughout its entire length (McKeon et al., 1986; Fischer et al., 1986; Parry et al., 1986; Steinert and Roop, 1988). Generally speaking, rod domains of

subunits within a sequence type show 70-95% homology, but those in different types show 30% or less homology (Parry and Fraser, 1985; Conway and Parry, 1988).

End domains (head and tail) have hypervariable amino acid sequences among different types of intermediate filament proteins compared with the rod domain, and their sizes are also variable (Geisler and Weber, 1986; Steinert and Roop, 1988). The predicted secondary structure of the end domains yields no common feature among the different types of subunits. There is little predicted α-helical structure in the C-terminal domains except for type III and part of type IV chains. These regions of α-helical structure do not have the heptad repeat (Conway and Parry, 1988; Parry, 1990). The variability of the terminal domains among intermediate filament proteins is significant both structurally and functionally. In desmin, the N-terminal domain contains no acidic residues, and 15% of the residues are arginine (Geisler and Weber, 1982). This domain is the site for proteolysis (Traub and Vorgias, 1983, 1984; Traub 1985; Kaufmann et al., 1985) and enzymatic phosphorylation (Geisler and Weber, 1988). It is also known that the N-terminus but not the C-terminus is required for assembly of desmin into filaments (Traub and Vorgias, 1983, 1984; Kaufmann et al., 1985; van den Heuvel et al., 1987). On the other hand, the C-terminus of desmin contains only one cysteine residue that has been extensively used for chemical cross-linking experiments to study the number of subunits in a single protofilament (Geisler and Weber, 1982; Pang et al., 1983). In

addition, the C-terminus and N-terminus can also be hydrolyzed by certain proteases (Kaufmann et al., 1985).

Assembly properties of intermediate filament proteins

Assembly of intermediate filament protein monomers is a sequential process, which progresses from dimers, protofilaments (tetramers), protofibrils (subfilaments), and 10-nm intermediate filaments (Stromer et al., 1981; Ip et al., 1985a, b; Steinert and Roop 1988; Aebi et al., 1988; Ip, 1988; Hisanaga et al., 1990; Hisanaga and Hirokawa, 1990). Among these steps, the dimer is a well characterized and documented species (Aebi et al., 1986; Quinlan et al., 1986; Steinert, 1990). Dimers consist of two intermediate filament monomers arranged in parallel and in register. These conclusions have been verified by sequencing studies with partially hydrolyzed keratin dimers (Woods and Inglis, 1984; Parry et al., 1985), cross-linking studies (Quinlan et al., 1985), electron microscope observations (Aebi et al., 1986), and theoretical calculations of maximal ionic interactions between two subunits (Fraser et al., 1985). Dimers are also termed "mini-myosin" type molecules because the two C-terminal end domains fold into a globular head that appears similar to myosin (Aebi et al., 1988). The forces involved in dimer formation are still uncertain. On the basis of a theoretical analysis of the distribution of ionic charges along a single subunit, it has been shown that ionic interactions are the primary binding force between

the two chains (Fraser et al., 1985). By characterizing the dimer subunits and by using binding assays, it has, however, been proposed that hydrophobic instead of ionic interactions are the main force for the formation of dimers (Quinlan et al., 1986; Hatzfeld et al., 1987).

The second step in assembly is the formation of protofilaments. Results from early physicochemical studies suggested that protofilaments consisted of a three-stranded coiled-coil (Skerrow et al., 1973; Steinert, 1978; Steinert et al., 1980; Geisler and Weber, 1981b). More direct evidence from cross-linking studies has indicated, however, that protofilaments are composed of four subunits in the form of a pair of coiled-coils (Ahmadi and Speakman, 1978; Gruen and Woods, 1983; Geisler and Weber, 1982; Pang et al., 1983; Woods and Inglis, 1984; Ip et al., 1985b).

The precise arrangement of the two dimers in a protofilament, however, is still unclear. The two dimers may be arranged either parallel or antiparallel, and the length of a protofilament may be approximately 50 nm (axial register of two dimers) or 70 nm (half-stagger of two dimers). Geisler et al. (1985) found that Fab fragments of a monoclonal antibody whose epitope is close to the carboxyl end of the desmin rod bound to both ends of the protofilaments and produced dumpbell-shaped particles. It was proposed that the two dimers may be arranged in an antiparallel direction without major stagger. Interestingly, Ip (1988) used a monoclonal antibody whose epitope is close to the N-terminal end of the desmin rod and found that antibodies generally bound to only one end of the protofilaments

and rarely encountered labeling at both ends. This result implies that the two dimers may be arranged in parallel fashion (Ip, 1988; Robson, 1989) and is consistent with current evidence from the assembly of neurofilaments (Hisanaga et al., 1990). Based on theoretical predictions from experiments on keratin, the maximum number of ionic interactions would occur between segment 1B and segment 2 in two dimers in an antiparallel arrangement (Crewther et al., 1983; Fraser et al., 1985). Although the half-staggered arrangement of two dimers to form a 70 nm protofilament is favored in theory (Crewther et al., 1983), the in register arrangement of two dimers to produce a 45-50 nm protofilament is supported by length measurements of protofilaments from several laboratories. In general, the length of a single protofilament is approximately 50 nm by X-ray diffraction (Fraser et al., 1976) and by measuring the length of protofilaments from electron micrographs (Steinert et al., 1981; Stromer et al., 1981; Geisler et al., 1982, 1985; Ip et al., 1985a, b; Quinlan et al., 1984). This length implies that the two dimers are in axial register within a protofilament. Aebi et al. (1988), therefore, hypothesized the presence of a "tetramer switch." This means that both in-register and half-staggered dimers, in either antiparallel or parallel conformation, may be converted into the other under appropriate conditions. More evidence will be needed to clear up this discrepancy.

The next step in assembly is packing protofilaments into 10-nm filaments. Exactly how the 10-nm filaments are constructed is still in doubt. Current evidence favors the proposition that 10-nm filaments

are built according to a common plan, i. e., backbones of 10-nm filaments are composed of helically packed rod domains oriented approximately parallel to the filament axis with end domains protruding from the backbone (Steinert and Roop, 1988).

Scanning transmission electron microscopy has been used to measure the mass-per-unit-length of certain intermediate filaments. Steven et al. (1982; 1983a, b) determined that, for vimentin, desmin and both bovine and human epidermal keratins, the majority of native and mature reconstituted intermediate filaments have a mass-per-unit-length of 33-38 kd/nm. Minor linear density variants of 23 kd/nm were found in native vimentin filaments (Steven et al., 1982) and of 26-28 kd/nm and 44-48 kd/nm in reconstituted bovine epidermal keratin and in vimentin/desmin heteropolymeric intermediate filaments (Steven et al., 1983a). Reconstituted human epidermal keratin filaments, however, had a major mass-per-unit-length peak between 17 and 20 kd/nm and two minor peaks, one at 25-29 kd/nm and another at 36-42 kd/nm (Engel et al., 1985). Steven et al. (1983b) also obtained principal mass-per-unit-length values of 22, 25 and 29 kd/nm if they measured immature or minimal form intermediate filaments. This may indicate that the protein used by Engel et al. (1985) was either not able to, or for some other reason did not, form mature filaments. The different mass-per-unit-length values for mature or native intermediate filaments are directly proportional to the average mass of their constituent subunits (Steven et al., 1983a, 1985). This suggests that all

intermediate filaments contain, in cross section, a common structural backbone element, namely, the conserved rod domains of eight intermediate filament protofilaments (Engel et al., 1985).

Electron microscopy of shadowed intermediate filaments emphasizes an intrinsic axial repeat of about 22 nm (Milam and Erickson, 1982; Henderson et al., 1982; Aebi et al., 1983; Sauk et al., 1984), which also can be seen in negatively stained intermediate filament samples (Ip et al., 1985a, b; Aebi et al., 1988). Moreover, this repeat correlates with the expected lengths of segments 1 and 2 calculated from the amino acid sequence (Geisler et al., 1985).

Electron microscopy has also been used to determine the size of particles produced when different kinds of intermediate filaments are disassembled or assembled. When desmin, keratin or vimentin intermediate filaments are partially unraveled under certain conditions, protofibrils with different sizes and protofilaments are present (Stromer et al., 1981; Franke et al., 1982; Aebi et al., 1983, 1988; Ip et al., 1985a, b; Ip, 1988). Evidence from this type of study also indicates that protofibrils have an average diameter of 4-5 nm, and may contain octamers, which are formed by two protofilaments that may either be in register or half-staggered. If the protofilaments are half-staggered, this may be responsible for the 22 nm axial repeat along the protofibrils. In addition, it has been suggested that the arrangement of the two tetramers in a neurofilament protofibril is antiparallel (Hisanaga et al., 1990). An intermediate filament, therefore, is built from four such protofibrils that are laterally

associated to produce 10 nm diameter particles, which are then elongated by longitudinal annealing of octamers (Stromer et al., 1981; Franke et al., 1982; Aebi et al., 1983, 1988; Quinlan et al., 1984; Ip et al., 1985a, b; Ip, 1988). The reverse order, however, has also been proposed. Elongation of neurofilament protofibrils may occur by adding octamers onto their ends followed by lateral packing of the elongated protofibrils to obtain 10 nm filaments (Hisanaga and Hirokawa, 1990).

Proteolytic digestion of intermediate filaments indicates that end domains are more susceptible to proteolysis than rod domains. This implies that end domains are located in more exposed areas, possibly protruding toward the surface of intermediate filaments (Steinert et al., 1983; Kaufmann et al., 1985).

In summary, the overall construction plan of intermediate filaments is a sequential process. It begins with the smallest unit, dimers, then progresses through tetramers, octamers and protofibrils, and finishes with intact intermediate filaments. Despite the substantial amount of information that supports this assembly scheme, there are still some areas that require further investigation. In addition, theoretical predictions of possible ionic interactions between the coiled-coil rod domains generated the basis for the concept that ionic interactions are the key forces responsible for assembly from alignment and registry of dimers to formation of intact filaments (Crewther et al., 1983; Fraser et al., 1985; Conway and Parry, 1988). This concept, however, has been questioned by

recent experimental evidence that indicates that hydrophobic instead of ionic interactions play major roles in the formation of dimers (Quinlan et al., 1986; Hatzfeld et al., 1987). Determination of critical concentrations required for desmin assembly, part of this dissertation, provides another piece of experimental evidence that indicates that hydrophobic interactions are dominant during assembly of desmin filaments (Chou et al., 1990). More evidence will be needed to fully understand the forces involved in assembly of intermediate filaments.

Factors affecting the assembly of intermediate filaments

The major factors affecting assembly of intermediate filaments are pH, temperature, ionic strength, and post-transcriptional modifications. The optimum pH for assembly of a specific type of intermediate filament varies. For instance, the optimum pH for desmin assembly is 7 (Huiatt, 1979) but is 6.25 for neurofilament assembly (NF-L) (Aebi et al., 1988). When the pH is either higher or lower than the optimum value, short filaments or aberrant structures are created (Aebi et al., 1988). Assembly of desmin or neurofilament intermediate filaments is more extensive as temperature increases (Stromer et al., 1987; Aebi et al., 1988). Short filamentous particles are generated as temperature decreases from 37 to 20°C in NF-L assembly, and these particles lose their assembly ability if temperature is again increased to 37°C. It has been suggested that

lower temperatures may produce "dead-end" precursor structures during NF-L assembly (Aebi et al., 1988).

It is a well-known fact that high ionic strength favors more extensive assembly of intermediate filament proteins (Huiatt, 1979; Huiatt et al., 1980; Renner et al., 1981; Steinert et al., 1981; Nelson and Traub, 1982; Hartzer, 1984; Ip et al., 1985a, b; Stromer et al., 1987). The main effect of increasing ionic strength is to increase the length of reassembled filaments (Huiatt, 1979). The presence of a specific type of cation and its concentration, however, can greatly influence assembly. At the same ionic strength, divalent cations are more effective promoters of assembly of macrofibers or bundles of keratin filaments (Fukuyama et al., 1978), or intermediate filaments per se than monovalent cations (Stromer et al., 1987; Yang and Babitch, 1988; Chou et al., 1990). Morphological evidence also indicates that the diameters of reassembled filaments are thicker as the concentration of divalent cations increases from .0 to 10 mM (Huiatt, 1979; Hartzer, 1984; Inagaki et al., 1989). This phenomenon may be related to the existence of specific divalent cation binding sites residing in intermediate filament proteins (Lefebvre and Mushynski, 1987, 1988; Yang et al., 1988). Moreover, divalent and monovalent cations may have different roles in the assembly process. Lateral association of neurofilament-L protofilaments is favored in the presence of divalent cations, but, elongation is favored in the presence of monovalent cations (Hisanaga and Hirokawa, 1990).

Two kinds of post-translational modification, namely limited proteolysis and phosphorylation, can regulate assembly of all types of intermediate filaments. As mentioned previously, it has been known since 1980 that limited proteolysis by a Ca^{2+}-activated proteinase, calpain, can remove the N-terminal head domain of desmin and vimentin, as well as impair the ability of protofilaments to assemble (O'Shea et al., 1979; Traub and Vorgias, 1983, 1984; Traub, 1985; Kaufmann et al., 1985). Recent studies have shown that in vitro phosphorylation of protofilaments also inhibits the assembly process and that in vitro phosphorylation of intact filaments causes disassembly (Inagaki et al., 1987, 1988; Evans, 1988). Three to four phosphorylation sites on desmin (Geisler and Weber, 1988) and on vimentin (Ando et al., 1989) are identified at the serine residues of the N-terminal head domain, particularly at the ß-turn region (Ando et al., 1989; Kitamura et al., 1989; Inagaki et al., 1989). Dephosphorylation of phosphorylated protein, however, reportedly restores the ability to assemble (Inagaki et al., 1988). Recent evidence however, suggests that phosphorylation, by itself, may not be adequate to explain the control of desmin assembly (Chou et al., 1990). This observation supports the earlier finding by Yang and Babitch (1988) that there is only a small correlation between glial fibrillary acidic protein phosphorylation and polymerization ability.

Intermediate Filaments in Smooth Muscle

Adult smooth muscle

Adult smooth muscle usually contains desmin filaments (Lazarides and Hubbard, 1976). Vimentin filaments, however, can also be detected in some smooth muscles (Bennett et al., 1978) especially in vascular smooth muscle (Franke et al., 1980; Hartzer, 1984). Two distinct structural features of intermediate filaments in smooth muscle are uniform diameter (10 nm) and great length (indeterminable) (Ashton et al., 1975; Small and Sobieszek, 1977; Campbell et al., 1979). Intermediate filaments can be distinguished from thin filaments not only by their constituents and diameters but also by the absence of heavy meromyosin binding (Bond and Somlyo, 1982; Tsukita et al., 1983). On the other hand, Fay and Cooke (1973) pointed out that intermediate filaments had been erroneously identified as thick filaments in early electron microscope studies. At one time, intermediate filaments were considered to be the core protein for thick filaments in smooth muscle (Small and Squire, 1972).

Many intermediate filaments are located around the periphery of cytoplasmic dense bodies in a ring-like zone in cross sections of smooth muscle cells (Shoenberg and Needham, 1976; Small, 1977; Small and Sobieszek, 1980; Berner et al., 1981a). Some of them loop tangentially near cytoplasmic dense bodies or are obliquely arranged

1985). Recent evidence has also shown that intermediate filaments terminate at or near membrane-associated dense bodies (Somlyo and Franzini-Armstrong, 1985).

Intermediate filaments also tend to be condensed in the axial regions of the cell rather than in the peripheral area, especially in stretched (Cooke and Fay, 1972; Fay and Cooke, 1973) and hypertrophic muscle (Berner et al., 1981b). Current evidence obtained from sectioned intact normal adult gizzard muscle by gold-labeling immunocytochemistry has shown that the major component of an axial bundle of intermediate filaments is identified as desmin. This bundle not only extends the entire length of the cell but also has individual intermediate filaments that form linkages with the nucleus and mitochondria at the poles of the nucleus (Stromer and Bendayan, 1988, 1989, 1990; Stromer, 1990). Colcemid and cytochalasin B treatments of cultured gizzard smooth muscle cells induce the formation of bundles or cables of intermediate filaments (Bennett et al., 1978). Cultured fibroblasts and nucleated chicken red blood cells contain a perinuclear concentration of intermediate filaments that is not altered by enucleation with cytochalasin B (Small and Celis, 1978).

The specific functions of intermediate filaments in smooth muscle are still unclear. Two types of roles, however, have been proposed. One role is solely cytoskeletal and suggests that intermediate filaments are associated with cytoplasmic dense bodies and are integrated into a cytoskeletal network that is separate from the contractile system (Cooke and Fay, 1972; Cooke, 1976, 1983; Small

and Sobieszek, 1977, 1980; Fürst et al., 1986). Evidence favoring a cytoskeletal role for the intermediate filament-cytoplasmic dense body network is: (1) the random distribution of cytoplasmic dense bodies in unstretched muscle changes to a centrally concentrated distribution in stretched muscle and is independent of the contractile state of the cells (Cooke and Fay, 1972); (2) intermediate filaments may be located between thick and thin filament domains rather than within myofilament domains (Small and Sobieszek, 1977, 1980); and (3) two distinct actin domains are present in cells. One domain contains caldesmon and interacts with myosin filaments for contraction. Another domain, however, contains filamin and is in the cytoskeletal domain (Cooke, 1983; Small et al., 1986; Fürst et al., 1986).

A second proposed role for the intermediate filament-cytoplasmic dense body network is not only cytoskeletal but also contractile (Bond and Somlyo, 1982; Tsukita et al., 1983; Fay et al., 1983; Kargacin et al., 1989). Evidence supporting this dual function is: (1) cytoplasmic dense bodies contain α–actinin, a Z-line protein in striated muscle (Schollmeyer et al., 1976); (2) actin filaments in smooth muscle have opposite polarity on opposite ends of dense bodies (Bond and Somlyo, 1982; Tsukita et al., 1983); (3) cytoplasmic dense bodies are arranged in a string-like fashion, and distance between them is decreased during contraction (Fay et al., 1983); and (4) there may be two groups of dense bodies in smooth muscle. Distance between one group of dense bodies is decreased during

contraction, while, distance between another group is kept constant, approximately 6 nm. This implies that the latter group of dense bodies may provide a framework for attachment of the contractile structures to the cytoskeleton (Kargacin et al., 1989).

Developing Smooth Muscle

Developmental changes in chicken gizzard have been investigated by transmission electron microscopy both in vivo (Bennett and Cobb, 1969; Bailey et al., 1984; Volberg et al., 1986; Bagby, 1986; Gabella, 1989) and in vitro (Campbell et al., 1971, 1974). Relatively little, however, is known about the arrangement of intermediate filaments in embryonic gizzard muscle. In general, size and number of muscle cells increase as embryo age increases (Gabella, 1989). The most active period of myoblast division is around day 6 in ovo, but most division of differentiated muscle cells occurs in the late stage of incubation, around day 19 (Gabella, 1989). On day 7, myoblasts begin to differentiate, i. e., cytoplasmic dense bodies appear and are closely associated with both intermediate and thin filaments (Bennett and Cobb, 1969; Cooke, 1983; Bailey et al., 1984). Thick filaments seem to first be present around day 9-10 in ovo (Bennett and Cobb, 1969). Evidence from another group, however, shows that thick filaments are absent on day 10 (Campbell et al., 1974). Both groups agree that the seemingly different time of thick filament appearance may be due to the fixative, OsO_4 only, used

thick filament appearance may be due to the fixative, OsO_4 only, used by Bennett and Cobb. Osmium tetroxide may induce aggregation of thin filaments and may have caused them to be incorrectly identified as thick filaments (Bennett and Cobb, 1969; Campbell et al., 1974). Another possibility is that intermediate filaments may have been incorrectly identified as thick filaments as mentioned by Fay and Cooke (1973). Interestingly, evidence from two-dimensional gel electrophoresis and fluorescent immunostaining demonstrates that myosin heavy chain, desmin, actin and tropomyosin can be detected as early as day 5 in ovo and that Ca^{2+}-dependent contractility of cells is detectable after day 7 (Hirai and Hirabayashi, 1983, 1986). Before day 14 in ovo, myofilaments are generally aligned but loosely packed in the axial regions of cells, and some intermediate filaments often are visible throughout entire cells. By day 16, however, myofilaments become tightly packed in a longitudinally parallel fashion as seen in adult cells (Gabella, 1989). After day 17, actin filaments approach and form visible connections with membrane-associated dense bodies (Bailey et al., 1984; Bagby, 1986; Volberg et al., 1986).

The chronology of appearance of filaments has also been studied in smooth muscle cells grown in tissue culture. Gizzard smooth muscle cells from 10-day embryos are ultrastructurally identical to gizzard cells isolated from 10-day-old embryos that have been grown in culture for three days. By 11 days in vitro, thick filaments appear,

In summary, although many biochemical characteristics of intermediate filaments have been determined, the specific roles of intermediate filaments, especially their relationship to cytoplasmic dense bodies, are either controversial in adult smooth muscle or are poorly understood in developing smooth muscle. More information will be needed to disclose the specific functions of intermediate filaments in smooth muscle cells.

Explanation of Dissertation Format

This dissertation is divided into two principal parts. The purpose of the first part is to investigate the effects of cations and temperature on the critical concentration of desmin required for filament assembly by using two independent assays. A full-length paper that describes this part has been published in the Biochemical Journal. The objective of the second part is to investigate developmental changes in cytoskeletal and contractile elements in embryonic gizzard cells by transmission electron microscopy and gold-labeling immunocytochemistry. The results are written in two full-length manuscripts that will be submitted for publication.

SECTION I: DETERMINATION OF CRITICAL CONCENTRATION REQUIRED FOR DESMIN ASSEMBLY

Determination of Critical Concentration Required for Desmin Assembly

Rong-Ghi R. Chou, Marvin H. Stromer,
Richard M. Robson and Ted W. Huiatt

Muscle Biology Group
Iowa State University, Ames, Iowa 50011

Running Title: Critical concentration for desmin assembly

All authors are with Iowa State University, Ames, Iowa 50011. Author Chou is with Department of Food Science and Human Nutrition. Authors Stromer, Robson, and Huiatt are with the Muscle Biology Group, Departments of Animal Science and of Biochemistry and Biophysics.

ABSTRACT

Critical concentration required for filament assembly in vitro from highly purified desmin was determined by both turbidity and centrifugation assays. Assembly was done in the presence of 2 mM Ca^{2+}, 2 mM Mg^{2+} or 150 mM Na^{+} at 2, 22 and 37°C. Similar values for critical concentration were obtained by both assays. As temperature increased, critical concentration decreased for each cation. Critical concentration was lowest in the presence of Ca^{2+} at 2, 22 and 37°C, but was highest in the presence of 150 mM Na^{+} at 2°C. Negative staining showed that supernatants from the centrifugation assays contained protofilaments, protofibrils and short particles (< 300 nm), but pellets contained long filaments (> 1 μm) with an average diameter of 10 nm. As temperature increased, both the average diameter and average length of particles in the supernatant increased. Thermodynamic analysis indicated that hydrophobic interactions were dominant during desmin assembly but that ionic interactions might also be involved. Our results demonstrated that the specific cation and temperature and temperature-cation interactions all are important in assembly of desmin intermediate filaments.

INTRODUCTION

Intermediate filaments, which are part of the cytoskeleton of most cells, average 10 nm in diameter and can be classified into six subclasses based on their origin: keratin (epithelial cells), vimentin (cells of mesenchymal origin), desmin (muscle cells), glial fibrillary acidic protein (GFAP) (glial cells), neurofilament proteins (neurons), and lamins (inner surface of the nuclear envelope). Recently, on the basis of comparisons among primary sequences, intermediate filament proteins have been grouped into five sequence types: Type I (acidic keratins); Type II (neutral/basic keratins); Type III (desmin, vimentin, GFAP); Type IV (neurofilaments: NF-L, NF-M, NF-H); and Type V (lamins A, B and C) (Steinert and Roop, 1988; Robson, 1989). Solubility of intermediate filament proteins in the filamentous state is relatively low, and their isolation and purification involve a denaturing solvent such as urea to solubilize the intermediate filament protein (Huiatt et al., 1980; O'Shea et al., 1981; Vorgias and Traub, 1983). Purified Type III intermediate filament proteins, however, will remain soluble without denaturing conditions if the ionic strength is kept low (< 0.01) and the pH is slightly alkaline. The properties of desmin and desmin intermediate filaments have recently been reviewed (Stromer, 1990).

It has been shown by various approaches that the basic building blocks of intermediate filament are protofilaments (Stromer et al., 1981; Aebi et al., 1983), which are tetramers composed of four

monomers in the form of a pair of coiled-coils (Geisler and Weber, 1982; Pang et al., 1983; Pang and Robson, 1984; Ip et al., 1985b). Monomers of intermediate filament proteins share a common structure that contains a conserved, alpha-helix-rich rod domain and nonhelical N- and C-terminal (head and tail, respectively) domains (Geisler and Weber, 1982; Robson, 1989). The N-terminal, but not the C-terminal domain, plays a functional role in filament formation (Traub and Vorgias, 1983, 1984; Kaufmann et al., 1985; van den Heuvel et al., 1987).

Purified Type III intermediate filament proteins, in general, are able to form filaments that are very similar to native intermediate filaments if the ionic strength is increased, if pH is decreased close to 7, or if both are done (Huiatt et al., 1980). Assembly is also greatly influenced by specific cations and temperature. Previous studies from our laboratory (Stromer et al., 1987) have shown that, at the same ionic strength, divalent cations are more effective promoters of desmin assembly than monovalent cations and that rate of assembly increases as temperature increases from 2 to 37°C. Similar results on assembly of GFAP were obtained by Yang and Babitch (1988). There are, however, no published data on the critical concentration required for desmin assembly under a specific set of conditions. Knowing the critical concentration under different conditions has the potential to help us understand the mechanism and forces involved in assembly. The purpose of this study, therefore, was to determine the critical concentration required for desmin assembly in the presence of

specific combinations of cations and temperature. Assembly was monitored by two independent methods, namely, turbidity and centrifugation, and was verified by negative staining of pellets and supernatants obtained during the centrifugation assay.

MATERIALS AND METHODS

Desmin preparation

Desmin was isolated and purified from fresh turkey gizzards by the method of Huiatt et al. (1980). Urea was removed from the purified desmin by extensive dialysis against 10 mM Tris-acetate, pH 8.5, at 2°C. Before desmin was used for assembly, it was dialyzed overnight against two changes of 1 mM $NaHCO_3$, pH 8.0, at 2°C and then clarified at 110,000 x g ($r_{av.}$ = 59.1 cm) for 30 min. The desmin concentration in the supernatant was determined by spectrophotometry, $E^{1\%}_{278nm}$= 5.57 (Huiatt et al., 1980). This value is consistent with that reported for desmin by Steinert et al. (1981).

Assembly of desmin

Desmin assembly was initiated by adding 0.6 ml of filament-forming buffer (30 mM imidazole-HCl, pH 7.0, plus the respective cation) to 1.2 ml of desmin. Final desmin concentrations tested were 100-350 µg/ml for assembly at 2°C, 50-250 µg/ml at 22°C and 25-125 µg/ml at 37°C. The final concentrations of cations were 2 mM $CaCl_2$, 2 mM $MgCl_2$ or 150 mM NaCl. Assembly was monitored by measuring the turbidity at 300 nm when maximum absorbance was reached (16 hr for 2°C; 8 hr for 22°C; 3 hr for 37°C). Turbidity was corrected for absorbance due to unassembled desmin by using control

solutions of desmin in 1 mM $NaHCO_3$ and due to the assembly buffer by using blanks in which no desmin was present.

Another aliquot was centrifuged after maximum absorbance was reached to pellet desmin filaments and leave a constant amount of protein in the supernatant at different starting protein concentrations. Centrifugation was done either at 40,000 x g ($r_{av.}$ 59.1 cm) for 30 min for desmin assembly in the presence of 2 mM $CaCl_2$ or $MgCl_2$ at 2 and 22°C or at 12,000 x g ($r_{av.}$ 59.1 cm) for 30 min for the other temperature-cation combinations. The centrifugal force selected was based on our experience with the length of filaments formed under a given set of conditions, the force required to sediment them and the requirement that the amount of desmin remaining in the supernatant must remain constant as the starting desmin concentration is increased. The desmin concentration in the supernatant was determined by the Bradford method (1976) using desmin to determine the standard curve.

Negative staining

Aliquots from both pellets and supernatants were negatively stained for electron microscopy. A drop of the sample was added to a glow-discharged carbon-coated grid. After 3 min, each grid was washed with 5 drops of glass-distilled water, stained with 2% uranyl acetate, and then examined at 80 kV in a JEOL JEM-100CXII electron microscope. Images were recorded on Kodak SO-163 electron image

film at a nominal magnification of x40,000. Actual magnification was determined by photographing a carbon-grating replica (E. F. Fullam Inc., Latham, NY, U.S.A.). A clear acetate sheet with lines 4 mm apart was randomly placed over the negative. Diameters and lengths of all recognizable particles that intersected a grid line, including protofilaments, protofibrils and filaments, were measured with a Bioquant Image Analysis System (R and M Biometrics, Nashville, TN, U.S.A.) by the method of Stromer et al. (1987).

RESULTS

Turbidity

Figure 1 shows an average of four replications of a turbidity assay done at 37°C with three cations. At 37°C, the highest final turbidity was obtained with Ca^{2+}, followed in decreasing order by the turbidities obtained with 2 mM Mg^{2+} and with 150 mM Na^{+}. When identical experiments were done at 22 or 2°C, the order for the final turbidities was 150 mM Na^{+} > 2 mM Ca^{2+} > 2 mM Mg^{2+} (data not shown). These results indicate that there is a temperature-cation interaction with Ca^{2+} at 37°C that affects the turbidity of desmin particles in suspension and confirms the previous observation of Stromer et al. (1987). For a given cation, turbidity is directly proportional to the desmin concentration. Critical concentration is determined by extrapolating an individual straight line for each cation to determine the intercept on the x-axis where the turbidity increment is equal to zero. The intercepts, therefore, represent the highest desmin concentrations with no detectable turbidity increase or assembly, i. e., the critical concentration. Figure 1 indicates that critical concentration for desmin assembly at 37°C in the presence of 2 mM Ca^{2+} or 150 mM Na^{+} is 11.6 μg/ml, but in the presence of 2 mM Mg^{2+} is 15.4 μg/ml. In addition, for assembling a given total amount of desmin, considerably higher turbidity was observed in the presence of 2 mM Ca^{2+} than in the presence of 2 mM Mg^{2+} or 150

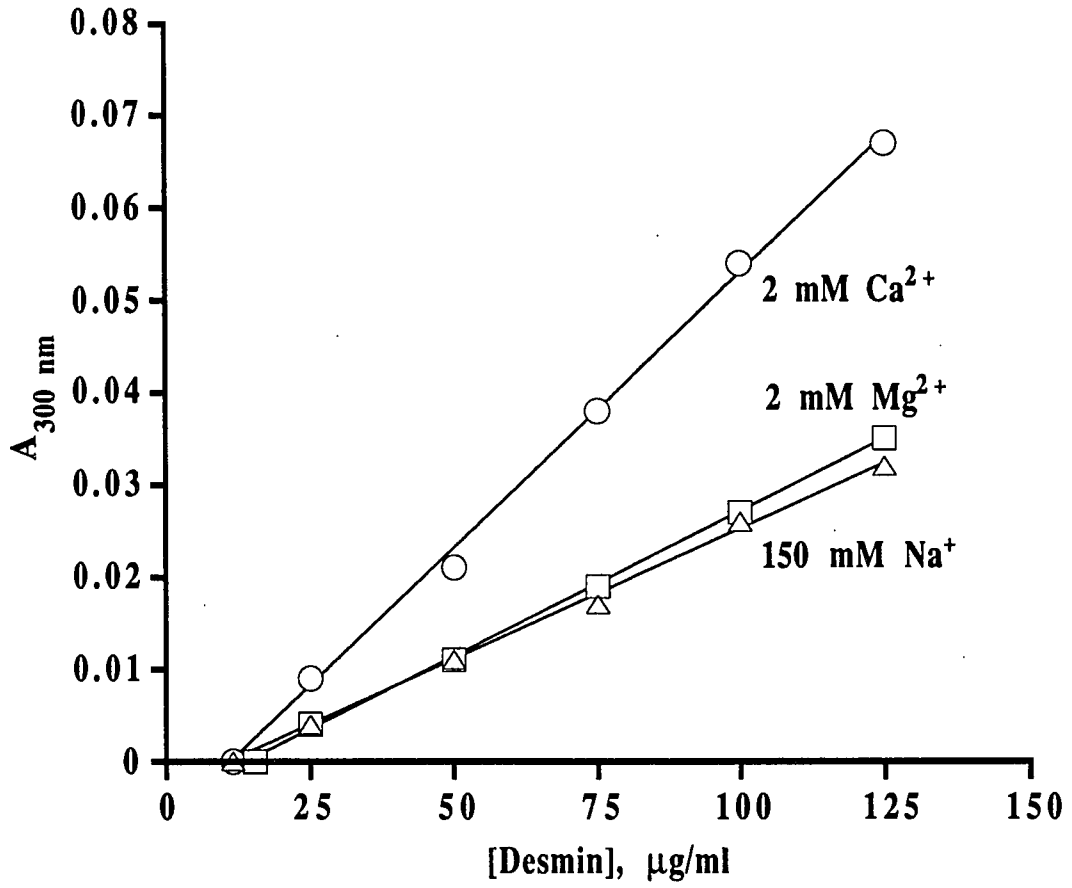

Figure 1 Desmin assembly at 37°C in the presence of three cations. Desmin was assembled at 37°C in 2 mM $CaCl_2$ (O-O), in 2 mM $MgCl_2$ (□-□) or in 150 mM NaCl (Δ-Δ), each buffered with 10 mM imidazole/HCl, pH 7.0. Each point is the average of four separate determinations. Values were corrected for desmin and buffer absorbance as described in the MATERIALS AND METHODS section

mM Na^+ at 37°C (Figure 1). The higher turbidity in the presence of Ca^{2+} involved formation of larger particles that are aggregates of filaments. These filamentous aggregates did not all remain suspended in the filament-forming buffer and gradually settled as a small amount of flocculent material at the bottom of the cuvette. This phenomenon also has been noted in our previous desmin studies (Huiatt, 1979; Stromer et al., 1987), in keratin assembly (Fukuyama et al., 1978), in vimentin assembly (Hartzer, 1984) and in GFAP assembly (Yang and Babitch, 1988). Values for critical concentrations that were determined by the turbidity method with the three cations at 2 and 22°C are compared with these obtained at 37°C in Table 1.

Centrifugation

Critical concentration can also be defined as the minimum concentration required for initiating the intermediate filament assembly process. All protein in excess of the critical concentration will be assembled into filaments, but the amount of protein not assembled will remain virtually constant at the level of the critical concentration after assembly equilibrium is reached (Timasheff, 1981). The centrifugation method, therefore, is able to reveal critical concentration by separating filaments from a constant amount of desmin in the supernatant. The amount of desmin remaining in the supernatant will be the critical concentration for a specific set of conditions. Figure 2 shows an average of four replications of a

centrifugation assay done in the presence of 150 mM Na^+ at 2, 22 and 37°C. At each temperature, a nearly constant amount of desmin remains in the supernatant irrespective of the initial desmin concentration. The critical concentration of desmin required for assembly in the presence of 150 mM Na^+ is 51.8 μg/ml at 2°C, 20.4 μg/ml at 22°C and 8.5 μg/ml at 37°C (Figure 2). Critical concentrations obtained by the centrifugation assay in the presence of 2 mM Ca^{2+} and 2 mM Mg^{2+} at these temperatures are compared with those obtained with 150 mM Na^+ in Table 2.

Critical concentration

Critical concentrations obtained from both turbidity and centrifugation assays (Tables 1 and 2) indicate that critical concentration decreases for each cation as temperature increases and that this trend is very consistent with both methods. Because both methods show similar trends, we have averaged the values from the two methods to facilitate comparisons among the temperature-cation combinations (Table 3). Critical concentration is lowest in the presence of 2 mM Ca^{2+} at each temperature. The critical concentration is highest in the presence of 150 mM Na^+ at 2°C. When averaged over the three temperatures, the trend shows that critical concentrations are lower in the presence of the 2 mM divalent cations than with 150 mM Na^+ (Table 3).

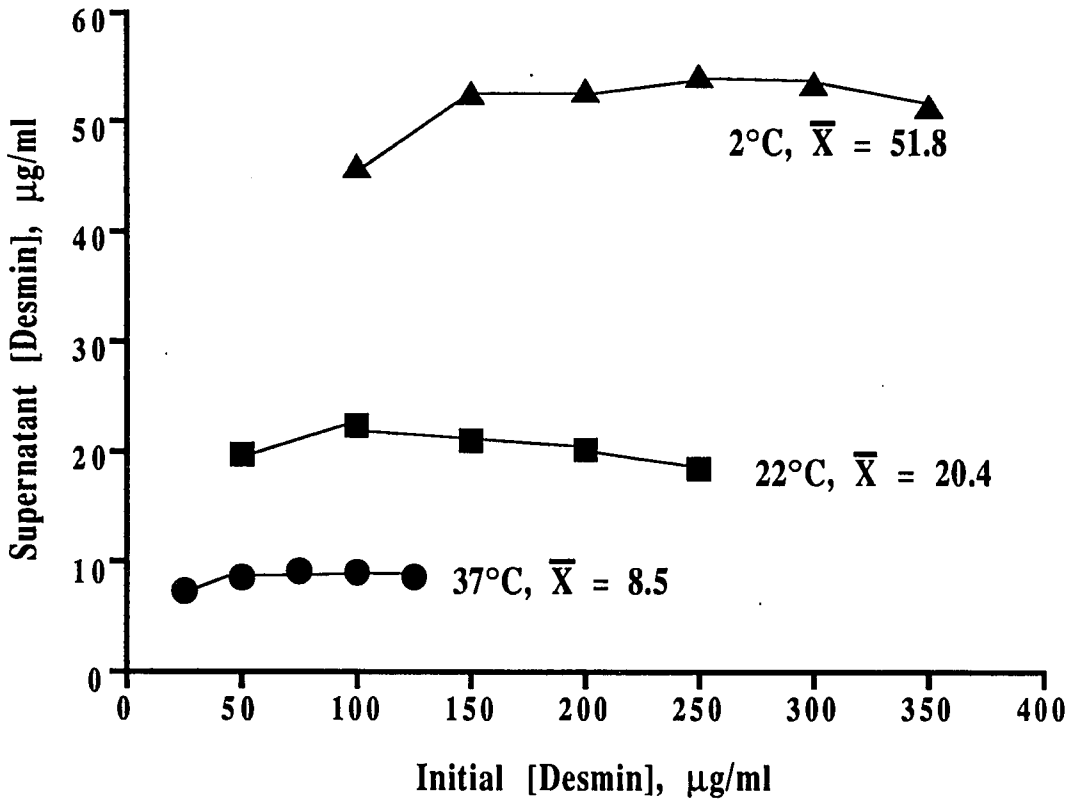

Figure 2. Supernatant desmin concentration after centrifugation of desmin assembled at three temperatures in the presence of 150 mM Na^+. After desmin assembly in 150 mM NaCl, 10 mM imidazole/HCl, pH 7.0, at 2°C (▲-▲), at 22°C (■-■) or at 37°C (●-●) reached maximum absorbance, samples were centrifuged at 12,000 x g ($r_{av.}$ 59.1 cm) for 30 min, and the concentration of desmin remaining in the supernatant was determined as described in the MATERIALS AND METHODS section. Values are the average of four separate experiments

Table 1. Critical concentration (μg/ml) of desmin determined by turbidity assay

Temperature	2 mM Ca^{2+}	2 mM Mg^{2+}	150 mM Na^{+}
2°C	30.4±6.6	36.7±5.3	55.5±8.1
22°C	20.0±5.5	26.2±4.7	28.2±2.5
37°C	11.6±2.0	15.4±2.8	11.6±2.7

Table 2. Critical concentration (μg/ml) of desmin determined by centrifugation assay

Temperature	2 mM Ca^{2+}	2 mM Mg^{2+}	150 mM Na^{+}
2°C	29.1±3.6	31.5±5.0	51.8±2.8
22°C	17.6±2.1	25.2±2.7	20.4±1.3
37°C	3.7±0.4	14.0±1.8	8.5±0.7

Table 3. Overall critical concentration, μg/ml

Temperature	2 mM Ca^{2+}	2 mM Mg^{2+}	150 mM Na^{+}
2°C	29.8±7.8	34.1±7.5	53.7±9.8
22°C	18.8±6.9	25.2±2.7	24.3±3.7
37°C	7.7±3.2	14.0±4.3	10.1±3.1
$\bar{X}$	18.8±9.7	24.8±10.3	29.4±15.7

Negative staining

The distribution of diameters of particles remaining in the supernatant is shown in Table 4. As temperature increases to 37°C, the percentage of protofilaments (2.5 nm diameter) and protofibrils (5 nm diameter) decreases when compared with values obtained at 2 and 22°C. Measurements of average diameters and lengths of particles that remained in the supernatant (Figure 3a) after centrifugation are shown in Tables 5 and 6. When averaged over all cations and temperatures, the diameter is about 5-6 nm, while the length is generally below 300 nm. Fully formed desmin filaments, however, have a diameter of about 10-11 nm and are several micrometers long. The particles remaining in the supernatant, therefore, are protofilaments, protofibrils or partly formed filaments in early stages of the assembly process (Figure 3a). In addition, as temperature increases, average diameters and lengths of particles increase (Table 2). This suggests that higher temperatures favor a more extensive assembly process. On the other hand, the overall average diameter of filaments formed at 2, 22 or 37°C and collected in the pellet (Figure 3b) is very close to 10 nm (Table 7). The filaments in Figure 3b were assembled in the presence of 150 mM Na^+ at 37°C and show some lateral aggregation which is common when high salt and higher temperatures are used. Filament diameters were measured only where the edges of single filaments could be unambiguously recognized. Although length of individual

Figure 3. Negatively stained samples from the centrifugation assay. (a) Supernatants from each temperature-cation combination typically contain protofilaments (arrow), short aggregates (double arrow) and partly formed desmin filaments with average lengths < 300 nm and with average diameters of 5-6 nm. These particles were in the supernatant of a sample assembled with 2 mM $MgCl_2$, 10 mM imidazole/HCl, pH 7.0, at 2°C and centrifuged at 40,000 x g ($r_{av.}$ 59.1 cm) for 30 min. (b) Filaments in the pellet from a sample assembled with 150 mM NaCl, 10 mM imidazole/HCl, pH 7.0, at 37°C and centrifuged at 12,000 x g ($r_{av.}$ 59.1 cm) for 30 min show some lateral aggregation. Individual filaments, however, have average diameters of 10 nm, a value typical of all pelleted filaments in these experiments. The bar represents 100 n m

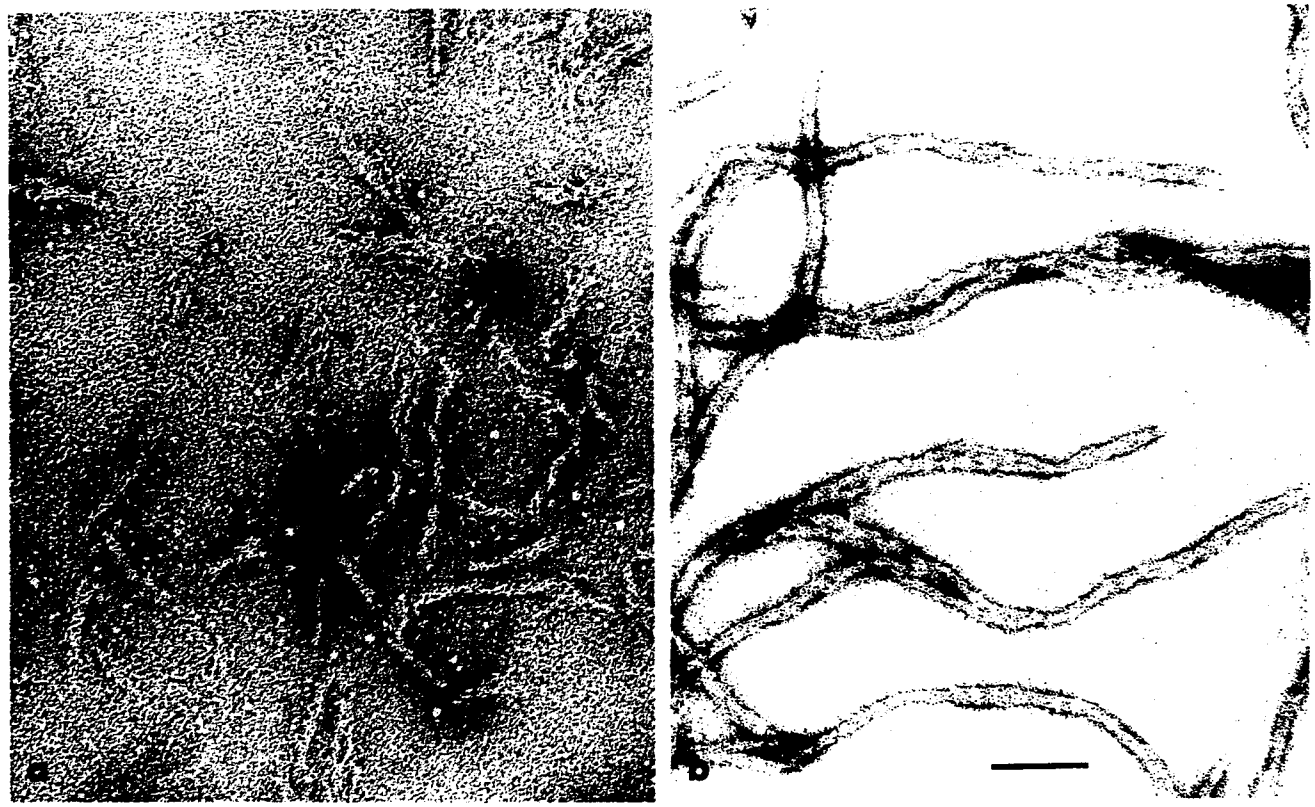
a
b

Table 4. The distribution of diameters of particles remaining in supernatant. [a]Particles are grouped by diameter into four ranges. [b]Each percentage (%) is calculated on the basis of 150 measurements

	2 mM Ca^{2+}			2 mM Mg^{2+}			150 mM Na^{+}		
Particle[a] Diameter (nm)	2°C	22°C	37°C	2°C	22°C	37°C	2°C	22°C	37°C
2.50±1.25	35[b]	28	4	30	21	9	27	15	5
5,00±1.25	60	56	30	65	64	39	42	40	35
7.50±1.25	5	16	38	5	15	35	25	37	41
10.00±1.25	----	----	28	----	----	17	6	8	19

Table 5. Average diameter (nm) of particles remaining in supernatant. Each mean value with its standard error is calculated from 150 measurements

Temperature	2 mM Ca^{2+}	2 mM Mg^{2+}	150 mM Na^{+}
2°C	4.27±1.41	4.38±1.36	5.25±2.15
22°C	4.70±1.63	4.85±1.50	5.97±2.07
37°C	7.37±2.30	6.57±2.23	6.88±2.08

Table 6. Average length (nm) of particles remaining in supernatant. Each mean value with its standard error is calculated from 120 measurements

Temperature	2 mM Ca^{2+}	2 mM Mg^{2+}	150 mM Na^{+}
2°C	105±57	129±68	223±94
22°C	110±67	122±64	273±120
37°C	158±69	209±95	326±120

Table 7. Average diameter (nm) of desmin filaments in pellet. Each mean value with its standard error is calculated from 150 measurements

Temperature	2 mM Ca^{2+}	2 mM Mg^{2+}	150 mM Na^{+}
2°C	10.00±1.60	9.75±1.62	9.63±1.40
22°C	10.02±1.44	9.78±1.29	9.77±1.34
37°C	11.13±2.07	10.33±1.44	10.30±1.60

filaments in the pellet could usually not be determined because of tangling of the filaments, many could be followed accurately for more than 1 μm (data not shown).

Thermodynamic data

Critical concentration can also be defined as the reciprocal of the equilibrium constant (K_{eq}) of the nucleation-elongation assembly reaction (Timasheff, 1981). Therefore, the free energy (ΔG), enthalpy (ΔH) and entropy (ΔS) for assembly can be estimated from the van't Hoff equation (Chang, 1977);

$$\ln C = -\ln K_{eq} = (-\Delta H/R)(1/T) + \Delta S/R$$

where, C = molar critical concentration,

R = universal gas constant, and

T = degrees Kelvin.

ΔH is estimated from the slope of the van't Hoff plot of the natural logarithm of molar critical concentration versus 1/T, and ΔS is estimated from the y-intercept. Then, ΔG is directly calculated from the relationship, $\Delta G = \Delta H - T\Delta S$. The results (Table 8), which were calculated from the average values in Table 3, indicate that desmin assembly, in the presence of each cation, is endothermic ($\Delta H > 0$) and is driven by entropy. This implies that hydrophobic interactions are dominant during desmin assembly in the presence of these cations (Cantor and Schimmel, 1980).

Table 8. Thermodynamic data of desmin assembly in the presence of cations. van't Hoff plots are calculated from the values in Table 3. r is the correlation coefficient. ΔH ($KJmol^{-1}$) with its standard error is estimated from the slope of the plot, and ΔS ($Jmol^{-1}K^{-1}$) with its standard error is estimated from the y-intercept. ΔG ($KJmol^{-1}$) is calculated from the relationship, $\Delta G = \Delta H - T\Delta S$

	2 mM Ca^{2+}	2 mM Mg^{2+}	150 mM Na^{+}
van't Hoff plot	lnC=3183(1/T)-26 r=0.956	lnC=1978(1/T)-21 r=0.955	lnC=4002(1/T)-28 r=0.990
ΔH	+26.5±8.0	+16.4±5.0	+33.6±5.0
ΔS	+218±25	+176±17	+235±17
ΔG_{275}	-33.6	-32.3	-31.1
ΔG_{295}	-37.8	-35.7	-35.7
ΔG_{310}	-41.2	-38.2	-39.9

DISCUSSION

Turbidity

The validity of using turbidity to measure the weight concentration of particles in suspension is based on both theoretical calculations (Berne, 1974) and experimental evidence (Gaskin et al., 1974). Turbidity is a function of the total concentration of scattering particles and is independent of the length distribution of the particles (Berne, 1974; Gaskin et al., 1974). There are, however, two requirements that need to be met before using the turbidity assay: (1) the length (L) of rod-like particles should be large in comparison to the wavelength (λ) of light used for measurement, and (2) turbidity should be proportional to the inverse third power of wavelength (λ^{-3}). Timasheff (1981) has stated that turbidity assays are valid if the ratio of particle length (L) to the λ used is greater than 3.5. Our results show that most filaments in our samples are longer than 1 μm, and that would provide a ratio of $L/\lambda 300nm > 3.5$. Reassembled desmin filaments, therefore, meet the rod-like requirement. This conclusion is consistent with our previous study (Huiatt, 1979) and with the work of Steinert et al. (1976) on keratin filaments. Referring to the second point, Camerini-Otero and Day (1978) suggested that presence of aberrant structures or nonideality of the solution might be responsible for a deviation of the wavelength exponent from the theoretical value of -3. Zackroff and Goldman

(1979) also suggested that the wavelength exponent of reassembled vimentin filaments might be influenced by the pH and ionic strength of the filament-forming buffer. Our results (data not shown), however, indicated that the dependence of turbidity on wavelength gave wavelength exponents close to -3 for each temperature-cation combination tested. In addition, results from this study and others (Huiatt, 1979; Steinert et al., 1976) demonstrated that, for each temperature-cation combination, turbidity in the plateau region was linearly related to total protein concentration and was independent of the length distribution of particles. Although the turbidity method has limitations (Timasheff and Grisham, 1980), results from our laboratory and from others indicate that it is an appropriate assay for measuring protein assembly.

Centrifugation

Centrifugation was used in this study to pellet desmin filaments and to leave a constant amount of desmin in the supernatant. For this approach to be valid, the following criteria should be met: (1) rate of disassembly must be slow relative to the duration of centrifugation so that the equilibrium distribution is not disturbed during the course of the experiment; and (2) the assembly equilibrium should not be affected significantly by pressure (Timasheff, 1981). Timasheff (1981) pointed out that the second criterion might be very difficult to meet. In the case of actin assembly, Ikkai and Ooi (1966)

demonstrated that high pressure generated near the bottom of the tubes during centrifugation shifted the assembly equilibrium of actin to the monomer state and finally induced irreversible denaturation of the actin monomer. It was suggested that assembly was associated with an increase in the volume of the actin solution; that is, the difference in partial specific volume between polymer and monomer ($\Delta\bar{v}$) was changed (Ikkai et al., 1966). Because many assembly processes are accompanied by a significant value of $\Delta\bar{v}$ (Harrington and Kegeles, 1973), desmin assembly may also be affected by pressure. Unfortunately, there are no published data on this aspect for desmin assembly.

The criteria used to select the centrifugal force used in our experiments were based on a report by Timasheff (1981) and on previous studies from our laboratory. Timasheff (1981) proposed two criteria for determining if appropriate centrifugal force has been used. First, the concentration of protein in the supernatant should be comparable to the critical concentration determined by another method. Second, the protein remaining in the supernatant must be unable to assemble at atmospheric pressure. We obtained similar values for critical concentrations by two independent methods, namely, turbidity and centrifugation (Tables 1 and 2). Negative staining of aliquots of supernatants immediately after centrifugation and 40 or 60 min after centrifugation showed that particle length did not increase as time after centrifugation increased (data not shown). This indicates that the amount of desmin remaining in the

supernatant did not exceed the critical concentration.

Our laboratory had previously developed a low speed (12,000 x g, $r_{av.}$ 59.1cm) centrifugation method to determine the effect of ionic strength on desmin and vimentin assembly. Huiatt et al. (1980) demonstrated that over 95% of desmin could be pelleted as filaments during a 30 min spin if assembly was done in the presence of 150 mM Na^+ at 2°C. Negative staining showed that pellets contained long filaments with average diameters of 10-11 nm but that supernatants contained protofilaments, protofibrils and short (< 300 nm) particles (Hartzer, 1984). On the basis of these observations, 12,000 x g ($r_{av.}$ 59.1 cm) was selected to reveal critical concentration required for desmin assembly in the presence of 150 mM Na^+ at 2°C. This g force was also used to reveal critical concentrations in the presence of 150 mM Na^+ at 22 and 37°C and of 2 mM Ca^{2+} or Mg^{2+} at 37°C because the turbidities observed for assembling a given amount of protein were higher with those temperature-cation combinations than in the presence of 150 mM Na^+ at 2°C. The 12,000 x g force was initially tried with the 2 mM Ca^{2+} and with the 2 mM Mg^{2+} samples at 2 and at 22°C, but the desmin concentration in the supernatant did not remain constant as the starting desmin concentration was increased (data not shown). A greater centrifugal force (40,000 x g, $r_{av.}$ 59.1 cm), therefore, was needed to reveal critical concentration in the presence of 2 mM Ca^{2+} or Mg^{2+} at 2 or 22°C. The criterion of leaving a constant concentration of desmin in the supernatant independent of the initial desmin concentration was met by using this higher

centrifugal force.

Factors affecting particle morphology

Our laboratory previously investigated the effects of pH and concentration of Mg^{2+} or Na^{+} on yield and morphology of desmin intermediate filaments (Huiatt, 1979). The optimum pH for assembly of desmin filaments was 7, the same as that utilized in these experiments. The studies by Huiatt (1979) also demonstrated that ionic strength had no effect on dimensions of the protofilaments. A comparison of desmin filaments formed in 10 mM imidazole-HCl, pH 7, with those formed in the same buffer plus 150 mM NaCl showed that the major effect of increasing ionic strength at pH 7 was to increase filament length. The purpose of the experiments described in the present paper was to determine the critical concentration required for desmin assembly at pH 7 in the presence of two divalent cations or a frequently utilized monovalent cation at three temperatures. Based both on our previous studies and on the results shown in Table 6, an increase in ionic strength is associated with an increase in filament length. Data shown in Table 7 indicate, however, that there is little variation in filament diameters for all experimental conditions tested and that differences in ionic strength had little effect on diameter of filaments.

Factors affecting critical concentration

Our data show that both temperature and cations modify the critical concentration of desmin. Between 2 and 37°C, critical concentration decreases as temperature increases. This implies that higher temperature favors more extensive assembly because of higher K_{eq}. This is consistent with our previous results showing that desmin assembly increased as temperature increased from 2 to 37°C (Stromer et al., 1987). Secondly, our results show that, when averaged over the three temperatures, critical concentration for desmin assembly in the presence of 2 mM divalent cations is lower than in the presence of 150 mM Na^+, a monovalent cation frequently used at this concentration for assembly (Huiatt et al., 1980; Inagaki et al., 1988). This also agrees with our previous studies (Stromer et al., 1987) and with studies on other intermediate filament proteins (Fukuyama et al., 1978; Yang and Babitch, 1988). Yang et al. (1988) have demonstrated that there are three classes of divalent cation binding sites, one of which is calcium specific and is in the rod domain of GFAP protein. Because the rod domains of intermediate filament proteins are the most highly conserved regions of the molecules, it is possible that calcium binding sites may also exist in desmin and that binding of calcium may cause a molecular change that favors filament assembly. Our data suggest that desmin assembly is a complex, multistep process. One possible interpretation of the data in Table 4 is that Na^+ favors filament elongation and that Ca^{2+} and Mg^{2+} at 2

and 22°C favor nucleation.

Recent studies by Inagaki et al. (1988) have shown that in vitro phosphorylation of desmin tetramers inhibits the assembly process and that in vitro phosphorylation of desmin filaments causes disassembly. Geisler and Weber (1988) determined that the three phosphorylation sites on desmin are in the N-terminal head domain, the region that has an important functional role in filament assembly (Traub and Vorgias, 1983, 1984; Kaufmann et al., 1985; van den Heuvel et al., 1987). The desmin used in the studies reported in this paper was prepared by the method of Huiatt et al. (1980) and contained 20% α-(more acidic) and 80% ß-desmin variants. Although phosphorylation affects assembly, all of our preparations contained a consistent ratio of α and ß variants, thus making comparisons among the treatments valid. If phosphorylation, by itself, controls desmin assembly, when the initial desmin concentration and thus the amount of the α variant is increased in an assembly assay, there should be some increase in the amount of unassembled desmin remaining in the supernatant. The results shown in Figure 2 indicate that this did not occur. This may indicate that the predominant ß variant can serve as a template for rod-to-rod associations that incorporate both α and ß desmin into the assembling particles.

Forces involved in assembly

Theoretical calculations of possible ionic interactions between the coiled-coil rods of intermediate filament proteins (Crewther et al., 1983; Fraser et al., 1985; Conway and Parry, 1988) formed the basis for the concept that ionic interactions are the key force responsible for alignment and registry of dimers in the intermediate filament. Our thermodynamic data indicate that desmin assembly in the presence of cations is endothermic and is driven by entropy. This implies that hydrophobic rather than ionic interactions are dominant during assembly, especially in the presence of high salt (because of charge masking by cations). This conclusion is supported by the fact that higher ionic strength favors more extensive assembly of intermediate filament proteins (Huiatt, 1979; Huiatt et al., 1980; Renner et al., 1981; Steinert et al., 1981; Nelson and Traub, 1982; Hartzer, 1984; Ip et al., 1985a, b; Stromer et al., 1987). Hatzfeld et al. (1987) also demonstrated that formation of the heterotypic cytokeratin complex did not depend solely on ionic interactions. Our data do not address the question of involvement of ionic interactions in alignment and registry of subunits but suggest that hydrophobic interactions are the major force for desmin intermediate filament assembly in the presence of cations.

ACKNOWLEDGEMENTS

We thank Kathy Schneider, Martha Bushlow, Mary Bremner, Stephan Bilak and Russell Poyner for excellent technical assistance. We also thank Dr. J. B. Applequist from the Department of Biochemistry and Biophysics for his assistance with the analysis of the thermodynamics data, Dr. D. F. Cox for assistance with the statistical analysis, and Marylou Weigel for typing the manuscript. This research was supported, in part, by a grant from the American Heart Association, Iowa Affiliate. This is Journal Paper J-13847 of the Iowa Agriculture and Home Economics Experiment Station, Ames, IA 50011, projects 2361, 2921 and 2127.

REFERENCES

Aebi, U., W. E. Fowler, P. Rew, and T.-T. Sun. 1983. The fibrillar substructure of keratin filaments unraveled. J. Cell Biol. 97:1131-1143.

Berne, B. J. 1974. Interpretation of the light scattering from long rods. J. Mol. Biol. 89:755-758.

Bradford, M. 1976. A rapid and sensitive method for the quantitation of microgram quantities of protein utilizing the principle of protein-dye binding. Anal. Biochem. 72:248-254.

Camerini-Otero, R. D., and L. A. Day. 1978. The wavelength dependence of the turbidity of solutions of macromolecules. Biopolymers 17:2241-2249.

Cantor, C. R., and P. R. Schimmel. 1980. Biophysical chemistry. Part I: The conformation of biological macromolecules. Pages 253-309 in Chapter 5. Conformational analysis and forces that determine protein structure. W. H. Freeman and Company, San Francisco, CA.

Chang, R. 1977. Physical chemistry with applications to biological systems. Page 243 in Chapter 12. Thermodynamics. Macmillan Publishing Co., Inc. New York, NY.

Conway, J. F., and D. A. D. Parry. 1988. Intermediate filament structure: 3. Analysis of sequence homologies. Int. J. Biol. Macromol. 10:79-88.

Crewther, W. G., L. M. Dowling, P. M. Steinert, and D. A. D. Parry. 1983. Structure of intermediate filaments. Int. J. Biol. Macromol. 5:267-274.

Fraser, R. D. B., T. P. MacRae, E. Suzuki, and D. A. D. Parry. 1985. Intermediate filament structure: 2. Molecular interactions in the filament. Int. J. Biol. Macromol. 7:258-274.

Fukuyama, K., T. Murozuka, R. Caldwell, and W. L. Epstein. 1978. Divalent cation stimulation of in vitro fibre assembly from epidermal keratin protein. J. Cell Sci. 33:255-263.

Gaskin, F., C. R. Cantor, and M. L. Shelanski. 1974. Turbidimetric studies of the in vitro assembly and disassembly of porcine microtubules. J. Mol. Biol. 89:739-758.

Geisler, N., and K. Weber. 1982. The amino acid sequence of chicken muscle desmin provides a common structural model for intermediate filament proteins. EMBO J. 1:1649-1656.

Geisler, N., and K. Weber. 1988. Phosphorylation of desmin in vitro inhibits formation of intermediate filaments; identification of three kinase A sites in the aminoterminal head domain. EMBO J. 7:15-20.

Harrington, W. F., and G. Kegeles. 1973. Pressure effects in ultracentrifugation of interacting systems. Methods Enzymol. 27:306-345.

Hatzfeld, M., G. Maier, and W. W. Franke. 1987. Cytoskeleton domains involved in heterotypic complex formation determined by in vitro binding assays. J. Mol. Biol. 197:237-255.

Hartzer, M. K. 1984. Purification and properties of porcine cardiac desmin and vascular smooth muscle vimentin. Ph. D. Dissertation. Iowa State University, Ames.

Huiatt, T. W. 1979. Studies on the 55,000-dalton protein from vertebrate smooth muscle intermediate filaments. Ph. D. Dissertation. Iowa State University, Ames.

Huiatt, T. W., R. M. Robson, N. Arakawa, and M. H. Stromer. 1980. Desmin from avian smooth muscle: Purification and partial characterization. J. Biol. Chem. 255:6981-6989.

Ikkai, T., and T. Ooi. 1966. The effect of pressure on F-G transformation of actin. Biochemistry 5:1551-1560.

Ikkai, T., T. Ooi, and H. Noguchi. 1966. Actin: Volume change on transformation of G-form to F-form. Science 152:1756-1757.

Inagaki, M., Y. Gonda, M. Matsuyama, K. Nishizawa, Y. Nishi, and C. Sato. 1988. Intermediate filament reconstitutuion in vitro: The role of phosphorylation on the assembly-disassembly of desmin. J. Biol. Chem. 263:5970-5978.

Ip, W., M. K. Hartzer, Y.-Y. S. Pang, and R. M. Robson. 1985a. Assembly of vimentin in vitro and its implications concerning the structure of intermediate filaments. J. Mol. Biol. 183:365-375.

Ip, W., J. E. Heuser, Y.-Y. S. Pang, M. K. Hartzer, and R. M. Robson. 1985b. Subunit structure of desmin and vimentin protofilaments and how they assemble into intermediate filaments. Ann. N. Y. Acad. Sci. 455:185-199.

Kaufmann, E., K. Weber, and N. Geisler. 1985. Intermediate filament forming ability of desmin derivatives lacking either the amino-terminal 67 or the carboxy-terminal 27 residues. J. Mol. Biol. 185:733-742.

Nelson, W. T., and P. Traub. 1982. Effect of the ionic environment on the incorporation of the intermediate-sized filament protein vimentin into residual cell structures upon treatment of Ehrlich ascites tumour cells with triton X-100. J. Cell Sci. 53:77-95.

O'Shea, J. M., R. M. Robson, M. K. Hartzer, T. W. Huiatt, W. E. Rathbun, and M. H. Stromer. 1981. Purification of desmin from adult mammalian skeletal muscle. Biochem. J. 195:345-356.

Pang, Y.-Y. S., R. M. Robson, M. K. Hartzer, and M. H. Stromer. 1983. Subunit structure of the desmin and vimentin protofilament units. J. Cell Biol. 97:226a. (Abstract)

Pang, Y.-Y. S., and R. M. Robson. 1984. Dissociation of desmin protofilaments with increase in pH or urea concentration. J. Cell Biol. 99:320a. (Abstract).

Renner, W., W. W. Franke, and E. Schmid. 1981. Reconstitution of intermediate-sized filaments from denatured monomeric vimentin. J. Mol. Biol. 149:285-306.

Robson, R. M. 1989. Intermediate filaments. Curr. Opinion Cell Biology 1:36-43.

Steinert, P. M., W. W. Idler, and S. B. Zimmerman. 1976. Self-assembly of bovine epidermal keratin filaments in vitro. J. Mol. Biol. 108:547-567.

Steinert, P. M., W. W. Idler, F. Cabral, M. M. Gottesman, and R. D. Goldman. 1981. In vitro assembly of homopolymer and copolymer filaments from intermediate filament subunits of muscle and fibroblastic cells. Proc. Natl. Acad. Sci. USA 78:3692-3696.

Steinert, P. M., and D. R. Roop. 1988. Molecular and cellular biology of intermediate filaments. Ann. Rev. Biochem. 57:593-625.

Stromer, M. H., T. W. Huiatt, F. L. Richardson, and R. M. Robson. 1981. Disassembly of synthetic 10-nm desmin filaments from smooth muscle into protofilaments. Eur. J. Cell Biol. 25:136-143.

Stromer, M. H., M. A.Ritter, Y.-Y. S. Pang, and R. M. Robson. 1987. Effect of cations and temperature on kineitcs of desmin assembly. Biochem. J. 246:75-81.

Stromer, M. H. 1990. Intermediate (10-nm) filaments in muscle. Pages 19-36 in R. D. Goldman, and P. M. Steinert, eds. Cellular and molecular biology of intermediate filaments. Plenum Publishing Corp., New York, NY.

Timasheff, S. N., and L. M. Grisham. 1980. In vitro assembly of cytoplasmic microtubules. Ann. Rev. Biochem. 49:565-591.

Timasheff, S. N. 1981. The self-assembly of long rodlike structures. Pages 315-336 in C. Frieden, and L. W. Nichol, eds. Protein-protein interactions. John Wiley Sons, Inc., New York, NY.

Traub, P., and C. E. Vorgias. 1983. Involvement of the N-terminal polypeptide of vimentin in the formation of intermediate filaments. J Cell Sci. 63:43-67.

Traub, P., and C. E. Vorgias. 1984. Differential effect of arginine modification with 1,2-cyclohexanedione on the capacity of vimentin and desmin to assemble into intermediate filaments and to bind to nucleic acids. J Cell Sci. 65:1-20.

van den Heuvel, R. M. M., G. J. J. M. van Eys, F. C. S. Ramaekers, W. J. Quax, W. T. M. Vree Egberts, G. Schaart, H. T. M. Cuypers, and H. Bloemendal. 1987. Intermediate filament formation after transfection with modified hamster vimentin and desmin genes. J. Cell Sci. 88:475-482.

Vorgias, C. E., and P. Traub. 1983. Isolation, purification and characterization of the intermediate filament protein desmin from porcine smooth muscle. Prep. Biochem. 13:227-243.

Yang, Z. W., and J. A. Babitch. 1988. Factors modulating filament formation by bovine glial fibrillary acidic protein, the intermediate filament component of astroglial cells. Biochemistry 27:7038-7045.

Yang, Z. W., F. K. Chung, and J. A. Babitch. 1988. Characterization and location of divalent cation binding sites in bovine glial fibrillary acidic protein. Biochemistry 27:7045-7050.

Zackroff, R. V., and R. D. Goldman. 1979. In vitro assembly of intermediate filaments from baby hamster kidney (BHK-21) cells. Proc. Natl. Acad. Sci. USA 76:6226-6230.

SECTION II IN VIVO STRUCTURAL CHANGES IN CONTRACTILE AND CYTOSKELETAL ELEMENTS IN DEVELOPING SMOOTH MUSCLE CELLS

In vivo structural changes in contractile and cytoskeletal elements in developing smooth muscle cells

Rong-Ghi R. Chou, Marvin H. Stromer,
Richard M. Robson and Ted W. Huiatt

Muscle Biology Group
Iowa State University, Ames, Iowa 50011

All authors are with Iowa State University, Ames, Iowa 50011. Author Chou is with the Department of Food Science and Human Nutrition. Authors Stromer, Robson, and Huiatt are with the Muscle Biology Group, Departments of Animal Science and of Biochemistry and Biophysics.

ABSTRACT

The in vivo development of smooth muscle cells in chicken gizzard was studied by both transmission electron microscopy (TEM) and immunoelectron microscopy (IEM). For TEM, smooth muscle was obtained from gizzards of 6-, 8-, 10-, 12-, 14-, 16-, 18-, and 20-day embryos and from 1- and 7-day post-hatch chickens. For IEM, smooth muscle was obtained from gizzards of 1- and 7-day post-hatch chickens. Myoblasts were actively replicating in tissue from 6-day embryos. Cytoplasmic dense bodies (CDBs) first appeared at day 8 and were recognized as patches of increased electron density that consisted of actin filaments (AFs), intermediate filaments (IFs), and cross-connecting filaments (CCFs). Although the assembly of CDBs was not synchronized, the number, size and electron density of CDBs increased as age increased. Membrane-associated dense bodies (MADBs) could also be recognized at embryonic day 8. The number and size of MADBs increased as age increased, especially after day 16. Filaments with the diameter of thick filaments first appeared at embryonic day 12. Smooth muscle cells were able to divide as late as embryonic day 20. The axial intermediate filament bundle (IFB) first appeared in 1-day post-hatch cells and became larger and more prominent in 7-day post-hatch cells. Immunogold labeling with anti-desmin showed that the IFB contained desmin IFs. The developmental events which occurred during this 23 day period could be sequentially classified into 7 stages, primarily based on the

appearance and the growth of contractile and cytoskeletal elements. These stages have been identified as follows: myoblast proliferation, dense body appearance, thick filament appearance, dense body growth, muscle cell replication, IFB appearance, and appearance of adult type cells. Smooth muscle cells in each stage express similar developmental characteristics. These sequential events clearly indicated that smooth muscle myogenesis in vivo is a sequential process in which contractile elements (AFs and thick filaments) and filament attachment sites (CDBs and MADBs) were assembled earlier than the axial IFB, a major cytoskeletal element.

INTRODUCTION

The development of chicken gizzard smooth muscle cells both in intact embryos (Bennett and Cobb, 1969; Gabella, 1989) and in cell culture (Campbell et al., 1971, 1974; Chamley-Campbell et al., 1979; Burnstock, 1981) has been studied by light and electron microscopy. It is believed, however, that the developmental process in cell culture is not identical to that in intact embryo. For instance, differentiated smooth muscle cells are able to divide in intact embryos, but not in cell culture (Campbell et al., 1974; Gabella, 1989).

Generally speaking, weight of the gizzard increases as age increases. This increase is believed mainly due to the increase in muscle cell number. Gap junctions appear at embryonic day 16, and their size increases as age increases. Caveolae become more common near the end of embryonic life and continue to increase in number after hatching. The size of the myofilament area inside smooth muscle cells also increases as age increases. On the other hand, mitochondria, which initially make up 8% of the cell volume by day 14, decrease to 5% in the adult (Gabella, 1989).

Previous studies of intact embryos have provided a general but incomplete sequence in the appearance of contractile and cytoskeletal elements and little information about the appearance and changes in cytoplasmic dense bodies (CDBs) in developing smooth muscle cells. In the early stages of embryonic development, myoblasts, with a high nucleus-to-cytoplasm ratio, are not differentiated and resemble

fibroblasts in their cellular and subcellular structure (Bennett and Cobb, 1969). Intermediate filaments (IFs) can be found as early as embryonic day 4, and the number of IFs increases as age increases (Bailey et al., 1984). By day 7, CDBs associated with both actin filaments (AFs) and IFs begin to appear (Bennett and Cobb, 1969; Bagby, 1986). Membrane-associated dense bodies (MADBs) (Bagby, 1983) or dense bands (Gabella, 1981) first appear at day 10 (Bennett and Cobb, 1969) and become more prominent in the late stages of embryonic development (Bennett and Cobb, 1969; Volberg et al., 1986; Gabella, 1989).

The appearance of structurally recognizable thick filaments is a matter of controversy. Bennett and Cobb (1969) observed thick filaments by embryonic day 9, but Campbell et al. (1974) found no thick filaments until after day 10. Results from two-dimensional gel electrophoresis and immunofluorescent staining showed, however, that myosin heavy chain can be detected as early as embryonic day 5 and that Ca^{2+}-dependent contractility of cells is detectable in cells prepared from 7 day old embryos (Hirai and Hirabayashi, 1983, 1986).

The axial intermediate filament bundle (IFB), a major cytoskeletal element, was identified by Stromer and Bendayan (1988) as a unique feature of intact adult gizzard smooth muscle cells. The IFB is linked to other IFs in the cytoplasm to construct an intracellular cytoskeletal network. It is believed that this cytoskeletal network may serve as a cellular organizer to retain the positions of organelles

during contraction and relaxation of smooth muscle cells (Stromer and Bendayan, 1988; 1990; Stromer, 1990). When the IFB can first be recognized in the developing smooth muscle cells is not known.

The organization of contractile and cytoskeletal elements in adult smooth muscle cells is still unclear (see reviews by Bagby, 1983; 1986; 1990). The purpose of these studies, therefore, was to investigate the changes in contractile and cytoskeletal elements, especially CDBs, in developing smooth muscle cells and to identify the changes that occur during development. This study was done on gizzard smooth muscle cells from 6-day embryonic to 7-day post-hatch chicks. Knowing the changes in filament attachment sites (CDBs and MADBs) and contractile and cytoskeletal elements during development may facilitate our understanding of the three-dimensional organization of these structures in adult smooth muscle cells.

MATERIALS AND METHODS

Tissue preparation for transmission electron microscopy

Smooth muscle samples for transmission electron microscopy were taken from gizzards of 6-, 8-, 10-, 12-, 14-, 16-, 18-, and 20-day embryos and from 1- and 7-day post-hatch chickens. Five to six embryos from each age were randomly selected and were examined to determine their developmental progress. At least two embryos from each age were again randomly selected from those that exhibited identical, normal developmental characteristics when compared with the Hamilton-Hamburger classification system. Tissue preparation for transmission electron microscopy and staining of sections were done by the method of Stromer and Bendayan (1988). In general, thin strips of tissue were cut parallel to the cell axis and were isometrically clamped before the ends of the strips were severed. Samples from 6- to 14-day embryonic gizzard could not be clamped because of the small organ size. Tissue samples were doubly fixed in Karnovsky's fixative with 2 mM $MgCl_2$ and 2 mM $CaCl_2$, pH 7.2, at 2°C for 2.5 hr and then in 1 % osmium tetroxide for 60 min. Dehydration in graded acetones was followed by embedding in Epon-Araldite resin. At least six blocks were randomly selected from each sample for thin sectioning. Sections were positively stained with methanolic uranyl acetate and Reynold's lead citrate.

.Tissue preparation for immunoelectron microscopy

Smooth muscle samples for immunoelectron microscopy were taken from gizzards of 1- and 7-day post-hatch chickens. Duplicate samples were used for each age examined. Tissue preparation was done by the method of Stromer and Bendayan (1988) and Bendayan (1984). Thin strips of tissue from 1- and 7-day post-hatch chickens were cut and clamped as described in the previous section. Samples were fixed in 2% paraformaldehyde, 1.5% glutaraldehyde, 2 mM $MgCl_2$, and 2 mM $CaCl_2$ buffered with Millonig's phosphate, pH 7.2, for 2.5 hr at 2°C. After fixation, the samples were immersed in 0.15 M glycine for 1 hr to block free aldehyde groups. Dehydration in graded methanol, infiltration, embedding in Lowicryl K4M resin, polymerization and thin sectioning (at least six blocks by random selection from each sample) were done by the method of Bendayan (1984).

Antibody labeling

Polyclonal antibodies to avian gizzard desmin were produced in a rabbit and used at 1:20 dilution on thin sections prepared for immunoelectron microscopy. The specificity of this anti-serum has been shown previously (Stromer et al., 1981; Stromer and Bendayan, 1988) and was also confirmed by immunoblotting (Chou et al., 1991). Details of the labeling method are described in Bendayan (1984).

Colloidal gold particles (15 nm) were complexed with protein A (Sigma Chemical Co., St. Louis, MO, U.S.A.) by the method of Bendayan (1984). Controls, either pre-absorption of anti-serum with desmin or substituting phosphate buffered saline for the anti-serum, showed that labeling was reduced to background level.

Sample evaluation

All sections were examined at 80 kV in a JEOL JEM-100CXII electron microscope. Images were recorded on Kodak SO-163 electron image film. Longitudinal cell profiles were analyzed with a Bioquant Image Analysis System (R & M Biometrics, Nashville, TN, U.S.A.). The average number of CDBs per μm^2 of myofilament area in cells from each age was analyzed by randomly selecting 10 representative cell profiles. The average apparent diameter and length of CDBs and MADBs at each age were also measured from separate negatives. The CDBs (100) and MADBs (50) to be measured were selected by randomly placing a clear acetate sheet with lines 4 mm apart over the negative. Measurements were done only where a single CDB or MADB that intersected a grid line could be unambiguously recognized. The apparent diameter and length of the CDB or MADB were defined as the length of two perpendicular lines that corresponded to the maximum width and the maximum length, respectively, of the CDB or MADB. Statistical analysis was done by using Duncan's multiple range test (SAS User's Guide: Statistics, 1986, SAS Institute Inc., Cary, NC, U.S.A.).

RESULTS

Sequential events in smooth muscle cells during development

Based primarily on appearance and growth of contractile and cytoskeletal elements during development, sequential changes in smooth muscle cells can be observed. These sequential changes, which occurred during the first 28 days of development, can be classified into 7 stages. These stages have been identified as follows: myoblast proliferation stage; dense body appearance stage; thick filament appearance stage; dense body growth stage; muscle cell replication stage; IFB appearance stage; and appearance of adult type cells stage.

Myoblast proliferation stage (6-day embryos)

In the early embryo, smooth muscle cells are mainly in the form of undifferentiated myoblasts. The major event is active myoblast division. Chromosome condensation in nuclei and dividing nuclei are frequently observed (Figure 1). Nuclei occupy most of the cell space, and the cytoplasmic area is small. The cytoplasm contains endoplasmic reticula, Golgi bodies and numerous ribosomes. This indicates that these cells are capable of synthesizing proteins required in developing cells. Occasionally, a few filaments with diameters of 3 to 8 nm, presumably AFs, are visible in the cytoplasm. No CDBs,

however, can be observed at this stage. In addition, the contour of the cells is not smooth because of appendages protruding from the cell membrane. Myoblasts are seemingly loosely and irregularly arranged because various cell orientations can be observed in one section plane and intercellular spaces are large. As age increases, the contour of the cells becomes smoother, the intercellular spaces become smaller, and the arrangement of elongating cells becomes more parallel.

Dense body appearance stage (8- to 10-day embryos)

This stage is characterized by the first appearance of CDBs, which are closely associated with AFs and IFs in the cytoplasm. These CDBs can first be recognized at embryonic day 8 as small patches of increased electron density that consist of two types of longitudinal filaments, one with a diameter similar to AFs (7-8 nm) and a second type with a diameter similar to IFs (10-12 nm), and of cross-connecting filaments (CCFs) with an average diameter of 2-3 nm. The CCFs are perpendicular to the longitudinal axis of CDBs and apparently link the longitudinal filaments (Figure 2). Filaments that have the diameter of thick myosin-containing filaments are not present. Cytoplasmic filaments are irregularly arranged, i.e., the filaments are not parallel to the long axis of the cell as in adult smooth muscle cells. MADBs are frequently visible, but no connections between MADBs and cytoplasmic filaments are observed at day 8 (Figure 2). Occasionally, connections between cytoplasmic filaments (both AFs and IFs) and

some MADBs are visible by day 10 (Figure 3). As age increases, however, more MADBs are linked to cytoplasmic filaments, and the number of cytoplasmic filaments attached to individual MADBs also increases.

Thick filament appearance stage (12- to 14-day embryos)

Filaments with the diameter of thick filaments appear by day 12 (Figure 4). The other myofilaments begin to change their orientation from random to more nearly parallel to the long axis of cells when thick filaments appear. This arrangement becomes more apparent as age increases. Another important feature is that the assembly of CDBs is not synchronous (Figure 4). The majority of the CDBs in the cell is still in early stages of assembly. Some CDBs in the same cell, however, are nearly completely assembled. The assembling CDBs, compared with the completely assembled CDBs, are not only smaller but also less electron dense, so that the filaments inside these CDBs are still visible. On the other hand, filaments inside the more completely assembled CDBs are obscured by the increased electron density (Figure 4). This phenomenon of asynchronous assembly of CDBs is present at each age of tissue that we examined, but especially from embryonic day 8 through day 16. As age increases, however, completely assembled CDBs progressively become the dominant form.

Figure 1. A dividing nucleus in early telophase is clearly seen in this putative myoblast in embryonic day 6. N = nucleus, G = Golgi bodies, E = endoplasmic reticulum, Bar= 0.9 μm

Figure 2. CDBs (large arrows) are first recognized as patches of increased electron density in filament-rich zones in 8-day embryonic gizzard smooth muscle cell. Small arrow = MADBs, Bar = 0.45 μm. Inset: At higher magnification, IFs (large arrow), AFs (small arrow), and some CCFs (arrow heads) are visible in the developing CDB. Bar = 72 nm

Figure 3. Connections between some MADBs and cytoplasmic filaments (large arrow = IF, small arrow = AF) begin to be visible at embryonic day 10. Bar = 0.18 μm

Figure 4. Thick filaments (large arrow) begin to appear in 12-day embryonic gizzard smooth muscle cells. Note also that assembly of CDBs is not synchronized. Longitudinal filaments are still visible inside some CDBs (small arrows) but are obscured by the increased density in another CDB (double arrow). Bar = 0.22 μm.

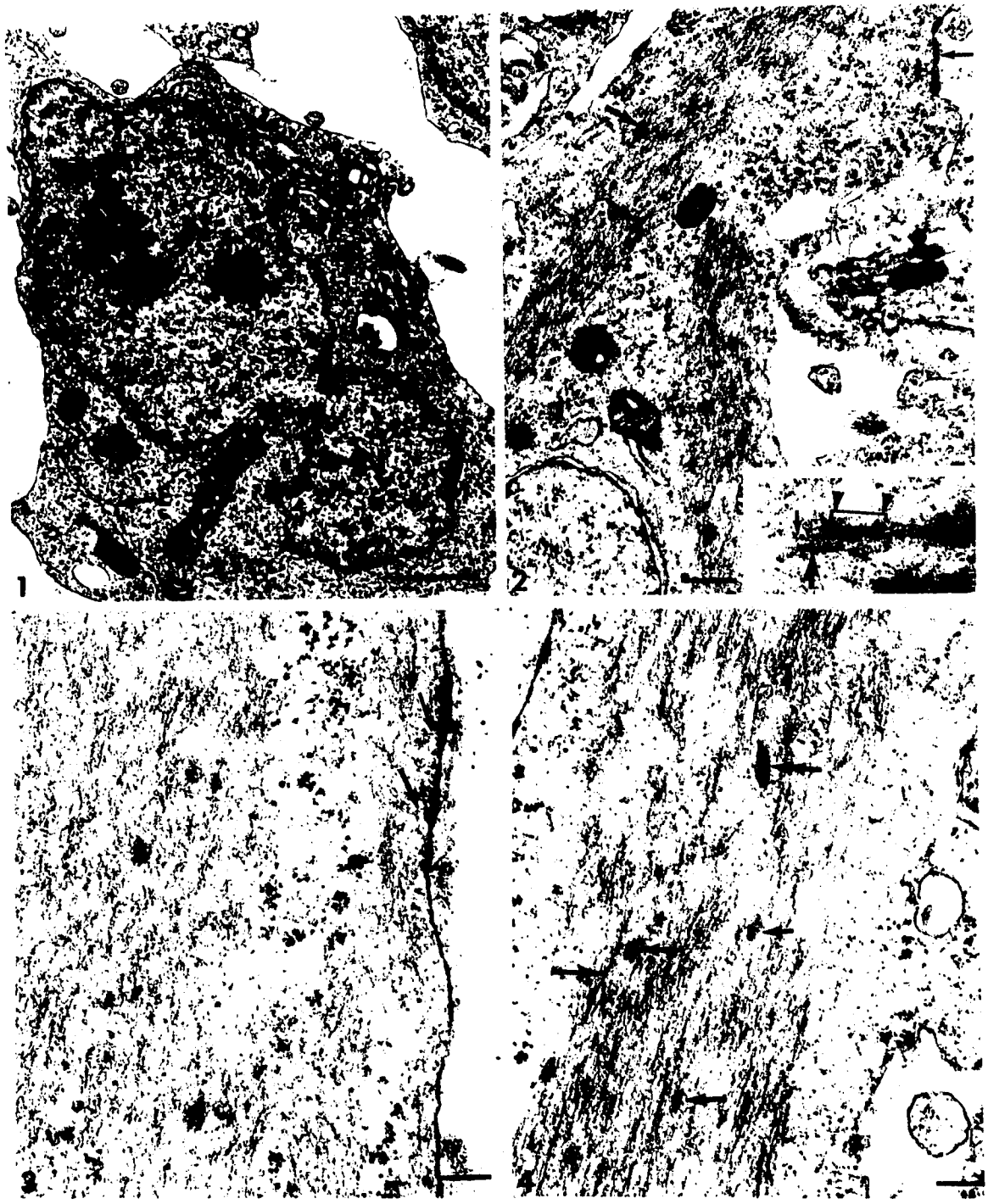

Dense body growth stage (16- to 18-day embryos)

The major event that characterizes this stage is the rapid increase in both number and size of dense bodies. The CDB number per μm^2 of myofilament area from embryonic day 8 to day 12 is nearly constant (Figure 5). After day 12, however, the number of CDBs increases as age increases, and this increase is most noticeable between day 12 and 16. This increase is also seen if sections from 16-day embryos (Figure 8) are compared with those from younger embryos. The rapid increase in CDB number that occurs between day 12 and 14 is not statistically significant ($P > 0.05$). This increase in CDB number continues at a similar rate between day 16 and 14 but, because the increase is relatively small, it, too, is not significant ($P > 0.05$). The CDB number in day 16 cells, however, is significantly ($P < 0.05$) greater when compared with those in day 8, 10 and 12. Although the number of MADBs in cells is very difficult to measure because it is almost impossible to visualize the entire cell surface, MADB numbers also increase at this time. This observation is consistent with the observations of Volberg et al. (1986) and Gabella (1989) who stated that MADBs are more numerous at embryonic day 16 than in previous ages.

Changes in length and diameter of CDBs with development are shown in Figure 6. The increase in the average apparent length of CDBs has a similar trend as the change in CDB number during development. This increase, however, is more evident after day 14.

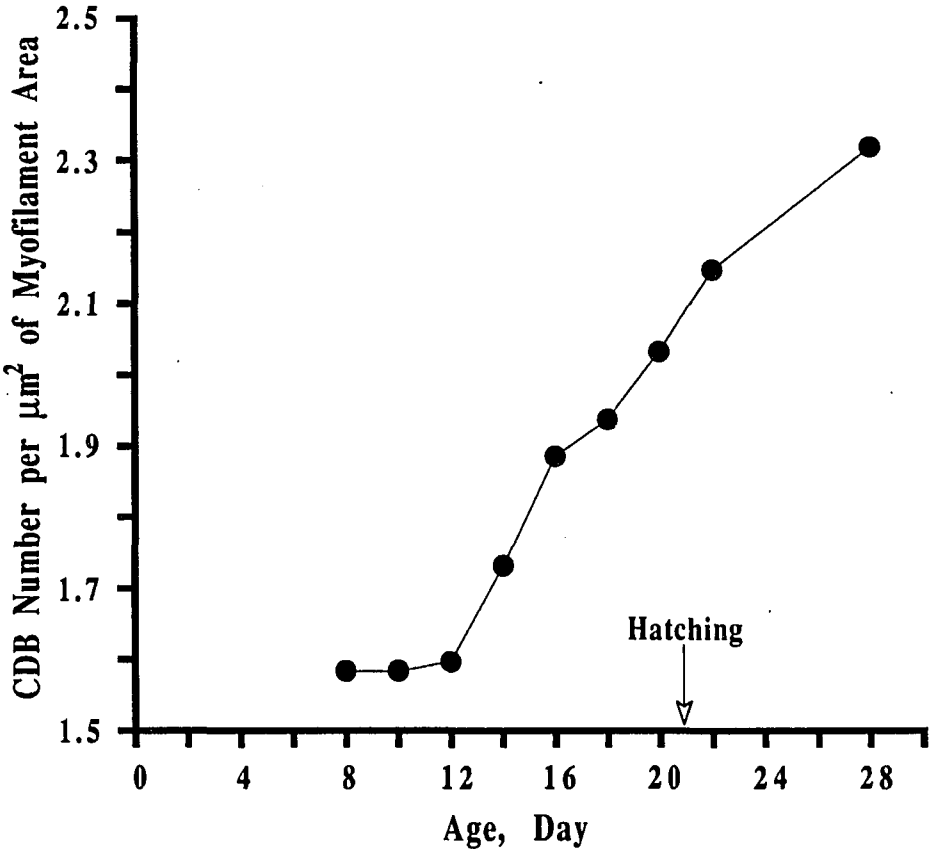

Figure 5. The change in CDB number per μm^2 myofilament area during development. Each point is the average of ten measurements. Standard error of means (S. E. M.) is 0.10

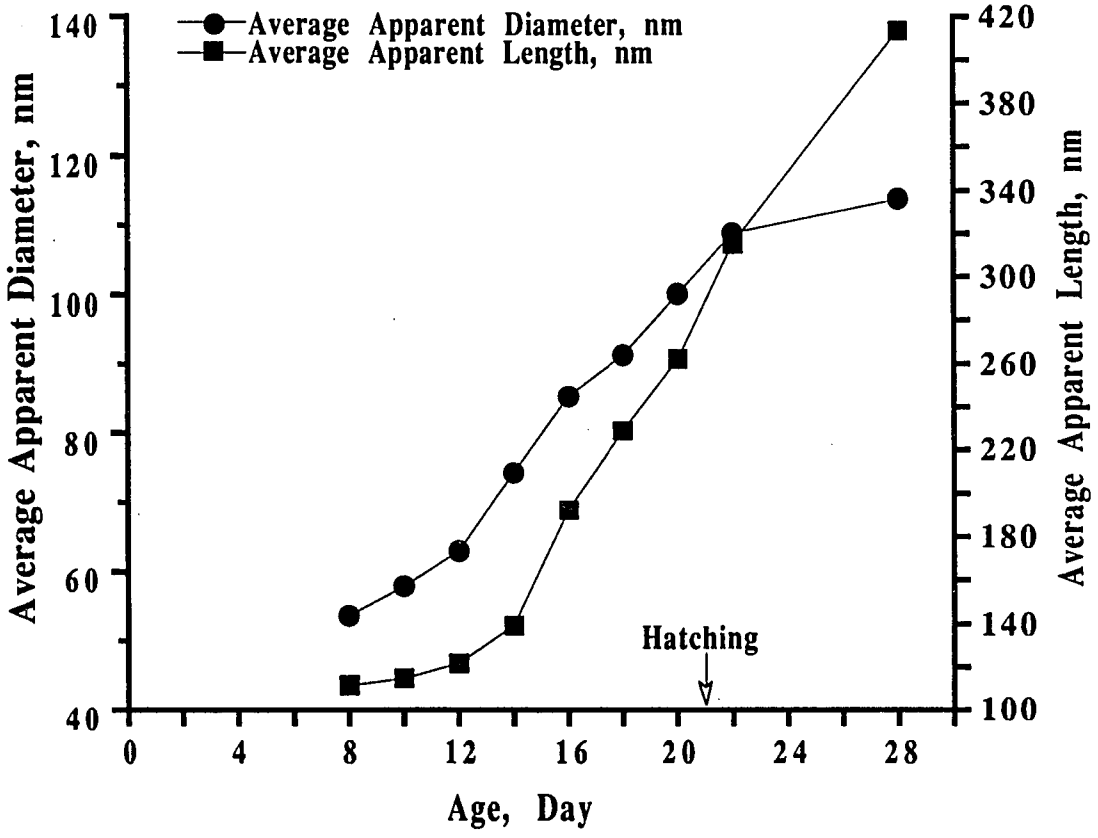

Figure 6. The changes in average apparent diameter and length of CDBs during development. Each point is the average of 100 measurements. Standard error of means (S. E. M.) for average apparent diameter is 2.84 and for average apparent length is 10.32

The average apparent diameter of CDBs, on the other hand, increases nearly linearly from day 8 until hatching and increases only slightly after hatching (Figure 6). The average apparent diameter and length of CDBs in day 16 cells are significantly ($P < 0.05$) larger than those in younger cells. In addition, the average apparent length and diameter of MADBs also increases as age increases (Figure 7). MADB length increases more rapidly from day 16 through day 28 than before day 16. The apparent diameter of MADBs increases linearly from day 8 to day 16, increases more rapidly between day 16 to day 18, and then increases more slowly after day 18. The size of MADBs in 18-day embryos is significantly ($P < 0.05$) larger than those in younger embryos. It is for these reasons that the embryonic age from day 16 to 18 is defined as the dense body growth stage.

The growth of CDBs in 16- to 18-day embryos appears to be mainly due to the addition of AFs, IFs and CCFs (Figure 8 inset). After day 16-18, however, the increase in size and electron density of CDBs occurs simultaneously, although partially assembled CDBs with low electron density sometimes can be found in older cells. The increase in electron density of the CDBs results in obscuring the filaments inside the CDBs. This phenomenon makes it difficult to distinguish the precise causes for increases in either size or electron density of the CDBs when both are increasing simultaneously. On the other hand, MADB size and electron density appear to increase simultaneously throughout development. This causes similar problems in determining which components are responsible for changes in MADB

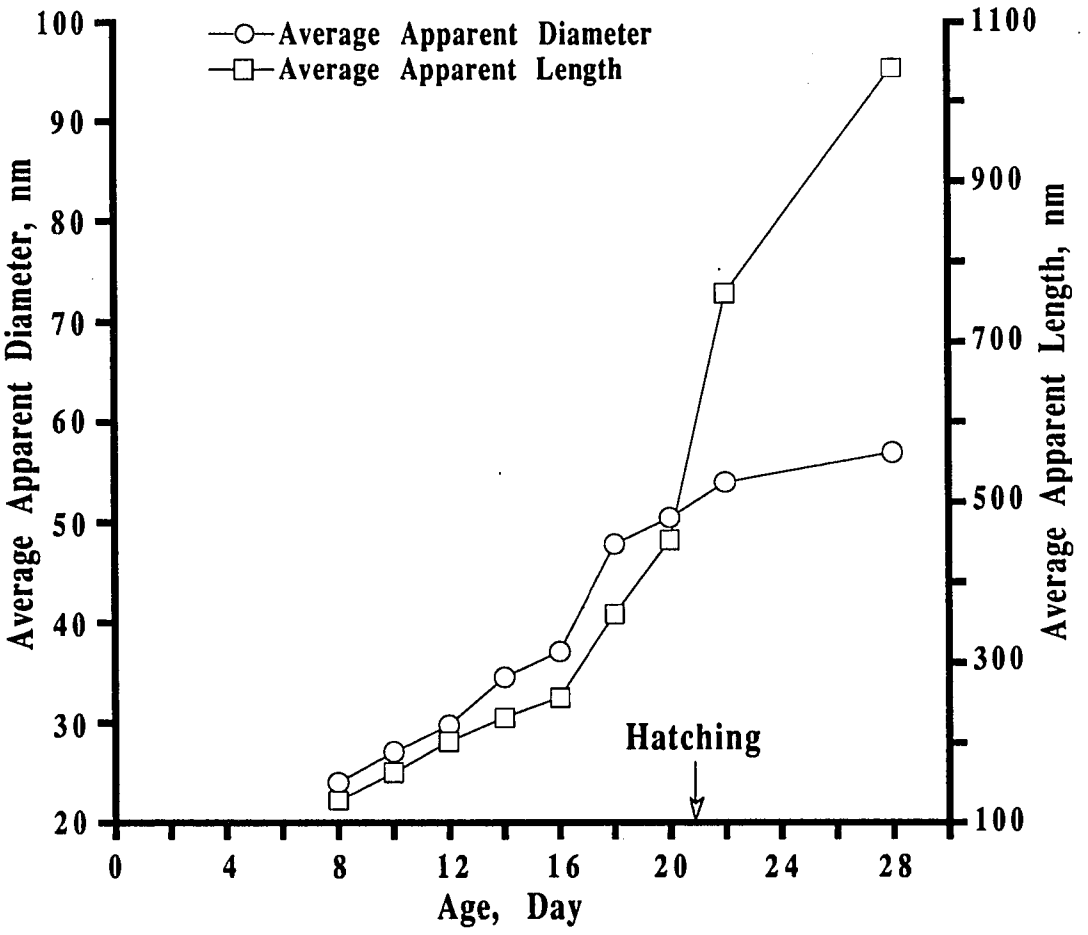

Figure 7. The changes in average apparent diameter and length of MADBs during development. Each point is the average of 50 measurements. Standard error of means (S. E. M.) for average apparent diameter is 1.77 and for average apparent length is 28.43

Figure 8. CDBs (arrows) and myofilaments are prominent in embryonic day 16 cells. Myofilaments are becoming oriented more nearly parallel to the cell axis. Bar = 0.96 μm. Inset: The increase in CDB size may be due to increased number of filaments inside the CDBs (cf. Fig. 2). IFs = large arrow, AFs = small arrow, and some CCFs = arrow head. Bar = 0.096 μm

Figure 9. Dividing smooth muscle cells are frequently visible in embryonic day 20 cells. Two daughter cells are connected by the constriction ring (double arrow). Myofilaments with CDBs in the cytoplasm (large arrow) and MADBs (small arrow) are evident in the two connected daughter cells. Bar = 1.92 μm

Figure 10. (a). Early stages in the formation of the IFB (bracket) are visible in 1-day post-hatch chicken gizzard cells and are characterized by small areas of irregularly arranged IFs (arrow). N = nucleus, Bar = 0.475 μm. (b). Labeling with anti-desmin and a protein A-gold complex shows that the IFB (bracket) contains desmin IFs. N = nucleus, Bar = 0.475 μm

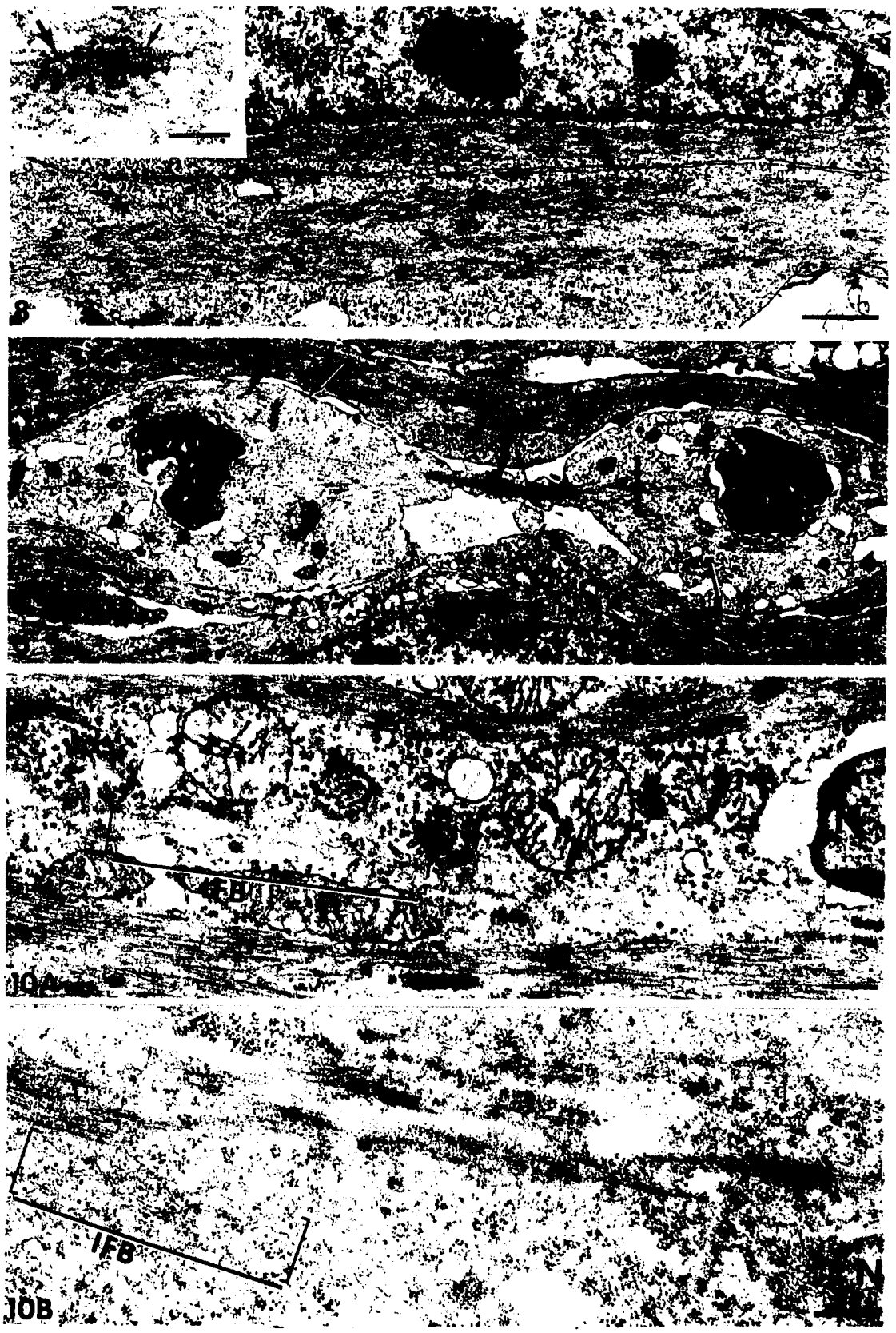
IFB
IFB

appearance.

Smooth muscle cell replication stage (20-day embryos)

Smooth muscle cells in mitosis are more frequently observed at day 20 (two embryos; one out of three to four blocks) compared with those seen in younger embryos (two to three embryos; one out of 12 to 16 blocks). Two dividing smooth muscle cells are joined by a characteristic structure referred to as a mid body or constriction ring (Figure 9). This constriction ring is responsible for the dumb-bell shape of dividing cells and contains densely packed microtubules which are remnants of the mitotic spindle. The myofilaments, CDBs, and MADBs are still recognizable in dividing cells. The maximal diameter of the ends of the cell is two to three times greater than the diameter of a non-dividing cell. The contractile elements from the mother cell appear to be evenly distributed to the daughter cells.

Axial intermediate filament bundle (IFB) appearance stage (1-day post-hatch chicken)

The axial IFB is a characteristic of intact adult chicken gizzard smooth muscle. This axial desmin-containing IFB was first identified both immunocytochemically and morphologically by Stromer and Bendayan (1988). The presence of the IFB, therefore, indicates that developing smooth muscle cells are reaching the late stages of

development. This axial bundle, in early stages of formation, is frequently found in the juxtanuclear region in 1-day post-hatch cells. This axial IFB is small and is irregularly arranged (Figure 10a). Immunogold labeling, with anti-desmin and a protein A-gold complex, demonstrates that this IFB contains desmin IFs (Figure 10b).

When compared with younger cells, CDBs have increased both their size and electron density. MADBs also are larger and frequently are connected to AFs and IFs. The orientation of myofilaments is more nearly parallel to the long axis of the cells. In general, the shape of the cell becomes smoother because of the disappearance of appendages which were evident in most younger cells.

Appearance of adult type cells stage (7-day post-hatch chicken)

A major change occurring between 1-day and 7-day post-hatch cells is the growth of the axial IFB. A segment of the IFB is clearly recognizable in the juxtanuclear region in either longitudinal (Figure 11a) or transverse (Figure 11b) cell profiles. The IFB is larger and more prominent than in one day old cells. Immunogold labeling, again, confirms that desmin-containing IFs are the major component of the IFB (Figure 11c). No thick filaments, AFs or CDBs can be detected inside the IFB.

The number and size of CDBs continue to increase. The larger the CDBs, in general, the greater the electron density (Figure 11a). A few assembling CDBs, with low electron density, however, are sometimes

Figure 11. The axial IFB is larger and contains more IFs in 7-day post-hatch cells than in 1-day post-hatch cells (cf. Fig. 10a). (a). A segment of the IFB (bracket) is visible in this longitudinal section. N = nucleus, Bar = 0.27 μm. (b). In cross-section, the triangular-shaped, juxtanuclear area occupied by the IFB contains only IFs. N = nucleus, Bar = 0.18 μm. (c). Labeling with anti-desmin and a protein A-gold complex confirms that the IFB contains desmin IFs. M = mitochondria, Bar = 0.27 μm


N
14B

visible in cells confirming that CDB formation continues through 7-day post-hatching. On the other hand, MADBs are prominent, and their average apparent length is over 1 μm. In addition, the myofilament arrangement, the cell shape, and the relationships of smooth muscle cells to each other are similar to those in adult gizzard cells as described by Gabella (1985; 1989).

DISCUSSION

The development of smooth muscle cells from 6-day embryonic to 7-day post-hatch chicken gizzard is a continuous process. Based primarily on the appearance and the growth of contractile and cytoskeletal elements, this process can be subdivided into 7 stages, namely, myoblast proliferation, dense body appearance, thick filament appearance, dense body growth, muscle cell replication, axial IFB appearance, and appearance of adult type cells. This process clearly suggests that the development of contractile elements and dense bodies occurs earlier than that of the major cytoskeletal element, the axial IFB. In addition, cells in each stage express a similar degree of maturity, an observation consistent with the work of Gabella (1989), who suggested that gizzard smooth muscle cell growth is synchronized.

Myoblast replication and dense body appearance

Myoblasts at embryonic day 6 rapidly divide and, based on the appearance of ribosomes, endoplasmic reticulum, and Golgi bodies, are potentially able to carry on active protein synthesis, a result consistent with the work of Bennett and Cobb (1969). This suggests that myoblasts are preparing themselves for differentiation into smooth muscle cells.

The first appearance of CDBs, which are closely associated with AFs and IFs at embryonic day 8, signals the beginning of the differentiation process as defined by Bennett and Cobb (1969) and by Bagby (1986). These CDBs, which average 54 nm in diameter and 112 nm in length (Figure 6), can be recognized as patches of increased electron density that consist of AFs, IFs, and CCFs as their filamentous backbone. High resolution immunoelectron microscope studies have identified the IFs inside CDBs as desmin-containing IFs and the CCFs as α-actinin-containing filaments (Chou et al., 1991). Our results confirm those from previous studies (Ashton et al., 1975; Bond and Somlyo, 1982; Small et al., 1986) that AFs are located inside CDBs. Two types of AFs, filamin-containing AFs and caldesmon-containing AFs, have been identified in adult cells. Filamin-containing AFs are present in the cytoskeletal domain, and caldesmon-containing AFs are in the contractile domain (Fürst et al., 1986; Small et al., 1986). It is not known what type of AF is present in CDBs and in the cytoplasm at this age.

Small MADBs that average 24 nm in diameter and 128 nm in length are also frequently observed at embryonic day 8. This result agrees with that of Bailey et al. (1984). Bennett and Cobb (1969), however, observed that MADBs were not found before day 10. The reason for this discrepancy is unknown but may be due to the use of an osmium tetroxide fixative by Bennett and Cobb.

Presence of thick filaments

We could identify thick filaments at embryonic day 12 but not earlier in the differentiation process. This result is in agreement with the work of Campbell et al. (1974). Other evidence has suggested that thick filaments are first present at day 9 (Bennett and Cobb, 1969). Both Bennett and Cobb (1969) and Campbell et al. (1974) agreed that the seemingly different time of thick filament appearance may be due to the fixative, osmium tetroxide only, used by Bennett and Cobb. Osmium tetroxide may induce aggregation of thin filaments and may have caused them to be incorrectly identified as thick filaments. Another possibility is that IFs may have been incorrectly identified as thick filaments as mentioned by Fay and Cooke (1973). In addition, evidence from two-dimensional gel electrophoresis and immunofluorescent staining demonstrates that myosin heavy chain can be detected as early as day 5 and that Ca^{2+}-dependent contractility of cells is detectable after day 7 (Hirai and Hirabayashi, 1983, 1986). Results from our laboratory indicate that myosin heavy chain are present at day 10 (Chou et al., 1991). It is, therefore, possible that thick filaments in early stages of assembly may have a diameter less than 16 nm, the average diameter of completely assembled thick filaments, or that the concentration of myosin heavy chain in cells before embryonic day 12 has not reached the critical concentration required for assembly of thick filaments.

Growth of dense bodies

In younger cells (< 16- to 18-day embryos), most CDBs are small and have low electron density. As age increases, CDBs become more numerous and larger, and their electron density increases. MADBs also become larger and more numerous. The increase in number of CDBs is most noticeable when smooth muscle from day 14-16 embryos is compared with tissue from younger embryos (Figure 5). The apparent length of CDBs begins to increase rapidly in 14-day embryos and continues at a similar rate through 7-day post-hatch (Figure 6). The apparent diameter of CDBs increases in a nearly linear fashion until 1-day post-hatch. This indicates that most CDB growth after hatching is due to an increase in CDB length. The increase in MADB size occurs slightly later. Both the apparent MADB diameter and length increase more rapidly after day 16 (Figure 7). A smaller rate of diameter increase occurs after day 18, and the rate remains nearly constant after hatching. The increase in MADB size is, therefore, due to an increase in the area of the sarcolemma occupied by MADBs which is seen in sections as an apparent increase in length of MADBs.

In the 7-day post-hatch chicken, the apparent diameter of CDBs is 114 nm and the length is 414 nm. This is a doubling in width and nearly a four-fold increase in length when compared with CDBs in 8-day embryos. A similar comparison of MADB size shows that, in the 7-day post-hatch chicken, MADBs average 57 nm wide and 1042 nm long, an increase of 2.5 times in width and an eight-fold increase in

length when compared with MADBs in 8-day embryos. The diameter of CDBs in adult smooth muscle has been reported to be about 100 nm but the length could not determined (Ashton et al., 1975; Bagby, 1983). Gabella (1984) found the MADB diameter was usually 100-400 nm but could be up to 1,000 nm in visceral muscle cells and that length was 2,000 nm or more. McGuffee et al. (1991), who used computer-assisted three-dimensional reconstruction of dense bodies in adult rabbit renal artery smooth muscle, reported that CDBs can be up to 2,000 nm long, 200 nm wide and 300-500 nm deep and that MADBs can be up to 3,500 nm long, 250 nm wide and 2,000 nm deep. When the smaller size of dense bodies that we observed in 7-day post-hatch cells is compared with those in the adult, it clearly suggests that growth of both classes of dense body continues from 7-day post-hatch until adult size occurs. Bennett and Cobb (1969) found that smooth muscle cells were not fully grown until 14 weeks after hatching. It is reasonable to speculate that dense body growth may continue over a similar interval.

Mitosis of smooth muscle

Differentiated smooth muscle cells are able to divide in situ without de-differentiation, i.e., the disappearance of contractile elements and filament attachment sites, a result consistent with the work of Bennett and Cobb (1969) and Gabella (1989). This property allows the number of differentiated cells to be increased efficiently.

In contrast, the mitotic process in cultured smooth muscle cells requires de-differentiation (Campbell, 1974). We observed the highest incidence of division in differentiated smooth muscle cells at embryonic day 20. This compares favorably with Gabella (1989), who indicated that the peak of active muscle cell division occurs at day 17-19. Gabella (1989) has suggested that the daughter cells can only grow in length at opposite ends as long as the daughter cells are connected end-to-end by the constriction ring during mitosis. It is not known if the dividing cells can contract.

Growth of the axial IFB

Since the IFB is a unique feature of adult cells, the presence of the axial IFB suggests that developing cells are reaching the later stages of development. The axial IFB in initial stages of assembly can first be recognized in 1-day post-hatch chicken gizzard cells. The IFB becomes larger and more prominent in 7-day post-hatch cells. No thick filaments, AFs or CDBs are present in this bundle. Immunogold labeling with anti-desmin and a protein A-gold complex demonstrated that the IFB mainly contains desmin IFs. These results are consistent with the results of Stromer and Bendayan (1988) in adult cells. Our results from both immunogold labeling with anti-desmin and structural approaches show that the axial IFB can also be observed in developing smooth muscle cells. Draeger et al. (1990) stated that bundles of IFs that labeled with anti-desmin could be observed with

light microscopy in some, but not all, isolated adult gizzard cells. It is possible that the IFB may be more difficult to detect in isolated cells, may be more difficult to see with the light microscope than with electron microscope, or may be different from the bundle observed by Draeger et al. (1990).

In conclusion, we have identified seven sequential stages that characterize avian smooth muscle development in situ. These stages are: myoblast proliferation; dense body appearance; thick filament appearance; dense body growth; muscle cell replication; IFB appearance; and adult type cell appearance. Although maturity of smooth muscle cells seems to be very similar at all ages that we investigated, the development of CDBs is not synchronized and many levels of assembly are evident in any given cell. Future studies hopefully will determine if this sequence of developmental events is a pattern for smooth muscle development from other sources.

ACKNOWLEDGEMENTS

We thank Mary Sue Mayes, Kim Ho, Janet Stephenson, and Jo Philips for excellent technical assistance. We also thank Dr. D. F. Cox from the Department of Satistics for assistance with the statistical analysis and Marylou Weigel for typing the manuscript. This research was supported, in part, by a grant from the American Heart Association, Iowa Affiliate. This is Journal Paper J- of the Iowa Agriculture and Home Economics Experiment Station, Ames, IA 50011, project 2921 and 2127.

REFERENCES

Ashton, F., A. V. Somlyo, and A. P. Somlyo. 1975. The contractile apparatus of vascular smooth muscle: Intermediate high voltage stereo electron microscopy. J. Mol. Biol. 98:17-29.

Bagby, R. M. 1983. Organization of contractile-cytoskeletal elements. Pages 1-84 in N. L. Stephens, ed. Biochemistry of smooth muscle. Vol. 1. CRC Press, Inc., Boca Raton, FL.

Bagby, R. M. 1986. Toward a comprehensive three-dimensional model of the contractile system of vertebrate smooth muscle cells. Int. Rev. Cytol. 105:67-128.

Bagby, R. M. 1990. Ultrastructure, cytochemistry, and organization of myofilaments in vertebrate smooth muscle. Pages 23-61 in P. M. Motta, ed. Ultrastructure of smooth muscle. Kluwer Acad. Publishers, Norwell, MA.

Bailey, C. G., R. M. Bagby, and M. C. Kreyling. 1984. Morphogenesis of the contractile system in embryonic chick gizzard smooth cells. I. Ultrastructure. J. Cell Biol. 99:29a. (Abstract).

Bennett, T., and J. L. S. Cobb. 1969. Studies of avian gizzard: the development of the gizzard and its innervation. Z. Zellforsch. Mikrosk. Anat. 98:599-621.

Bond, M., and A. V. Somlyo. 1982. Dense bodies and actin polarity in vertebrate smooth muscle. J. Cell Biol. 95:403-413.

Burnstock, G. 1981. Development of smooth muscle and its innervation. Pages 431-457 in E. Bülbring, A. F. Brading, A. W.

Jones, and T. Tomita, eds. Smooth muscle: An assessment of current knowledge. University of Texas Press, Austin, TX.

Campbell, G. R., Y. Uehara, G. Mark, and G. Burnstock. 1971. Fine structure of smooth muscle cells grown in tissue culture. J. Cell Biol. 49:21-34.

Campbell, G. R., J. H. Chamley, and G. Burnstock. 1974. Development of smooth muscle cells in tissue culture. J. Anat. 117:295-312.

Chamley-Campbell, J., G. R. Campbell, and R. Rose. 1979. The smooth muscle cell in culture. Physiol. Rev. 59:1-61.

Chou, R. R., M. H. Stromer, R. M. Robson, and T. W. Huiatt. 1991. Substructure of CDBs and change in content and distribution of desmin and α-actinin in developing smooth muscle cells. Submitted.

Draeger, A., E. H. K. Stelzer, M. Herzog, and J. V. Small. 1989. Unique geometry of actin-membrane anchorage sites in avian gizzard smooth muscle cells. J. Cell Sci. 94:703-711.

Draeger, A., W. B. Amos, M. Ikebe, and J. V. Small. 1990. The cytoskeletal and contractile apparatus of smooth muscle: Contraction bands and segmentation of the contractile elements. J. Cell Biol. 111:2463-2473.

Fay, F. S., and P. H. Cooke. 1973. Reversible disaggregation of myofilaments in vertebrate smooth muscle. J. Cell Biol. 56:399-411.

Fürst, D. O., R. A. Cross, J. De Mey, and J. V. Small. 1986. Caldesmon is an elongated, flexible molecule located in the actomyosin domains of smooth muscle. EMBO J. 5:251-257.

Gabella, G. 1981. Structure of smooth muscles. Pages 1-46 in E. Bülbring, A. F. Brading, A. W. Jones, and T. Tomita, eds. Smooth muscle: An assessment of current knowledge. University of Texas Press, Austin, TX.

Gabella, G. 1984. Structural apparatus for force transmission in smooth muscles. Physiol. Rev. 64:455-477.

Gabella, G. 1985. Chicken gizzard: The muscle, the tendon and their attachment. Anat. Embryol. 171:151-162.

Gabella, G. 1989. Development of smooth muscle: Ultrastructural study of the chick embryo gizzard. Anat. Embryol. 180:213-226.

Hirai, S., and T. Hirabayashi. 1983. Developmental change of protein constituents in chicken gizzards. Dev. Biol. 97:483-493.

Hirai, S., and T. Hirabayashi. 1986. Development of myofibrils in the gizzard of chicken embryos: Intracellular distribution of structural proteins and development of contractility. Cell Tissue Res. 243:487-493.

McGuffee, L. J., J. Mercure, and S. A. Little. 1991. Three-dimensional structure of dense bodies in rabbit renal artery smooth muscle. Anat. Rec. 229:499-504.

Small, J. V., D. O. Fürst, and J. De Mey. 1986. Localization of filamin in smooth muscle. J. Cell Biol. 102:210-220.

Somlyo, A. V., and C. Franzini-Armstrong. 1985. New views of smooth muscle structure using freezing, deep-etching and rotary shadowing. Experientia 41:841-856.

Stromer, M. H., and M. Bendayan. 1988. Arrangement of desmin intermediate filaments in smooth muscle cells as shown by high-resolution immunocytochemistry. Cell Motil. Cytoskeleton 11:117-125.

Stromer, M. H. 1990. Intermediate (10-nm) filaments in muscle. Pages 19-36 in R. D. Goldman, and P. M. Steinert, eds. Cellular and molecular biology of intermediate filaments. Plenum Publishing Corp., New York, NY.

Stromer, M. H., and M. Bendayan. 1990. Immunocytochemical identification of cytoskeletal linkages to smooth muscle cell nuclei and mitochondria. Cell Motil. Cytoskeleton 17:11-18.

Volberg, T., H. Sabanay, and B. Geiger. 1986. Spatial and temporal relationships between vinculin and talin in the developing chicken gizzard smooth muscle. Differentiation 32:34-43.

SECTION III. SUBSTRUCTURE OF CYTOPLASMIC DENSE BODIES AND CHANGES IN CONTENT AND DISTRIBUTION OF DESMIN AND α-ACTININ IN DEVELOPING SMOOTH MUSCLE CELLS

Substructure of cytoplasmic dense bodies and changes in content and distribution of desmin and α-actinin in developing smooth muscle cells

Rong-Ghi R. Chou, Marvin H. Stromer,
Richard M. Robson and Ted W. Huiatt

Muscle Biology Group
Iowa State University, Ames, Iowa 50011

All authors are with Iowa State University, Ames, Iowa 50011. Author Chou is with the Department of Food Science and Human Nutrition. Authors Stromer, Robson, and Huiatt are with the Muscle Biology Group, Departments of Animal Science and of Biochemistry and Biophysics.

ABSTRACT

Substructure of cytoplasmic dense bodies (CDBs) and changes in the distribution of desmin and α-actinin during development of smooth muscle were studied in samples taken from gizzards of 10- and 16-day embryos and from 1- and 7-day post-hatch chickens. SDS-PAGE showed that the amount of major muscle proteins (myosin heavy chain, α-actinin, desmin, and actin) increased as age increased. Immunogold labeling with polyclonal anti-desmin and a protein A-gold (15 nm) complex indicated that the amount of desmin intermediate filaments (IFs) increased as age increased. The labeling with anti-desmin in embryonic day 10 and 16 cells was located both at the periphery of the myofilament compartment and on or close to desmin IFs inside CDBs. Stereo pairs from unlabeled samples clearly indicated that IFs insert into the CDBs in 16-day embryonic cells. After hatching, gold particles were gradually confined to the perimeters of CDBs. This suggests that the antigenic sites on desmin IFs inside the CDBs are covered by the material responsible for the increasing electron density of the CDBs as age increased. Seven days after hatching, gold particles heavily labeled the axial intermediate filament bundle (IFB). Immunogold labeling with monoclonal anti-α-actinin and a goat anti-mouse IgM-gold (10 nm) complex indicated that the amount of α-actinin increased as age increased. The α-actinin was mainly located on the cross-connecting filaments (CCFs) (average diameter of 2-3 nm) inside the CDBs and sometimes on membrane-

associated dense bodies (MADBs). Actin filaments, desmin IFs and α-actinin-containing CCFs, therefore, are the principal components of CDB substructure. A proposed model for CDB assembly and the relationship between CDBs and the IFB are also presented.

INTRODUCTION

Adult or mature smooth muscle cells contain thick filaments, actin filaments (AFs), dense bodies, and cytoskeletal intermediate filaments (IFs). Thick filaments are side polar with 14-nm axial repeat of cross-bridge projections (Cooke et al., 1989). Two types of AFs, filamin-containing AFs and caldesmon-containing AFs, are present in adult cells. Filamin-containing AFs are present in the cytoskeletal domain, and caldesmon-containing AFs are in the contractile domain (Fürst et al., 1986; Small et al., 1986).

Two types of dense bodies are present in smooth muscle cells. Membrane-associated dense bodies (MADBs) (Bagby, 1983) or dense bands (Gabella, 1981) are located at the thickened areas where the sarcolemma is very electron dense and free of caveolae. Both AFs (Ashton et al., 1975; Small and Sobieszek, 1980; Bagby, 1983; Gabella, 1985; Somlyo and Franzini-Armstrong, 1985) and IFs (Cooke and Fay, 1972; Small and Sobieszek, 1980; Bagby, 1983; Gabella, 1985; Somlyo and Franzini-Armstrong, 1985) are associated with the cytoplasmic side of the MADBs.

Another type of dense body, cytoplasmic dense bodies (CDBs), is located in the cytoplasm (Gabella, 1981; Bagby, 1983). AFs are inserted into, but do not penetrate through the CDBs (Ashton et al., 1975) and have opposite polarity at the two ends of the CDBs, identical to the polarity of AFs at the Z-lines in skeletal muscle (Bond and Somlyo, 1982). The arrangement of CDBs is in a chain-like fashion

(Bond and Somlyo, 1982; Fay et al., 1983). The distance between two successive CDBs decreases during smooth muscle contraction (Fay et al., 1983). Moreover, Kargacin et al. (1989) found that, during contraction, some longitudinally aligned dense bodies move rapidly toward each other while others, not longitudinally aligned, move little within a cell. This observation suggested that the dense bodies in semirigid groups may serve as a structural connection between contractile and cytoskeletal elements (Kargacin et al., 1989). This observation was confirmed by McGuffee et al. (1991), who presented a three-dimensional structure of CDBs and MADBs in artery smooth muscle. Draeger et al. (1990) also proposed that CDBs, attached to both AFs from contractile units and IFs, may serve as coupling elements between the cytoskeletal and contractile systems. It is generally agreed that CDBs contain actin (Small et al., 1986) and α-actinin (Schollmeyer et al,. 1976; Bagby, 1986; 1990). It is unclear, however, whether desmin (a major IF protein in smooth muscle) is one of the components of CDBs. Furthermore, the linkage between CDBs and IFs is also unknown.

Desmin-containing IFs are abundant in smooth muscle. The desmin content of gizzard smooth muscle is typically about 8% of the myofibrillar proteins (Huiatt et al., 1980). IFs sometimes tangentially contact CDBs or may be obliquely oriented between adjacent CDBs in vascular smooth muscle (Ashton et al., 1975; Bond and Somlyo, 1982; Garfield and Somlyo, 1985). On the other hand, IFs also terminate at or near MADBs (Somlyo and Franzini-Armstrong, 1985). In general,

however, IFs in the cytoplasm appear to concentrate near the periphery of CDBs (Bagby, 1983).

Recently, Stromer and Bendayan (1988) identified an axial intermediate filament bundle (IFB) that is present in intact adult chicken gizzard smooth muscle cells. The IFs from this IFB also directly link the nucleus and some of the mitochondria at the poles of the nucleus (Stromer and Bendayan, 1990). It was suggested, therefore, that the IFB may couple with other IFs remaining in the cytoplasm to form an intact cytoskeletal system to retain the positions of cellular organelles during contraction and relaxation (Stromer and Bendayan, 1988, 1990; Stromer, 1990).

The structural arrangement and the function of IFs and CDBs in smooth muscle cells, however, are still unclear (see reviews in Bagby, 1983; 1986; 1990). The major problem has been to identify the specific relationships between CDBs and IFs. A fundamental question is whether IFs penetrate into and contribute to the substructures of the CDB. It is very difficult to test this question in adult cells because of the great electron density of the CDBs. Structural studies of developing smooth muscle cells (Chou et al., 1991) indicated, however, that the addition of electron density to the CDBs occurs in the late stages of CDB assembly. The purpose of this study, therefore, was to investigate the distribution of desmin IFs and α-actinin and to identify the relationship between desmin IFs and CDBs by antibody localization studies in developing smooth muscle cells. Several

possible steps in CDB assembly are delineated, and the relationship between CDBs and IFB is further clarified.

MATERIALS AND METHODS

SDS-PAGE and immunoblotting

Smooth muscle samples were taken from gizzards of 10- and 16-day embryos and 1- and 7-day post-hatch chickens. Tissue was dissolved and prepared for SDS-PAGE by the method of Huiatt et al. (1980). Protein concentrations were determined by the biuret method (Robson et al., 1968). Electrophoresis was performed on 10% polyacrylamide gels (weight ratio of acrylamide to methylenebisacrylamide is 37.5 to 1) according to the methods of Laemmli (1970). The same amount of protein (70 μg for Coomassie blue stained gels and 45 μg for transblotting) from each sample was loaded on gels. After electrophoresis, proteins were transferred to a nitrocellulose membrane (Towbin et al., 1979). Overall protein staining of nitrocellulose blots by the colloidal gold method and the silver enhanced immunogold staining method with anti-desmin (1:100) and anti-α-actinin (1:20,000) were both done by the method of Moeremans et al. (1989). Avian desmin, isolated and purified by the method of Huiatt et al. (1980), was used as standard. Purified chicken gizzard α-actinin and bovine lens vimentin were also used as standards and were purchased from Sigma Chemical Company (St. Louis, MO, U.S.A.).

Tissue preparations for immunoelectron microscopy

Smooth muscle samples for immunoelectron microscopy were taken from gizzards of 10- and 16-day embryos and from 1- and 7-day post-hatch chickens. Duplicate samples were used for each age. Tissue preparations were done by the methods of Stromer and Bendayan (1988) and Bendayan (1984). In general, thin strips of tissue were cut parallel to the cell axis and were isometrically clamped before the ends of the strips were cut. Tissue from 10 day embryos was not clamped because of the relatively small gizzard size. Samples were fixed with 2% paraformaldehyde, 1.5% glutaraldehyde, 2 mM $MgCl_2$, and 2 mM $CaCl_2$ in Millonig's phosphate buffer, pH 7.2, for 2.5 hr at 2°C. After fixation, the samples were rinsed and immersed in 0.15 M glycine to block free aldehyde groups. Dehydration in graded methanol, infiltration, and embedding in Lowicryl K4M resin, and polymerization followed the method of Bendayan (1984).

Antibody labeling

Polyclonal antibodies produced in a rabbit to avian gizzard desmin were used at 1:20 dilution on tissue sections prepared for immunoelectron microscopy. The specificity of this anti-serum has been shown previously (Stromer et al., 1981; Stromer and Bendayan, 1988) and was also confirmed by immunoblotting in this study.

Monoclonal antibodies (IgM class) to α-actinin were purchased from Sigma Chemical Company (St. Louis, MO, U.S.A.) and used at 1:10,000 dilution on tissue sections. The specificity of this monoclonal antibody was determined by immunoblotting. The protein A-gold complex was produced by the method of Bendayan (1984), and the goat anti-mouse IgM-gold complex was purchased from Sigma Chemical Company. Labeling experiments both with polyclonal anti-desmin and a protein A-gold (15 nm) complex and with monoclonal anti-α-actinin and a goat anti-mouse IgM-gold (10 nm) complex were performed as described in Stromer and Bendayan (1988) and in Bendayan (1984). Controls, either pre-absorption of each anti-sera with its respective antigen or substituting phosphate buffered saline for the anti-sera, showed that labeling was reduced to background level. At least ten blocks were randomly selected from each sample for thin sectioning. Sections were examined at 80 kV in a JEOL JEM-100CXII electron microscope. Images were recorded on Kodak SO-163 electron image film.

RESULTS

Changes in major muscle proteins

Based on SDS-PAGE results (Figure 1a) and overall protein staining of blots (Figure 1b), bands with the relative mobilities of myosin heavy chain, α-actinin, desmin, actin, and tropomyosin are detectable in 10-day embryonic gizzards. The intensity of the myosin heavy chain, desmin and actin bands increases rapidly as age increases. The intensity of the α-actinin and tropomyosin bands, however, does not increase rapidly until hatching. The desmin and α–actinin bands were identified by labeling with anti-desmin (Figure 1c) and anti-α–actinin (Figure 1d) on blots, respectively, and each of the antibodies is highly specific. Myosin heavy chain, actin, and tropomyosin were identified by comparing their mobilities with those of the standard proteins (avian α–actinin, mammalian vimentin and avian desmin).

Distribution of desmin IFs

Anti-desmin produces a relatively low level of highly specific labeling on cells from 10 day embryos (Figure 2). Many gold particles are near the peripheral areas of the filament-rich zones, but others are in the interior of the filament-containing zone (Figure 2a). The labeling in the interior of the filament-containing zone is frequently

Figure 1. Change in major muscle proteins from 10 and 16 day old embryos and 1- and 7-day post-hatch cells. Content of myosin heavy chain (M), α-actinin (αA), desmin (D), actin (A), and tropomyosin (T) increases as age increases. (a). Coomassie blue stained gel. (b). Overall protein staining of blot. (c). Immunoblot with anti-α-actinin. (d). Immunoblot with anti-desmin. Protein loads for each lane were 70 μg for the Coomassie blue stained gel and 45 μg for the transblot. In each gel and blot, lane 1 is standard proteins, lane 2 is 10-day embryonic gizzard, lane 3 is 16-day embryonic gizzard, lane 4 is 1-day post-hatch chicken gizzard, and lane 5 is 7-day post-hatch chicken gizzard.

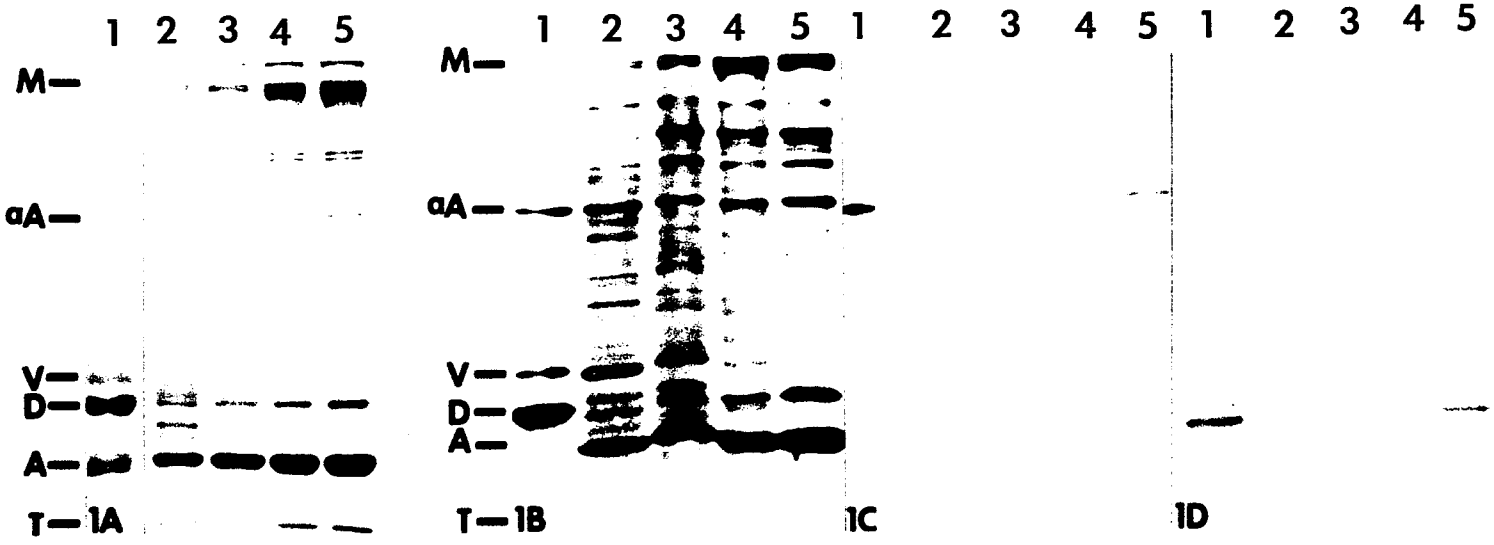
1 2 3 4 5
M
αA
V
D
A
T
1A
1 2 3 4 5
M
αA
V
D
A
T
1B
1C
1 2 3 4 5
1D

Figure 2. (a). The number of desmin IFs in embryonic day 10 cells is very low, and they are mainly located at the periphery of the myofilament compartment. Bar = 0.46 μm. (b). Some gold particles (arrows) also frequently label on or close to the CDBs inside this compartment. Bar = 0.23 μm

Figure 3. (a). Distribution of desmin IF in embryonic day 16 cells is mainly confined to the periphery of well-arranged myofilaments. Labeled CDBs (large arrows) appear to be arranged in a chain-like fashion. Some gold particles are located at or close to MADBs (small arrow). Bar = 0.46 μm. (b). At higher magnification, gold particles also heavily label the desmin IFs inside the CDBs. The desmin IFs are arranged in a side-by-side array inside the CDBs. Bar = 0.092 μm.

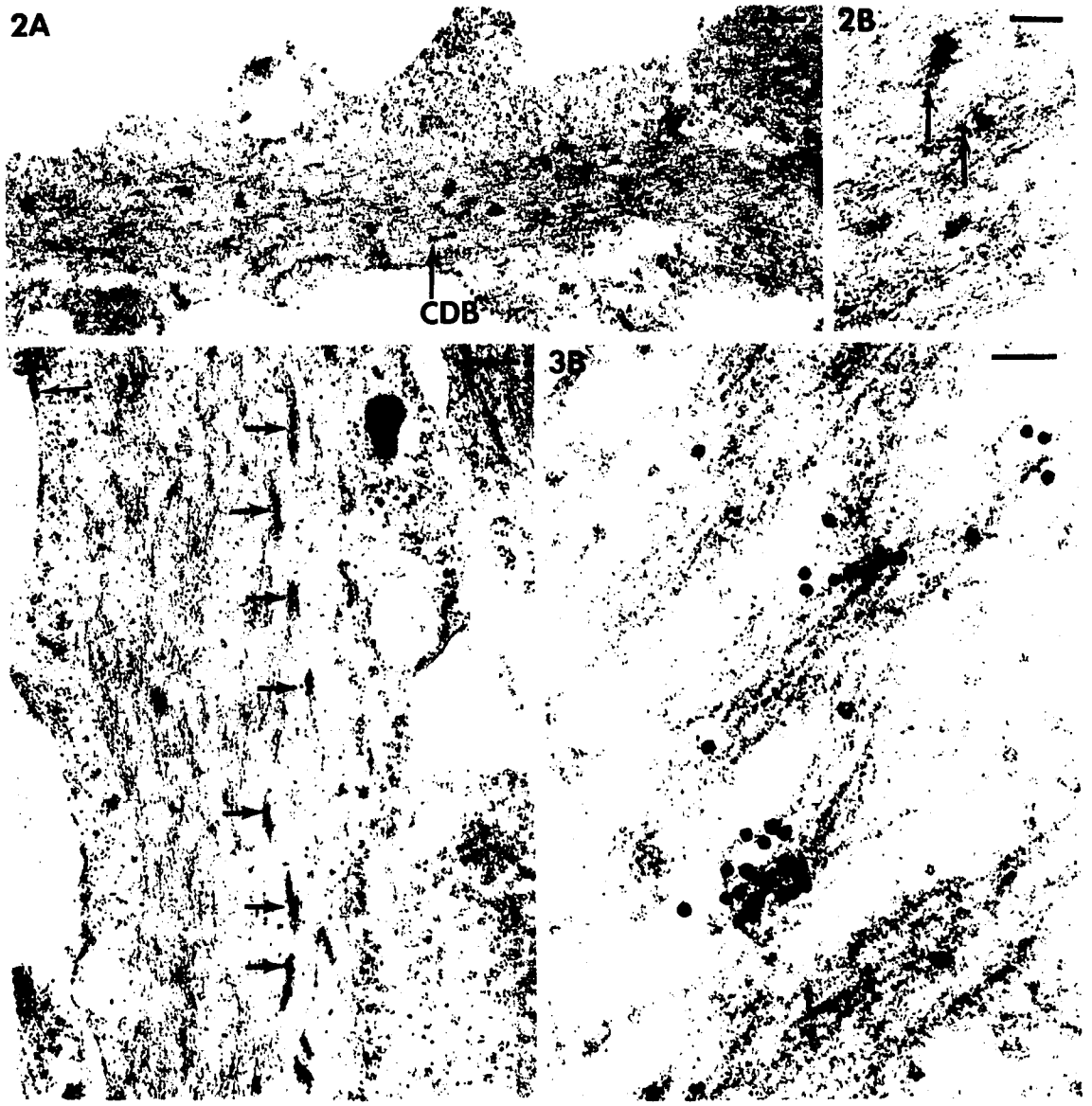
2A
CDB
2B
3A
3B

associated with small areas of increased electron density (Figure 2b). We have identified these areas as putative CDBs in the early stages of formation. Occasionally, a few gold particles label close to the cell membrane.

The labeling intensity with anti-desmin increases in 16-day embryonic smooth muscle cells. More gold particles are located on peripheral areas of the myofilament compartment or are associated with the chain-like arrays of CDBs (large arrows) (Figure 3a). Another major location of gold particles is on or close to the IFs inside the forming CDBs. These forming CDBs are characterized by side-by-side arrays of IFs that label heavily with anti-desmin (Figure 3b). In addition, some gold particles are located on or close to MADBs (small arrow) (Figure 3a). A stereo pair of a representative CDB in an unlabeled 16-day embryonic cell shows that an IF (arrows) penetrates into, but not through the interior of the CDB (Figure 4).

One-day post-hatch samples bind still more anti-desmin and the location of the label has shifted to the interior of the myofilament compartment (Figure 5). Within the myofilament compartment, more of the label is located at the perimeter of CDBs (arrows) rather than on the CDBs per se (c.f. Figure 3). The electron density of CDBs in 1-day post-hatch cells is greater than in younger cells. The increase in CDB density is associated with a diminution of desmin labeling directly on the CDB and an increase in perimeter (often at the ends) labeling. By 7-day post-hatch, the labeling pattern with anti-desmin is very similar to that seen in adult smooth muscle.

Figure 4. A stereo pair of a representative CDB in an unlabeled embryonic day 16 cell. A desmin IF is marked by arrows and penetrates into the interior of the CDB. Half tilt angle = 19°. Section thickness ≅ 150 nm, Bar = 50 nm.

Figure 5. Desmin IFs are not limited in the periphery of well-arranged myofilaments in 1-day post-hatch cells. Gold particles are more confined to the perimeter of CDBs (arrows) as age increases to 1-day post-hatching. Bar = 0.5 μm.

Figure 6. (a). Desmin IFs are concentrated in the axial IFB (arrow) in 7-day post-hatch cells. N = nucleus, Bar = 0.5 μm. (b). Gold particles near CDBs are confined to the perimeter of CDBs (large arrow). Gold particles also label on or close to MADBs (small arrow). Bar = 0.5 μm.


4


5


6A
IFB
N

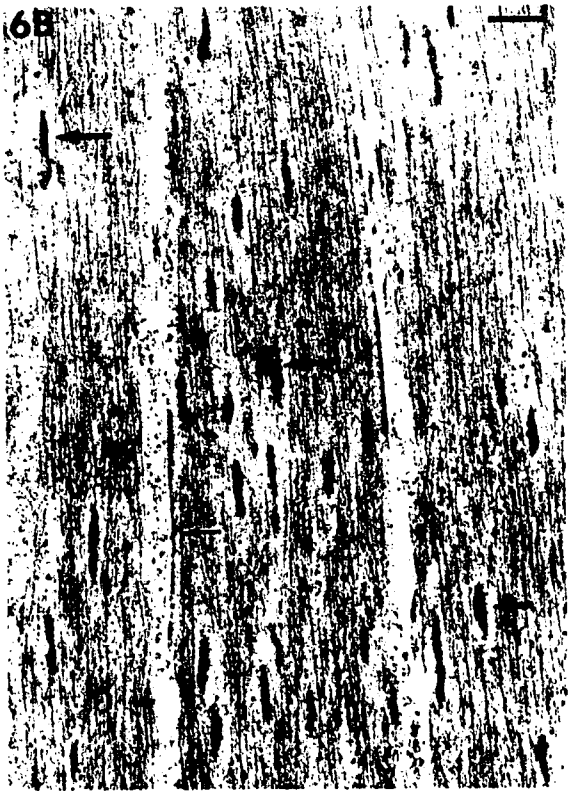
6B

Cells of this age often contain a well-formed IFB (arrows) that is heavily labeled with anti-desmin (Figure 6a). This indicates that, at 7-day post-hatch,desmin-containing IFs are the key component of the IFB. In another section, from a 7-day post-hatch sample, the plane of section does not include the IFB but shows the labeling at the perimeter of the CDBs (large arrows) (Figure 6b). In addition, gold particles also frequently label MADBs or desmin IFs which extend to MADBs (small arrow) (Figure 6b).

Distribution of α–actinin

Labeling experiments with monoclonal anti-α–actinin and goat anti-mouse IgM-gold complex demonstrate that most of the gold particles are located on the CDBs throughout development (Figure 7a-d) and that gold particles are sometimes present on MADBs (small arrow in Figure 7d). The intensity of labeling on the CDBs is similar in 10- and 16-day embryos, increases in 1-day post-hatch cells and further increases in 7-day post-hatch cells. In general, the larger the CDBs, the more heavily they are labeled (Figure 7d). Anti-α–actinin labeling of a developing CDB in a 7-day post-hatch cell shows that the label is located on the cross-connecting filaments (CCFs) (Figure 7d inset). These CCFs have an average diameter of 2-3 nm and are perpendicular to the AFs and IFs inside the CDB. This result suggests that α–actinin is one of the components of the CCFs inside CDBs.

Figure 7. Most anti-α-actinin labeling is on CDBs (large arrows) throughout development, but gold particles are sometimes also located on MADBs (small arrow). (a). embryonic day 10 cell. Bar = 0.435 μm, (b). embryonic day 16 cell. Bar = 0.174 μm, (c). 1-day post-hatch cell. Bar = 0.22 μm, and (d). 7-day post-hatch cell. Bar = 0.174 μm. Higher magnification inset in (d) shows that the gold particles are located on the CCFs (arrow head) inside a developing CDB in a 7-day post-hatch cell. Bar = 0.087 μm.

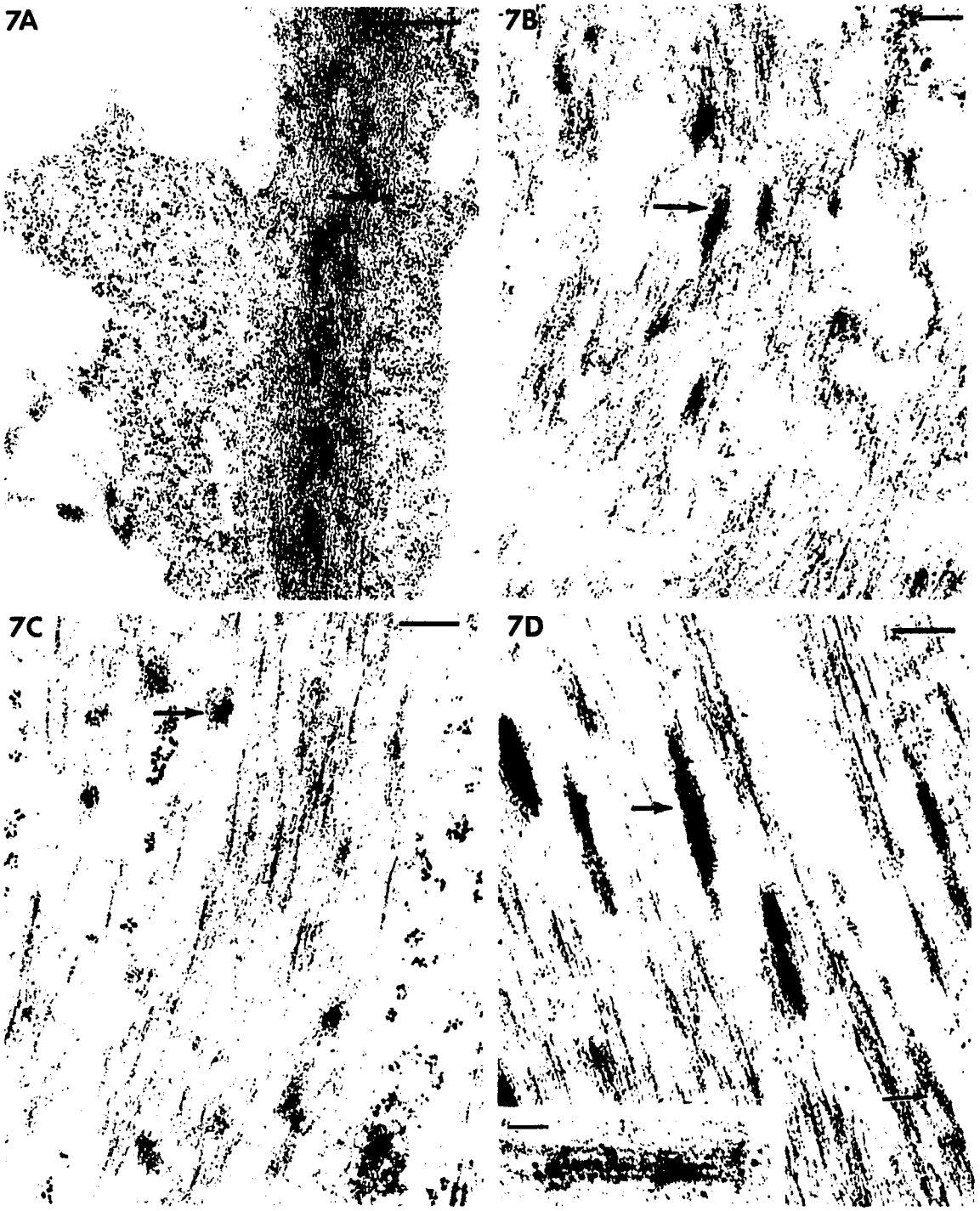
7A
7B
7C
7D

DISCUSSION

Changes in muscle proteins during development

Changes in content of several muscle proteins in developing smooth muscle cells were studied in developing gizzards from 10-day embryos through 7-days post-hatch chicks with both biochemical and immunochemical approaches. Based on SDS-PAGE and immunoblotting, myosin heavy chain, α–actinin, desmin, actin, and tropomyosin are detectable in gizzards from 10-day embryos, and the amount of the individual proteins increases as age increases. This result is consistent with that of Hirai and Hirabayashi (1983), who also found comparable increases in these proteins. The increases in amount of these proteins may be due to an increase in the number of muscle cells relative to other cell types or to an increase in myofibrillar protein content of individual muscle cells or both. Gabella (1989) indicated that the weight of gizzard increases from 60 mg at embryonic day 10 to 2,000 mg at seven days post-hatching and that this increase in weight is mainly due to an increase in cell number. It is also possible that the increase in the amount of desmin after hatching, which is consistent with the results of Cossette and Vincent (1991), may be due to the formation and enlargement of the axial IFB in the cells.

Distribution of desmin IFs during development

Immunogold labeling with anti-desmin and a protein A-gold complex shows that the amount of desmin-containing IFs increases as age increases, a result that is consistent with our biochemical results. In 10- and 16-day embryos, gold particles are located both at the periphery of the myofilament compartment and on, or close to, the IFs inside the CDBs. After hatching, additional gold particles are present inside the myofilament compartment. It is unclear whether the increase in labeling in this compartment is due only to the growth of the myofilaments. Gabella (1989) stated that the area of the myofilament compartment increases from 25% of cell volume at embryonic day 10 to 75% after hatching. It is, therefore, possible that the myofilament compartment expands and surrounds those IFs which were originally at the periphery of the compartment. It is also possible that the formation of additional CDBs in the myofilament compartment causes a reorganization of IFs in this compartment. In addition to the anti-desmin labeling associated with the perimeter of maturing CDBs, as the IFB forms and enlarges, it also is heavily labeled. This suggests that the principal IF type in the IFB, which first appears in 1-day post-hatch cells (Chou et al., 1991), is desmin.

Distribution of α–actinin during development

At all tissue ages examined in this study, anti-α–actinin labeling is constantly located on CDBs. If the filamentous substructure of the CDB is still visible, the gold label is mainly located on the CCFs. These CCFs have an average diameter of 2-3 nm (Chou et al., 1991) which is similar to the diameter of the α–actinin molecule (Suzuki et al., 1976). MADBs are not labeled as intensely or frequently as CDBs. These results are consistent with the widely reported presence of α–actinin in both CDBs and MADBs (Schollmeyer et al., 1976; Bagby, 1983; 1986; 1990; Fay et al., 1983; Small, 1985; Lemanski et al., 1985; Fujimoto and Ogawa, 1988). Based on experiments described but not shown, however, Draeger et al. (1990) stated that their polyclonal α–actinin stains only CDBs. The reason for the different levels of MADB labeling by different anti-α–actinin preparations is unknown. The properties of the antibodies can vary, and different sample preparations may have altered the epitopes needed for recognition by the antibody.

Anti-α–actinin labeling on CDBs is similar in 10- and 16-day embryos, increases in 1-day post-hatch cells and further increases in 7-day post-hatch cells. This result is consistent with our SDS-PAGE and immunoblotting data. In general, the larger the CDB, the more gold particles there are on the CDB. Increased electron density of CDBs is not necessarily associated with greater labeling. It is possible that the material responsible for the greater electron density obscured the

epitopes on the CDBs required for recognition by this monoclonal antibody.

Substructure of CDBs

Stereo pairs and labeling experiments with anti-desmin and a protein A-gold complex at embryonic day 16 demonstrate that desmin-containing IFs are one of the backbone filaments inside the CDBs in intact embryonic gizzard smooth muscle cells. This conclusion is consistent with the observations of Uehara et al. (1971), who studied the structures of cultured embryonic gizzard smooth muscle cells and suggested that the IFs compose the CDB backbones in cultured cells. Campbell et al. (1971) also observed that IFs are associated with the ends of CDBs, appeared to emanate from inside the CDBs and could have a role in forming the CDB backbone.

There are other reports that IFs are only laterally associated with CDBs, loop tangentially near CDBs, or are obliquely arranged between CDBs in adult vascular smooth muscle (Ashton et al., 1975; Bond and Somlyo, 1982; Garfield and Somlyo, 1985; Bagby 1990). In isolated CDB-IF fractions from 2-3 month old chicken gizzards (Tsukita et al., 1983), IF are reported to be attached laterally to CDBs. It is possible that the isolation procedure may have altered the IF-CDB relationship and/or may have partially extracted the CDB and thus exposed the IFs inside. In adult taenia coli, Cooke and Fay (1972) suggested that the IFs are directly attached to the CDBs. The major problem in

interpreting these results from laboratories that worked with adult tissues is the great electron density of the CDBs, which masks the filament backbone inside the CDBs. In embryonic cells, however, the assembly of CDBs is not synchronized so various stages of assembly can readily be studied. The interior filaments of CDBs, are frequently recognizable between the dense body appearance stage (embryonic day 8) and the dense body growth stage (embryonic day 16). The increase in CDB electron density mainly occurs at the late stages of development, approximately after embryonic day 16-18 (Chou et al., 1991).

Anti-desmin and protein A-gold labeling clearly demonstrate that gold particles are frequently located on the desmin IFs inside CDBs in 16-day embryos. As age increases to post-hatching, there is an increase in electron density of CDBs, and the gold particles are more confined to the perimeter of CDBs. This indicates that the increased electron density of CDBs, not only structurally obscures the desmin IFs inside the CDBs, but also blocks antigenic sites on these filaments.

Labeling with anti-α-actinin indicates that α-actinin is a component of the CCFs inside the CDBs. Moreover, these CCFs are oriented perpendicular to the AFs and desmin-containing IFs in developing CDBs (Figure 7d inset). Exactly what the CCFs are linking is unclear. On the other hand, by using stereo electron microscopy, it has been shown that actin filaments (AFs) are present inside CDB (Ashton et al., 1975). When decorated with heavy meromyosin S-1,

AFs are attached with opposite polarity to either end of CDBs (Bond and Somlyo, 1982; Tsukita et al., 1983). Recently, based on anti-actin staining experiments described but not shown, Small et al. (1986) stated that AFs are indeed a CDB component. Draeger et al. (1990) further proposed that AFs from contractile units, i. e., caldesmon-containing AFs, are attached to CDBs. In summary, three filamentous components, namely, AFs, desmin-containing IFs and α-actinin-containing CCFs, have been identified in CDBs.

Possible steps in CDB assembly

The results presented here and in a previous study (Chou et al., 1991) have shown that AFs and IFs run parallel to the longitudinal axis of CDBs and that the CCFs are perpendicular to the longitudinal axis of CDBs. Based on our observations, it is reasonable to propose the following steps for CDB assembly: (1) predominantly parallel alignment of AFs and desmin-containing IFs to form the long axis of CDBs, (2) cross-linking of AFs, possibly including desmin-containing IFs, by CCFs that are oriented perpendicular to the longitudinal filaments, and (3) addition of other components that contribute to the increase in electron density.

There is no evidence that AFs and IFs pass completely and continuously through a CDB. This is particularly clear for AFs because they have opposite polarity on opposite ends of the CDB (Bond and Somlyo, 1982; Tsukita et al., 1983). If these AFs were continuous, a

reversal of polarity within an AF would be required. No evidence for such a phenomenon exists. Because AFs are present inside CDBs, it is far more likely that AFs overlap inside CDBs with an arrangement similar to that observed in mammalian Z-lines (Yamaguchi et al., 1985) and in nemaline myopathy rod bodies, which are Z-line analogs (Stromer et al., 1976). Similarly stereo pair micrographs of developing CDBs (Figure 4) suggest that individual IFs penetrate into but do not pass through the CDB. This means that IFs also overlap inside the CDB.

The presence of CCFs that are oriented perpendicular to the long axis of the CDB, that are recognized by anti-α-actinin and that have diameters similar to that of α-actinin suggest that these filaments are α-actinin and could link longitudinal filaments in the CDB. The ability of α-actinin to cross-link AFs is well documented (Singh et al., 1981; Jockush and Isenberg, 1981; Isobe et al., 1988; Meyer and Aebi, 1990). Little information is available about the interaction between α-actinin and desmin. Isobe et al. (1988) suggested that α-actinin is involved in interlinking AFs and desmin IFs in cultured hamster heart cells. Preliminary results from our laboratory (unpublished results), obtained by immobilizing either α-actinin or desmin on nitrocellulose papers, then overlaying with either desmin or α-actinin respectively and detecting bound proteins with antibodies, suggest that α-actinin and desmin may interact. It is also possible that other unidentified components that contribute to the added electron density of the CDB are also involved in linking together the filamentous components.

Our data clearly indicate that growth of CDBs is accompanied by an increase in electron density. The component(s) responsible for this increase are not known. As more IFs, AFs and CCFs are added to the growing CDB, they may alone account for the increased density. We can not, however, exclude the possibility that other unidentified proteins are added during the later stages of CDB growth.

Relationship of the axial IFB to CDBs

The IFB can first be recognized in 1-day post-hatch chicken gizzard smooth muscle cells (Chou et al., 1991). This bundle becomes larger and more prominent in 7-day post-hatch cells (Figure 6a; Chou et al., 1991). The axial IFB is a characteristic of intact adult chicken gizzard smooth muscle cells (Stromer and Bendayan, 1988) and extends the entire length of the cell. Individual desmin IFs fray out from the IFB and directly link the nucleus and mitochondria at the poles of the nucleus to the IFB (Stromer and Bendayan, 1990). Although many IFs seem to be oriented parallel to the smooth muscle cell axis (Stromer, 1990), some IFs may be obliquely arranged between CDBs (Ashton et al., 1975; Bond and Somlyo, 1982; Garfield and Somlyo, 1985) and also terminate at or near MADBs located at the sarcolemma. This suggests that IFB may serve as an axial anchoring point for the IF-CDB network that extends outward toward the MADBs. Such an axial anchoring point would be consistent with the results of Cooke and Fay (1972) who observed that random

distribution of CDBs in unstretched smooth muscle change to a more central distribution in stretched samples. This suggests that CDBs are linked together into a cytoskeletal network. Draeger et al. (1990) also suggested that CDBs, via attached AFs from contractile units and IFs, are responsible for linking cytoskeletal and contractile units in smooth muscle cells.

We have used SDS-PAGE and Western blots together with colloidal gold labeled antibodies and electron microscopy to show that amounts of specific avian smooth muscle proteins increase during development and that proteins associated with the CDBs change both their structural arrangement and the accessibility to antibodies. Between 10-day embryonic age and 7-day post-hatch, amounts of myosin heavy chain, α-actinin, desmin and actin all increase. On the basis of structural changes in the CDB and immunoelectron microscopy labeling, we propose that CDB assembly is a three step process including: (1) alignment of AFs and desmin IFs; (2) cross-linking of major longitudinal filaments, probably by α-actinin; and (3) addition of components that increase the electron density of the CDB.

ACKNOWLEDGEMENTS

We thank Mary Sue Mayes, Kim Ho, Janet Stephenson, Jean Schmidt, Stephan Bilak, and Jo Philips for excellent technical assistance. We also thank Marylou Weigel for typing the manuscript. This research was supported, in part, by a grant from the American Heart Association, Iowa Affiliate. This is Journal Paper J- of the Iowa Agriculture and Home Economics Experiment Station, Ames, IA 50011, projects 2921 and 2127.

REFERENCES

Ashton, F., A. V. Somlyo, and A. P. Somlyo. 1975. The contractile apparatus of vascular smooth muscle: Intermediate high voltage stereo electron microscopy. J. Mol. Biol. 98:17-29.

Bagby, R. M. 1983. Organization of contractile-cytoskeletal elements. Pages 1-84 in N. L. Stephens, ed. Biochemistry of smooth muscle. Vol. 1. CRC Press, Inc., Boca Raton, FL.

Bagby, R. M. 1986. Toward a comprehensive three-dimensional model of the contractile system of vertebrate smooth muscle cells. Int. Rev. Cytol. 105:67-128.

Bagby, R. M. 1990. Ultrastructure, cytochemistry, and organization of myofilaments in vertebrate smooth muscle. Pages 23-61 in P. M. Motta, ed. Ultrastructure of smooth muscle. Kluwer Acad. Publishers, Norwell, MA.

Bendayan, M. 1984. Protein A-gold electron microscopic immunocytochemistry: Methods, applications, and limitations. J. Electron Microsc. Tech. 1:243-270.

Bond, M., and A. V. Somlyo. 1982. Dense bodies and actin polarity in vertebrate smooth muscle. J. Cell Biol. 95:403-413.

Campbell, G. R., Y. Uehara, G, Mark, and G. Burnstock. 1971. Fine structure of smooth muscle cells grown in tissue culture. J. Cell Biol. 49:21-34.

Chou, R. R., M. H. Stromer, R. M. Robson, and T. W. Huiatt. 1991. Structural changes in contractile and cytoskeletal elements in developing smooth muscle cells. Submitted.

Cooke, P. H., and F. S. Fay. 1972. Correlation between fiber length, ultrastructure, and the length-tension relationship of mammalian smooth muscle. J. Cell Biol. 52:105-116.

Cooke, P. H., F. S. Fay, and R. Craig. 1989. Myosin filaments isolated from skinned amphibian smooth muscle cells are side polar. J. Muscle Res. Cell Motil. 10:206-220.

Cossette, L. J., and M. Vincent. 1991. Expression of a developmentally regulated cross-linking intermediate filament-associated protein (IFAP-400) during the replacement of vimentin and for desmin in muscle cell differentiation. J. Cell Sci. 98:251-260.

Draeger, A., W. B. Amos, M. Ikebe, and J. V. Small. 1990. The cytoskeletal and contractile apparatus of smooth muscle: Contraction bands and segmentation of the contractile elements. J. Cell Biol. 111:2463-2473.

Fay, F., K. Fujiwara, D. Rees, and K. Fogarty. 1983. Distribution of α-actinin in single isolated smooth muscle cells. J. Cell Biol. 96:783-795.

Fujimoto, T., and K. Ogawa. 1988. Smooth muscle cells of the chicken aortic arch differ from those in the gizzard and the femoral artery in the distribution of F-actin, α-actinin and filamin. Histochem. 88:525-532.

Fürst, D. O., R. A. Cross, J. De Mey, and J. V. Small. 1986. Caldesmon is an elongated, flexible molecule located in the actomyosin domains of smooth muscle. EMBO J. 5:251-257.

Gabella, G. 1981. Structure of smooth muscles. Pages 1-46 in E. Bülbring, A. F. Brading, A. W. Jones, and T. Tomita, eds. Smooth muscle: An assessment of current knowledge. University of Texas Press, Austin, TX.

Gabella, G. 1985. Chicken gizzard: The muscle, the tendon and their attachment. Anat. Embryol. 171:151-162.

Gabella, G. 1989. Development of smooth muscle: Ultrastructural study of the chick embryo gizzard. Anat. Embryol. 180:213-226.

Garfield, R., and A. P. Somlyo. 1985. Structure of smooth muscle. Pages 1-36 in A. K. Grover, and E. E. Daniel, eds. Calcium and contractility: Smooth muscle. Humana Press, Clifton, NJ.

Hirai, S., and T. Hirabayashi. 1983. Developmental change of protein constituents in chicken gizzards. Dev. Biol. 97:483-493.

Huiatt, T. W., R. M. Robson, N. Arakawa, and M. H. Stromer. 1980. Desmin from avian smooth muscle: Purification and partial characterization. J. Biol. Chem. 225:6981-6989.

Isobe, Y., F. D. Warner, and L. F. Lemanski. 1988. Three-dimensional immunogold localization of α-actinin within the cytoskeletal networks of cultured cardiac muscle and nonmuscle cells. Proc. Natl. Acad. Sci. U.S.A. 85:6758-6762.

Jockusch, B. M., and G. Isenberg. 1981. Interaction of α-actinin and vinculin with actin: Opposite effects on filament network formation. Proc. Natl. Acad. Sci. U.S.A. 78:3005-3009.

Kargacin, G. J., P. M. Cooke, S. B. Abramson, and F. S. Fay. 1989. Periodic organization of the contractile apparatus of smooth muscle revealed by the motion of dense bodies in single cells. J. Cell Biol. 108:1465-1475.

Laemmli, U. K. 1970. Cleavage of structural proteins during the assembly of the head of bacteriophage T4. Nature 227, 680-685.

Lemanski, L. F., D. J. Paulson, C. S. Hill, L. A. Davis, L. C. Riles, and S.-S. Lim. 1985. Immunoelectron microscopic localization of α-actinin on Lowicryl-embedded thin sectioned tissues. J. Histochem. Cytochem. 33:515-522.

McGuffee, L. J., J. Mercure, and S. A. Little. 1991. Three-dimensional structure of dense bodies in rabbit renal artery smooth muscle. Anat. Rec. 229:499-504.

Meyer, R. K., and U. Aebi. 1990. Bundling of actin filaments by α-actinin depends on its molecular length. J. Cell Biol. 110:2013-2024.

Moeremans, M., G. Daneels, M. De Raeymaeker, B. De Wever, and J. De Mey. 1989. Chapter 2. The use of colloidal gold particles for testing the specificity of antibodies and/or the presence of antigen. Page 17-27 in A. J. Verkleij, and J. L. M. Leunissen, ed. Immuno-Gold Labeling in Cell Biology. CRC Press, Inc., Boca Raton, FL.

Robson, R. M., D. E. Goll, and M. J. Temple. 1968. Determination of protein in "Tris" buffer by the biuret reaction. Anal. Biochem. 24:339-341.

Schollmeyer, J. E., L. T. Furcht, D. E. Goll, R. M. Robson, and M. H. Stromer. 1976. Localization of contractile proteins in smooth muscle cells and in normal and transformed fibroblasts. Pages 361-388 in R. Goldman, T. Pollard, and J. Rosenbaum, eds. Cell motility. Book A. Cold Spring Harbor Laboratory, New York, NY.

Singh, I., D. E. Goll, R. M. Robson, and M. H. Stromer. 1981. Effect of α-actinin on actin structure: Viscosity studies. Biochim. Biophys. Acta 669:1-6.

Small, J., and A. Sobieszek. 1980. The contractile apparatus of smooth muscle. Int. Rev. Cytol. 64:241-306.

Small, J. V. 1985. Geometry of actin-membrane attachments in the smooth muscle cell: The localizations of vinculin and α-actinin. EMBO J. 4:45-49.

Small, J. V., D. O. Fürst, and J. De Mey. 1986. Localization of filamin in smooth muscle. J. Cell Biol. 102:210-220.

Somlyo, A. V., and C. Franzini-Armstrong. 1985. New views of smooth muscle structure using freezing, deep-etching and rotary shadowing. Experientia 41:841-856.

Stromer, M. H., L. B. Tabatabai, R. M. Robson, D. E. Goll, and M. G. Zeece. 1976. Nemaline myopathy, an integrated study: Selective extraction. Exptl. Neurol. 50:402-421.

Stromer, M. H., T. W. Huiatt, F. L. Richardson, and R. M. Robson. 1981. Disassembly of synthetic 10-nm desmin filaments from smooth muscle into protofilaments. Eur. J. Cell Biol. 25:136-143.

Stromer, M. H., and M. Bendayan. 1988. Arrangement of desmin intermediate filaments in smooth muscle cells as shown by high-resolution immunocytochemistry. Cell Motil. Cytoskeleton 11:117-125.

Stromer, M. H. 1990. Intermediate (10-nm) filaments in muscle. Pages 19-36 in R. D. Goldman, and P. M. Steinert, eds. Cellular and molecular biology of intermediate filaments. Plenum Publishing Corp., New York, NY.

Stromer, M. H., and M. Bendayan. 1990. Immunocytochemical identification of cytoskeletal linkages to smooth muscle cell nuclei and mitochondria. Cell Motil. Cytoskeleton 17:11-18.

Suzuki, A., D. E. Goll, R. E. Allen, R. M. Robson, and M. H. Stromer. 1976. Some properties of purified skeletal muscle α-actinin. J. Biol. Chem. 251:6860-6870.

Towbin, H., T. Staehelin, and J. Gordon. 1979. Electrophoretic transfer of proteins from polyacrylamide gels to nitrocellulose sheets: Procedure and some applications. Proc. Natl. Acad. Sci. USA 76:4350-4354.

Tsukita, S., S. Tsukita, and H. Ishikawa. 1983. Association of actin and 10 nm filaments with the dense bodies in smooth muscle cells of the chicken gizzard. Cell Tissue Res. 229:233-242.

Uehara, Y., G. R. Campbell, and G, Burnstock. 1971. Cytoplasmic filaments in developing and adult vertebrate smooth muscle. J. Cell Biol. 50:484-497.

Yamaguchi, M. M., M. Izuminoto, R. M. Robson, and M. H. Stromer. 1985. Fine structures of wide and narrow vertebrate muscle Z-lines: A proposed model and computer simulation of Z-line architecture. J. Mol. Biol. 184:621-644.

SUMMARY AND CONCLUSION

The purpose of the first section of my study was to determine the critical concentration required for desmin assembly in the presence of specific combinations of cations and temperature. Assembly was monitored by two independent methods, namely, turbidity and centrifugation, and was verified by negative staining of pellets and supernatants obtained during the centrifugation assay. Results from this section permit the following conclusions:

1. Both turbidity and centrifugation were appropriate assays to measure desmin critical concentration.

2. As temperature increased from 2 to 37°C, critical concentration decreased.

3. Divalent cations lowered critical concentration more than the monovalent cation.

4. Supernatants contained short aggregates or partially formed filaments, but pellets contained long filaments (>> 1 μm) with an average diameter of 10 nm.

5. Thermodynamic results indicated that hydrophobic interactions are dominant during assembly of desmin intermediate filaments.

The purpose of the second section of my study was to investigate and identify the structural changes in contractile and cytoskeletal elements, especially cytoplasmic dense bodies (CDBs), in developing

smooth muscle cells. Results from this section lead to the following conclusions:

1. The events which occurred during the first 28 days of development could be sequentially classified into 7 stages, primarily based on the appearance and growth of contractile and cytoskeletal elements. These stages have been identified as follows: myoblast proliferation; dense body appearance; thick filament appearance; dense body growth; muscle cell replication; IFB appearance; and appearance of adult type cells. Smooth muscle cells in each stage expressed a similar degree of maturity. These sequential events clearly indicate that smooth muscle myogenesis in vivo is a sequential process in which assembly of contractile elements (actin and thick filaments) and filament attachment sites (CDBs and membrane-associated dense bodies (MADBs)) is initiated earlier than the axial IFB, a major cytoskeletal element.

2. CDBs could first be recognized at embryonic day 8 as patches of increased electron density that consisted of actin filaments (AFs), intermediate filaments (IFs), and cross-connecting filaments (CCFs).

3. The number, size and electron density of CDBs increased as age increased. MADBs could also be recognized in embryonic day 8. Their number and size increased as age increased, especially after day 16.

4. Filaments with the diameter of thick filaments appeared at embryonic day 12.

5 Smooth muscle cells were able to divide, and the highest incidence of this mitosis was at embryonic day 20.

6. The desmin-containing axial IFB first appeared in 1-day post-hatch cells. This IFB became larger and more prominent in 7-day post-hatch cells. Immunogold labeling with anti-desmin showed that the IFB contained desmin IFs.

The purpose of the third section of my study was to investigate the substructure of CDBs and changes in the distribution of desmin and α-actinin during development of smooth muscle in samples taken from gizzards of 10 and 16 day embryos and from 1- and 7-day post-hatch chickens. Results from this section may be summarized as follows:

1. SDS-PAGE showed that the amount of major muscle proteins (myosin heavy chain, α-actinin, desmin, and actin) increased as age increased.

2. Immunogold labeling with polyclonal anti-desmin and with monoclonal anti-α-actinin indicated that the number of desmin IFs and the amount of α-actinin increased as age increased.

3. Anti-desmin labeling in embryonic day 10 and 16 cells was located both at the periphery of the myofilament compartment and on or close to desmin IFs inside CDBs. After hatching, gold particles associated with CDBs were gradually confined to the perimeters of CDBs. This suggested that the antigenic sites on desmin IFs inside

CDBs were blocked by the component(s) responsible for the increased electron density of the CDBs as age increased.

4. In 7-day post-hatch cells, anti-desmin heavily labeled the axial IFB and suggested that desmin was the constituent protein.

5. α-actinin was mainly located in the CDBs and sometimes in MADBs throughout development. Gold particles also revealed that α-actinin was mainly located in the CCFs which have an average diameter of 2-3 nm.

6. A proposed model for CDB assembly involves: (1) alignment of AFs and desmin-containing IFs parallel to the long axis of CDBs, (2) cross-linking of AFs, possibly including desmin IFs, by CCFs that are oriented perpendicular to the longitudinal filaments, and (3) an increase in electron density.

7. Desmin IFs, together with AFs, form the backbone of CDBs. These desmin IFs may interact with the desmin IFs in the axial IFB to form an intracellular cytoskeletal network inside smooth muscle cells.

LITERATURE CITED

Aebi, U., W. E. Fowler, P. Rew, and T.-T. Sun. 1983. The fibrillar substructure of keratin filaments unraveled. J. Cell Biol. 97:1131-1143.

Aebi, U., J. Cohn, L. Buhle, and L. Gerace. 1986. The nuclear lamina is a meshwork of intermediate-type filaments. Nature 323:560-564.

Aebi, U., M. Häner, J, Troncoso, R. Eichner, and A. Engel. 1988. Unifying principles in intermediate filament (IF) structure and assembly. Protoplasma 145:73-81.

Ahmadi, B., and P. T. Speakman. 1978. Suberimidate crosslinking shows that a rod-shaped, low cystine, high helix protein prepared by limited proteolysis of reduced wool has four protein chains. FEBS Letters 94:365-367.

Ando, S., K. Tanaba, Y. Ando, C. Sato, and M. Inagaki. 1989. Domain- and sequence-specific phosphorylation of vimentin induces disassembly of the filament structure. Biochemistry 28:2974-2979.

Ashton, F., A. V. Somlyo, and A. P. Somlyo. 1975. The contractile apparatus of vascular smooth muscle: Intermediate high voltage stereo electron microscopy. J. Mol. Biol. 98:17-29.

Bagby, R. M. 1983. Organization of contractile-cytoskeletal elements. Pages 1-84 in N. L. Stephens, ed. Biochemistry of smooth muscle. Vol. 1. CRC Press, Inc., Boca Raton, FL.

Bagby, R. M. 1986. Toward a comprehensive three-dimensional model of the contractile system of vertebrate smooth muscle cells. Int. Rev. Cytol. 105:67-128.

Bagby, R. M. 1990. Ultrastructure, cytochemistry, and organization of myofilaments in vertebrate smooth muscle. Pages 23-61 in P. M. Motta, ed. Ultrastructure of smooth muscle. Kluwer Acad. Publishers, Norwell, MA.

Bailey, C. G., R. M. Bagby, and M. C. Kreyling. 1984. Morphogenesis of the contractile system in embryonic chick gizzard smooth cells. I. Ultrastructure. J. Cell Biol. 99:29a. (Abstract).

Benavente, R., and G. Krohne. 1986. Involvement of nuclear lamins in post-mitotic reorganization of chromatin as demonstrated by microinjection of lamin antibodies. J. Cell Biol. 103:1847-1854.

Bennett, T., and J. L. S. Cobb. 1969. Studies of avian gizzard: the development of the gizzard and its innervation. Z. Zellforsch. Mikrosk. Anat. 98:599-621.

Bennett, G. S., S. A. Fellini, and H. Holtzer. 1978. Immunofluorescent visualization of 100 Å filaments in different cultured chick embryo types. Differentiation 12:71-82.

Bennett, G. S., S. A. Fellini, Y. Toyama, and H. Holtzer. 1979. Redistribution of intermediate filament subunits during skeletal myogenesis and maturation in vitro. J. Cell Biol. 82:577-5864.

Berner, P. F., E. Frank, H. Holtzer, and A. P. Somlyo. 1981a. The intermediate filament proteins of rabbit vascular smooth muscle:

Immunofluorescent studies of desmin and vimentin. J. Muscle Res. Cell Motil. 2:439-452.

Berner, P. F., A. V. Somlyo, and A. P. Somlyo. 1981b. Hypertrophy-induced increase of intermediate filaments in vascular smooth muscle. J. Cell Biol. 88:96-101.

Bilak, S. R., E. M. Bremner, and R. M. Robson. 1987. Composition of intermediate filament subunit proteins in embryonic, neonatal and post-natal porcine skeletal muscle. J. Anim. Sci. 64:601-606.

Bloemendal, H., and F. R. Piper. 1989. Intermediate filaments: Known structure, unknown function. Biochim. Biophys. Acta 1007:245-253.

Bond, M., and A. V. Somlyo. 1982. Dense bodies and actin polarity in vertebrate smooth muscle. J. Cell Biol. 95:403-413.

Bretscher, A. 1984. Smooth muscle caldesmon: Rapid purification and F-actin crosslinking properties. J. Biol. Chem. 259:12873-12880.

Burke, B., and L. Gerace. 1986. A cell free system to study reassembly of the nuclear envelope at the end of mitosis. Cell 44:639-652.

Burnstock, G. 1970. Structure of smooth muscle and its innervation. Pages 1-69 in E. Bülbring, A. Brading, A. Janes, and T. Tomita, eds. Smooth muscle. Edward Arnold (Publishers) Ltd., London.

Campbell, G. R., Y. Uehara, G, Mark, and G. Burnstock. 1971. Fine structure of smooth muscle cells grown in tissue culture. J. Cell Biol. 49:21-34.

Campbell, G. R., J. H. Chamley, and G. Burnstock. 1974. Development of smooth muscle cells in tissue culture. J. Anat. 117:295-312.

Campbell, G. R., J. Chamley-Campbell, U. Gröschel-Stewart, J. V. Small and P. Anderson. 1979. Antibody staining of 10-nm (100-Å) filaments in cultured smooth, cardiac and skeletal cells. J. Cell Sci. 37:303-322.

Chou, R. R., M. H. Stromer, R. M. Robson, and T. W. Huiatt. 1990. Determination of critical concentration required for desmin assembly. Biochem. J. 272:139-145.

Clark, T., P. K. Ngai, C. Sutherland, U. Gröschel-Stewart, and M. P. Walsh. 1986. Vascular smooth muscle caldesmon. J. Biol. Chem. 261:8028-8035.

Conway, J. F., and D. A. D. Parry. 1988. Intermediate filament structure: 3. Analysis of sequence homologies. Int. J. Biol. Macromol. 10:79-98.

Cooke, P. H., and F. S. Fay. 1972. Correlation between fiber length, ultrastructure, and the length-tension relationship of mammalian smooth muscle. J. Cell Biol. 52:105-116.

Cooke, P. 1976. A filamentous cytoskeleton in vertebrate smooth muscle fibers. J. Cell Biol. 68:539-556.

Cooke, P. 1983. Organization of contractile fibers in smooth muscle. Pages 57-77 in R. M. Dowben, and J. M. Shay, eds. Cell and muscle motility. Vol. 3. Plenum Publishing Corp., New York, NY.

Cooke, P. H., G. Kargacin, R. Craig, K. Fogerty, and F. S. Fay. 1987. Molecular structure and organization of filaments in single, skinned smooth muscle cells. Pages 1-25 in M. J. Siegman, A. P. Somlyo, and N. L. Stephens, eds. Regulation and contraction of smooth muscle. Alan R. Liss, New York, NY.

Cooke, P. H., F. S. Fay, and R. Craig. 1989. Myosin filaments isolated from skinned amphibian smooth muscle cells are side polar. J. Muscle Res. Cell Motil. 10:206-220.

Crewther, W. G., A. S. Inglis, and N. M. McKern. 1978. Amino acid sequence of α-helical segments from S-carboxymethylkerateine-A: Complete sequence of a type II segment. Biochem. J. 173:365-371.

Crewther, W. G., L. M. Dowling, P. M. Steinert, and D. A. D. Parry. 1983. The structure of intermediate filaments. Int. J. Biol. Macromol. 5:267-274.

Devine, C. E., A. V. Somlyo, and A. P. Somlyo. 1972. Sarcoplasmic reticulum and excitation-contraction coupling in mammalian smooth muscles. J. Cell Biol. 52:690-718.

Engel, A., A. Eichner, and U. Aebi. 1985. Polymorphism of reconstituted human epidermal keratin filaments: Determination of their mass-per-unit-length and width by scanning transmission electron microscopy (STEM). J. Ultrastruct. Res. 90:323-335.

Evans, R. M. 1988. Cyclic AMP-dependent protein kinase-induced vimentin filament disassembly involves modification of the N-

terminal domain of intermediate filament subunits. FEBS Letters 234:73-78.

Fay, F. S., and P. H. Cooke. 1973. Reversible disaggregation of myofilaments in vertebrate smooth muscle. J. Cell Biol. 56:399-411.

Fay, F., K. Fujiwara, D. Rees, and K. Fogarty. 1983. Distribution of α-actinin in single isolated smooth muscle cells. J. Cell Biol. 96:783-795.

Fisher, D. Z., N. Chaudhury, and G. Blobel. 1986. cDNA sequencing of nuclear lamins A and C reveals primary and secondary structure homology to intermediate filament proteins. Proc. Natl. Acad. Sci. USA 83:6450-6454.

Franke, W. W., E. Schmid, K. Weber, and M. Osborn. 1979. HeLa cells contain intermediate-sized filaments of the prekeratin type. Exp. Cell Res. 118:95-109.

Franke, W. W., E. Schmid, J. Vanderkerckhove, and K. Weber. 1980. A permanently proliferating rat vascular smooth muscle cell with maintained expression of smooth muscle characteristics, including actin of the vascular smooth muscle type. J. Cell Biol. 87:594-600.

Franke, W. W., D. Schiller, and C. Grund. 1982. Protofilamentous and annular structures as intermediates during reconstitution of cytokeratin filaments in vitro. Biol. Cell 46:257-268.

Franke, W. W. 1987. Nuclear lamins and cytoplasmic intermediate filament proteins: A growing multigene family. Cell 48:3-4.

Fraser, R. D. B., T. P. MacRae, and E. Suzuki. 1976. Structure of the α-keratin microfibril. J. Mol. Biol. 108:435-452.

Fraser, R. D. B., T. P. MacRae, E. Suzuki, and D. A. D. Parry. 1985. Intermediate filament structure: 2. Molecular interactions in the filament. Int. J. Biol. Macromol. 7:258-274.

Fukuyama, K., T. Murozuka, R. Caldwell, and W. L. Epstein. 1978. Divalent cation stimulation of in vitro fibre assembly from epidermal keratin protein. J. Cell Sci. 33:255-263.

Fürst, D. O., R. A. Cross, J. De Mey, and J. V. Small. 1986. Caldesmon is an elongated, flexible molecule located in the actomyosin domains of smooth muscle. EMBO J. 5:251-257.

Gabella, G. 1971. Caveolae intracellulares and sarcoplasmic reticulum in smooth muscle. J. Cell Sci. 8:601-609.

Gabella, G. 1981. Structure of smooth muscles. Pages 1-46 in E. Bülbring, A. Brading, A. Jones, and T. Tomita, eds. Smooth muscle: An assessment of current knowledge. University of Texas Press, Austin, TX.

Gabella, G. 1989. Development of smooth muscle: Ultrastructural study of the chick embryo gizzard. Anat. Embryol. 180:213-226.

Gard, D. L., P. B. Bell, and E. Lazarides. 1979. Coexsistence of desmin and the fibroblastic intermediate filament subunit in muscle and nonmuscle cells: Identification and comparative peptide analysis. Proc. Natl. Acad. Sci. USA 76:3894-3898.

Garfield, R. E., and E. E. Daniel. 1977. Relation of membrane vesicles to volume control and Na^+ transport in smooth muscle: Effect of

metabolic and transport inhibition on fresh tissues. J. Mechanochem. Cell Motility. 4:113-155.

Garfield, R., and A. P. Somlyo. 1985. Structure of smooth muscle. Pages 1-36 in A. K. Grover, and E. E. Daniel, eds. Calcium and contractility: Smooth muscle. Humana Press, Clifton, NJ.

Geisler, N., and K. Weber. 1980. Purification of smooth-muscle desmin and a proteinchemical comparison of desmin from chicken gizzard and hog stomach. Eur. J. Biochem. 111:425-433.

Geisler, N., and K. Weber. 1981a. Self-assembly in vitro of the 68,000 molecular weight component of the mammalian neurofilament triplet proteins into intermediate-sized filaments. J. Mol. Biol. 151:565-571.

Geisler, N., and K. Weber. 1981b. Comparison of the proteins of two immunologically distinct intermediate-sized filaments by amino acid sequence analysis: Desmin and vimentin. Proc. Natl. Acad. Sci. USA 78:4120-4123.

Geisler, N., and K. Weber. 1982. The amino acid sequence of chicken muscle desmin provides a common structural model for intermediate filament proteins. EMBO J. 1:1649-1656.

Geisler, N., E. Kaufmann, and K. Weber. 1982. Proteinchemical characterization of three structurally distinct domains along the protofilament unit of desmin 10 nm filaments. Cell 30:277-286.

Geisler, N., E. Kaufmann, and K. Weber. 1985. Antiparallel orientation of the two double-stranded coiled-coils in the tetrameric

protofilament unit in intermediate filaments. J. Mol. Biol. 182:173-177.

Geisler, N., and K. Weber. 1986. Structural aspects of intermediate filaments. Pages 41-68 in J. W. Shay, ed. Cell and molecular biology of the cytoskeleton. Plenum Publishing Corp., New York, NY.

Geisler, N., and K. Weber. 1988. Phosphorylation of desmin in vitro inhibits formation of intermediate filaments; identification of three kinase A sites in the aminoterminal head domain. EMBO J. 7:15-20.

Georgatos, S. D., and V. T. Marchesi. 1985. The binding of vimentin to human erythrocyte membranes: A model system for the study of intermediate filament-membrane interactions. J. Cell Biol. 100:1955-1961.

Georgatos, S. D., D. C. Weaver, and V. T. Marchesi. 1985. Site-specificity in vimentin-membrane interactions: Intermediate filament subunits associate with the plasma membrane via their head domains. J. Cell Biol. 100:1962-1967.

Georgatos, S. D., and G. Blobel. 1987a. Two distinct attachment sites for vimentin along the plasma membrane and the nuclear envelope in avian erythrocytes: A basis for vectorial assembly of intermediate filaments. J. Cell Biol. 105:105-115.

Georgatos, S. D., and G. Blobel. 1987b. Lamin B constitutes an intermediate filament attachment site at the nuclear envelope. J. Cell Biol. 105:117-125.

Georgatos, S. D., K. Weber, N. Geisler, and G. Blobel. 1987. Binding of two desmin derivatives to the plasma membrane and nuclear envelope of avian erythrocytes: Evidence for a conserved site-specificity in intermediate filament-membrane interaction. Proc. Natl. Acad. Sci. USA 84: 6780-6784.

Gerace, L., and G. Blobel. 1980. The nuclear envelope lamina is reversibly depolymerized during mitosis. Cell 19:277-287.

Gerace, L. 1986. Nuclear lamina and organization of nuclear architecture. Trends Biochem. Sci. 11:443-446.

Goldman, R. D., A. E. Goldman, K. J. Green, J. C. R. Jones, S. M. Jones, and H.-S. Yang. 1986. Intermediate filament network: Organization and possible functions of a diverse group of cytoskeletal elements. J. Cell Sci. Suppl. 5:69-97.

Goldman, R. D., R. V. Zackroff, and P. M. Steinert. 1990. Intermediate filaments: An overview. Pages 3-17 in R. D. Goldman, and P. M. Steinert, eds. Cellular and molecular biology of intermediate filaments. Plenum Publishing Corp., New York, NY.

Graceffa, P., C.-L. A. Wang, and W. F. Stafford. 1988. Caldesmon: Molecular weight and subunit composition by analytical ultracentrifugation. J. Biol. Chem. 263:14196-14202.

Granger, B. L., and E. Lazarides. 1982. Structural associations of synemin and vimentin filaments in avian erythrocytes revealed by immunoelectron microscopy. Cell 30:263-275.

Gruen, L. C., and E. F. Woods. 1983. Structural studies on the microfibrillar proteins of wool: Interaction between α-helical

segments and reassembly of a four-chain structure. Biochem. J. 209:587-595.

Guyton, A. C. 1986. Textbook of medical physiology. W. B. Saunders Company, Philadelphia, PA.

Hanukoglu, I., and E. Fuchs. 1983. The cDNA sequence of a type II cytoskeletal keratin reveals constant and variable structural domains among keratins. Cell 33:915-924.

Hartshorne, D. J., and A. Persechini. 1984. Regulatory mechanisms in smooth muscle: The role of myosin phosphorylation. Pages 271-282 in N. L. Stephens, ed. Smooth muscle contraction. Marcel Dekker Inc., New York, NY.

Hartzer, M. K. 1984. Purification and properties of porcine cardiac desmin and vascular smooth muscle vimentin. Ph. D. Dissertation. Iowa State University, Ames.

Hatzfeld, M., G. Maier, and W. W. Franke. 1987. Cytokeratin domains involved in heterotypic complex formation determined by in-vitro binding assays. J. Mol. Biol. 197:237-255.

Henderson, D., and K. Weber. 1981. Immuno-electron microscopical identification of the two types of intermediate filaments in established epithelial cells. Exp. Cell Res. 132:297-311.

Henderson, D., N. Geisler, and K. Weber. 1982. A periodic ultrastructure in intermediate filaments. J. Mol. Biol. 106:735-746.

Hirai, S., and T. Hirabayashi. 1983. Developmental change of protein constituents in chicken gizzards. Dev. Biol. 97:483-493.

Hirai, S., and T. Hirabayashi. 1986. Development of myofibrils in the gizzard of chicken embryos: Intracellular distribution of structural proteins and development of contractility. Cell Tissue Res. 243:487-493.

Hisanaga, S., A. Ikai, and N. Hirokawa. 1990. Molecular architecture of the neurofilament: I. Subunit arrangement of neurofilament L protein in the intermediate-sized filament. J. Mol. Biol. 211:857-869.

Hisanaga, S., and N. Hirokawa. 1990. Molecular architecture of the neurofilament: II. Reassembly process of neurofilament L protein in vitro. J. Mol. Biol. 211:871-882.

Huiatt, T. W. 1979. Studies on the 55,000-dalton protein from vertebrate smooth muscle intermediate filaments. Ph. D. Dissertation. Iowa State University, Ames.

Huiatt, T. W., R. M. Robson, N. Arakawa, and M. H. Stromer. 1980. Desmin from avian smooth muscle: Purification and partial characterization. J. Biol. Chem. 255:6981-6989.

Inagaki, M., Y. Nishi, K. Nishizawa, M. Matsuyama, and C. Sato. 1987. Site specific phosphorylation induces disassembly of vimentin filaments in vitro. Nature 328:649-652.

Inagaki, M., Y. Gonda, M. Matsuyama, K. Nishizawa, Y. Nishi, and C. Sato. 1988. Intermediate filament reconstitution in vitro: The role of phosphorylation on the assembly-disassembly of desmin. J. Biol. Chem. 263:5970-5978.

Inagaki, M., Y. Gonda, S. Ando, S. Kitamura, Y. Nishi, and C. Sato. 1989. Regulation of assembly-disassembly of intermediate filaments in vitro. Cell Struct. and Function. 14:279-286.

Ip, W., M. K. Hartzer, Y.-Y. S. Pang, and R. M. Robson. 1985a. Assembly of vimentin in vitro and its implications concerning the structure of intermediate filaments. J. Mol. Biol. 183:365-375.

Ip, W., J. E. Heuser, Y.-Y. S. Pang, M. K. Hartzer, and R. M. Robson. 1985b. Subunit structure of desmin and vimentin protofilaments and how they assemble into intermediate filaments. Ann. N. Y. Acad. Sci. 455:185-199.

Ip, W. 1988. Modulation of desmin intermediate filament assembly by a monclonal antibody. J. Cell Biol. 106:735-746.

Ishikawa, H., R. Bischoff, and H. Holtzer. 1968. Mitosis and intermediate-sized filaments in developing skeletal muscle. J. Cell Biol. 38:538-555.

Kargacin, G. J., P. M. Cooke, S. B. Abramson, and F. S. Fay. 1989. Periodic organization of the contractile apparatus of smooth muscle revealed by the motion of dense bodies in single cells. J. Cell Biol. 108:1465-1475.

Kaufmann, E., K. Weber, and N. Geisler. 1985. Intermediate filament forming ability of desmin derivatives lacking either the amino-terminal 67 or the carboxy-terminal 27 residues. J. Mol. Biol. 185:733-742.

Kitamura, S., S. Ando, M. Shibata, K. Tanaba, C. Sato, and M. Inagaki. 1989. Protein kinase C phosphorylation of desmin at four serine

residues within the non-helical head domain. J. Biol. Chem. 264:5674-5678.

Klymkowsky, M. W., R. H. Miller, and E. B. Lane. 1983. Morphology, behavior, and interaction of cultured epithelial cells after the antibody-induced disruption of keratin filament organization. J. Cell Biol. 96:494-509.

Klymkowsky, M. W., J. B. Bachant, and A. Domingo. 1989. Functions of intermediate filaments. Cell Motil. Cytoskeleton 14:309-331.

Lazarides, E., and B. D. Hubbard. 1976. Immunological characterization of the subunit of the 100 Å filaments from muscle cells. Proc. Natl. Acad. Sci. U.S.A. 73:4344-4348.

Lazarides, E. 1980. Intermediate filaments as mechanical integrators of cellular space. Nature 283:249-256

Lazarides, E. 1982. Intermediate filaments: A chemically heterogeneous, developmentally regulated class of proteins. Ann. Rev. Biochem. 51:219-250.

Lazarides, E., B. L. Granger, D. L. Gard, C. M. O'Connor, J. Breckler, M. Price, and S. I. Danto. 1982. Desmin- and vimentin-containing filaments and their role in the assembly of the Z disk in muscle. Cold Spring Harb. Symp. Quant. Biol. 46:351-378.

Lefebvre, S., and W. E. Mushynski. 1987. Calcium binding to untreated and dephosphorylated porcine neurofilaments. Biochem. Biophys. Res. Commun. 145:1006-1011.

Lefebvre, S., and W. E. Mushynski. 1988. Characterization of the cation-binding properties of porcine neurofilaments. Biochemistry. 27:8503-8508.

Lehman, W., A. Sheldon, and W. Madonia. 1987. Diversity in smooth muscle thin filament composition. Biochim. Biophys. Acta. 914:35-39.

Lehman, W., R. Craig, J. Lui, and C. Moody. 1989. Caldesmon and the structure of smooth muscle thin filaments: Immunolocalization of caldesmon on thin filaments. J. Muscle Res. Cell. Motil. 10:101-112.

Leonard, D. G. B., J. D. Gorham, P. Cole, L. A. Green, and E. B. Ziff. 1988. A nerve growth factor-regulated messenger RNA encodes a new intermediate filament protein. J. Cell Biol. 106:181-193.

Liem, R. K. H., and S. B. Hutchison. 1982. Purification of individual components of the neurofilament triplet: Filament assembly from the 70,000-dalton subunit. Biochemistry 21:3221-3226.

Malecki, M., and J. V. Small. 1987. Immunocytochemistry of contractile and cytoskeletal proteins in smooth muscle: Lowicryl, LR White and polyvinylalcohol compared. Protoplasma 139:100-169.

Malencik, D. A., J. Ausio, C. E. Byles, B. Modrell, and S. R. Anderson. 1989. Turkey gizzard caldesmon: Molecular weight determination and calmodulin binding studies. Biochemistry 28:8227-8233.

McKeon, F. D., M. W. Kirschner, and D. Caput. 1986. Homologies in both primary and secondary structure between nuclear envelope and intermediate filament proteins. Nature 319:463-468.

Metuzals, J., and W. E. Mushynski. 1974. Electron microscope and experimental investigations of the neurofilamentous network in Dieters' neurons: Relationship with the cell surface and nuclear pores. J. Cell Biol. 61:701-722.

Milam, L., and H. P. Erickson. 1982. Visualization of a 21-nm axial periodicity in shadowed keratin filaments and neurofilaments. J. Cell Biol. 94:592-596.

Moody, C., W. Lehman, and R. Craig. 1990. Caldesmon and the structure of smooth muscle thin filaments: Electron microscopy of isolated thin filaments. J. Muscle Res. Cell Motil. 11:176-185.

Nelson, W. T., and P. Traub. 1982. Effect of the ionic environment on the incorporation of the intermediate-sized filament protein vimentin into residual cell structures upon treatment of Ehrlich ascites tumour cells with triton X-100. J. Cell Sci. 53:77-95.

Newport, J. W., and D. J. Forbes. 1987. The nucleus: Structure, function and dynamics. Ann. Rev. Biochem. 56:535-565.

Osborn, M., W. Franke, and K. Weber. 1980. Direct demonstration of the presence of two immunologically distinct intermediate-sized filament systems in the same cell by double immunofluorescence microscopy: Vimentin and cytokeratin in cultured epithelial cells. Exp. Cell Res. 125:37-46.

Osborn, M., N. Geisler, G. Shaw, G. Sharp, and K. Weber. 1982. Intermediate filaments. Cold Spring Harb. Symp. Quant. Biol. 46:413-429.

Osborn, M., and K. Weber. 1982. Intermediate filaments: Cell type-specific markers in differentiation and pathology. Cell 31:303-306.

O'Shea, J. M., R. M. Robson, T. W. Huiatt, M. K. Hartzer, and M. H. Stromer. 1979. Purified desmin from adult mammalian skeletal muscle: A peptide mapping comparison with desmins from adult mammalian and avian smooth muscle. Biochem. Biophys. Res. Commun. 89:972-980.

O'Shea, J. M., R. M. Robson, M. K. Hartzer, T. W. Huiatt, W. E. Rathbun, and M. H. Stromer. 1981. Purification of desmin from adult mammalian skeletal muscle. Biochem. J. 195:345-356.

Pang, Y.-Y. S., R. M. Robson, M. K. Hartzer, and M. H. Stromer. 1983. Subunit structure of the desmin and vimentin protofilament units. J. Cell Biol. 97:226a. (Abstract)

Parry, D. A. D., and R. D. B. Fraser. 1985. Intermediate filament structure: 1. Analysis of IF protein sequence data. Int. J. Biol. Macromol. 7:203-213.

Parry, D. A. D., A. C. Steven, and P. M. Steinert. 1985. The coiled-coil molecules of intermediate filaments consist of two parallel chains in exact axial register. Biochem. Biophys. Res. Commun. 127:1012-1018.

Parry, D. A. D., J. F. Conway, and P. M. Steinert. 1986. Structural studies on lamin: Similarities and differences between lamin and intermediate filament proteins. Biochem. J. 238:305-308.

Parry, D. A. D., J. F. Conway, A. E. Goldman, R. D. Goldman, and P. M. Steinert. 1987. Nuclear lamin proteins: Common structures for paracrystalline, filamentous and lattice forms. Intl. J. Biol. Macromol. 9:137-145.

Parry, D. A. D. 1990. Primary and secondary structure of IF protein chains and models of molecular aggregation. Pages 175-204 in R. D. Goldman, and P. M. Steinert, eds. Cellular and molecular biology of intermediate filaments. Plenum Publishing Corp., New York, NY.

Parysek, L. M., and R. D. Goldman. 1988. Distribution of a novel 57kDa intermediate filament (IF) protein in the nervous system. J. Neurosci. 8:555-563.

Quinlan, R. A., J. A. Cohlberg, D. L. Schiller, M. Hatzfeld, and W. W. Franke. 1984. Heterotypic tetramer (A_2D_2) complexes of non-epidermal keratins isolated from cytoskeletons of rat hepatocytes and hepatoma cells. J. Mol. Biol. 178:365-388.

Quinlan, R. A., D. L. Schiller, M. Hatzfeld, T. Achtstatter, R. Moll, J. L. Jorcano, T. M. Magin, and W. W. Franke. 1985. Patterns of expression and organization of cytokeratin intermediate filaments. Ann. N. Y. Acad. Sci. 455:282-306.

Quinlan, R. A., M. Hatzfeld, W. W. Franke, A. Lustig, T. Schulthess, and J. Engel. 1986. Characterization of dimer subunits of intermediate filament proteins. J. Mol. Biol. 192:337-349.

Renner, W., W. W. Franke, and E. Schmid. 1981. Reconstitution of intermediate-sized filaments from denatured monomeric vimentin. J. Mol. Biol. 149:285-306.

Robson, R. M. 1989. Intermediate filaments. Curr. Opinion Cell Biology 1:36-43.

Sauk, J. J., M. Krumweide, D. Cocking-Johnson, and J. G. White. 1984. Reconstitution of cytokeratin filaments in vitro: Further evidence for the role of nonhelical peptides in filament assembly. J. Cell Biol. 99:1590-1597.

Schollmeyer, J. E., L. T. Furcht, D. E. Goll, R. M. Robson, and M. H. Stromer. 1976. Localization of contractile proteins in smooth muscle cells and in normal and transformed fibroblasts. Pages 361-388 in R. Goldman, T. Pollard, and J. Rosenbaum, eds. Cell motility. Book A. Cold Spring Harbor Laboratory, New York, NY.

Shoenberg, C. F., and D. M. Needham. 1976. A study of the mechanism of contraction in vertebrate smooth muscle. Biol. Rev. 51:53-104.

Skerrow, D., A. G. Matoltsy, and M. N. Matoltsy. 1973. Isolation and characterization of helical regions of epidermal prekeratin. J. Biol. Chem. 248:4820-4826.

Small, J. V., and J. M. Squire. 1972. Structural basis of contraction in vertebrate smooth muscle. J. Mol. Biol. 67:117-149.

Small, J. V. 1977. Studies on isolated smooth muscle cells: The contractile apparatus. J. Cell Sci. 24:327-349.

Small, J., and A. Sobieszek. 1977. Studies on the function and composition of the 10-nm (100-Å) filaments of vertebrate smooth muscle. J. Cell Sci. 23:243-268.

Small, J. V., and J. E. Celis. 1978. Direct visualization of the 10-nm (100-Å) -filament network in whole and enucleated cultured cells. J. Cell Sci. 31:393-409.

Small, J., and A. Sobieszek. 1980. The contractile apparatus of smooth muscle. Int. Rev. Cytol. 64:241-306.

Small, J., and A. Sobieszek. 1983. Contractile and structural proteins of smooth muscle. Pages 86-140 in N. L. Stephens, ed. Biochemistry of smooth muscle. Vol. 1. CRC Press, Inc., Boca Raton, FL.

Small, J. V., D. O. Fürst, and J. De Mey. 1986. Localization of filamin in smooth muscle. J. Cell Biol. 102:210-220.

Smith, C. W. J., and S. B. Marston. 1985. Disassembly and reconstitution of the Ca^{2+}-sensitive thin filaments of vascular smooth muscle. FEBS Letters 184:115-119.

Somlyo, A. P., C. F. Devine, A. V. Somlyo, and S. R. North. 1971. Sarcoplasmic reticulum and the temperature-dependent contraction of smooth muscle in calcium-free solutions. J. Cell Biol. 51:722-741.

Somlyo, A. P., A. V. Somlyo, H. Shuman, B. F. Sloane, and A. Scarpa. 1978. Electron probe analysis of calcium compartments in cryosections of smooth and striated muscles. Ann. N. Y. Acad. Sci. 307:523-544.

Somlyo, A. P., A. V. Somlyo, H. Shuman, and M. Endo. 1982. Calcium and monovalent ions in smooth muscle. Fed. Proc. 41:2883-2894.

Somlyo, A. V., P. Vinall, and A. P. Somlyo. 1969. Excitation-contraction coupling and electrical events in two types of vascular smooth muscle. Microvasc. Res. 1:354-373.

Somlyo, A. V. 1979. Bridging structures spanning the junctional gap at the triad of skeletal muscle. J. Cell Biol. 80:743-750.

Somlyo, A. V., M. Bond, P. F. Berner, F. T. Ashton, H. Holtzer, A. P. Somlyo, and T. M. Butler. 1984. The contractile apparatus of smooth muscle: An update. Pages 1-20 in N. L. Stephens, ed. Smooth muscle contraction. Marcel Dekker Inc., New York, NY.

Somlyo, A. V., and C. Franzini-Armstrong. 1985. New views of smooth muscle structure using freezing, deep-etching and rotary shadowing. Experientia 41:841-856.

Steinert, P. M. 1978. Structure of the three-chain unit of the bovine epidermal keratin filament. J. Mol. Biol. 123:49-70.

Steinert, P. M., W. W. Idler, and R. D. Goldman. 1980. Intermediate filaments of baby hamster kidney (BHK-21) cells and bovine epidermal keratinocytes have similar ultrastructures and subunit domain structures. Proc. Natl. Acad. Sci. USA 77:4534-4538.

Steinert, P. M., W. W. Idler, F. Cabral, M. M. Gottesman, and R. D. Goldman. 1981. In vitro assembly of homopolymer and copolymer filaments from intermediate filament subunits of muscle and fibroblastic cells. Proc. Natl. Acad. Sci. USA 78:3692-3696.

Steinert, P. M., R. V. Zackroff, M. Aynardi-Whitman, and R. D. Goldman. 1982. Isolation and characterization of intermediate filaments. Methods Cell Biol. 24A:399-419.

Steinert, P. M., R. H. Rice, D. R. Roop, B. L. Trus, and A. C. Steven. 1983. Complete amino acid sequence of a mouse epidermal keratin subunit and implications for the structure of intermediate filaments. Nature 302:794-800.

Steinert, P. M., and D. A. D. Parry. 1985. Intermediate filaments: Conformity and diversity of expression and structure. Ann. Rev. Cell Biol. 1:41-65.

Steinert, P. M., and D. R. Roop. 1988. Molecular and cellular biology of intermediate filaments. Ann. Rev. Biochem. 57:593-625.

Steinert, P. M. 1990. The two-chain coiled-coil molecule of native epidermal keratin intermediate filaments is a Type I-Type II heteropolymer. J. Biol. Chem. 265:8766-8774.

Steven, A. C., J. S. Wall, J. T. Hainfeld, and P. M. Steinert. 1982. Structure of fibroblastic intermediate filaments: Analysis by scanning transmission electron microscopy. Proc. Natl. Acad. Sci. USA 79:3101-3105.

Steven, A. C., J. F. Hainfeld, B. L. Trus, J. S. Wall, and P. M. Steinert. 1983a. The distribution of mass in heteropolymer intermediate filaments assembled in vitro. J. Biol. Chem. 258:8323-8329.

Steven, A. C., J. F. Hainfeld, B. L. Trus, J. S. Wall, and P. M. Steinert. 1983b. Epidermal keratin filaments assembled in vitro have masses-per-unit-length that scale according to average subunit in

mass: Structural basis for homologous packing of subunits in intermediate filaments. J. Cell Biol. 97: 1939-1944.

Steven, A. C., B. L. Trus, J. F. Hainfeld, J. S. Wall, and P. M. Steinert. 1985. Conformity and diversity in the structures of intermediate filaments. Ann. N. Y. Acad. Sci. 455:377-380.

Stromer, M. H., T. W. Huiatt, F. L. Richardson, and R. M. Robson. 1981. Disassembly of synthetic 10-nm desmin filaments from smooth muscle into protofilaments. Eur. J. Cell Biol. 25:136-143.

Stromer, M. H., M. A. Ritter, Y.-Y. S. Pang, and R. M. Robson. 1987. Effect of cations and temperature on kinetics of desmin assembly. Biochem. J. 246:75-81.

Stromer, M. H., and M. Bendayan. 1988. Arrangement of desmin intermediate filaments in smooth muscle cells shown by high-resolution immunocytochemistry. Cell Motil. Cytoskeleton 11:117-125.

Stromer, M. H., and M. Bendayan. 1989. Desmin filaments are directly connected to mitochondrial and nuclear membranes. J. Cell Biol. 109:256a. (Abstract)

Stromer, M. H. 1990. Intermediate (10-nm) filaments in muscle. Pages 19-36 in R. D. Goldman, and P. M. Steinert, eds. Cellular and molecular biology of intermediate filaments. Plenum Publishing Corp., New York, NY.

Stromer, M. H., and M. Bendayan. 1990. Immunocytochemical identification of cytoskeletal linkages to smooth muscle cell nuclei and mitochondria. Cell Motil. Cytoskeleton 17:11-18.

Traub, P., and C. E. Vorgias. 1983. Involvement of the N-terminal polypeptide of vimentin in the formation of intermediate filaments. J Cell Sci. 63:43-67.

Traub, P., and C. E. Vorgias. 1984. Differential effect of arginine modification with 1,2-cyclohexanedione on the capacity of vimentin and desmin to assemble into intermediate filaments and to bind to nucleic acids. J Cell Sci. 65:1-20.

Traub, P. 1985. Intermediate Filaments. Springer-Verlag, New York, NY.

Trybus, K. M. 1989. Filamentous smooth muscle myosin is regulated by phosphorylation. J. Cell Biol. 109:2887-2894.

Tsukita, S., S. Tsukita, and H. Ishikawa. 1983. Association of actin and 10 nm filaments with the dense body in smooth muscle cells of the chicken gizzard. Cell Tissue Res. 229:233-242.

van den Heuvel, R. M. M., G. J. J. M. van Eys, F. C. S. Ramaekers, W. J. Quax, W. T. M. Vree Egberts, G. Schaart, H. T. M. Cuypers, and H. Bloemendal. 1987. Intermediate filament formation after transfection with modified hamster vimentin and desmin genes. J. Cell Sci. 88:475-482.

Volberg, T., H. Sabanay, and B. Geiger. 1986. Spatial and temporal relationships between vinculin and talin in the developing chicken gizzard smooth muscle. Differentiation 32:34-43.

Vorgias, C. E., and P. Traub. 1983. Isolation, purification and characterization of the intermediate filament protein desmin from porcine smooth muscle. Prep. Biochem. 13:227-243.

Weber, K., and N. Geisler. 1987. Biochemistry and molecular structure of intermediate filaments. Fortsch. Zool. 34:251-260.

Woods, E. F., and A. S. Inglis. 1984. Organization of the coiled-coils in the wool microfibril. Int. J. Biol. Macromol. 6:277-283.

Wootton, G. S., and P. A. Goodford. 1975. An association between mitochondria and vesicles in smooth muscle. Cell Tissue Res. 161:119-132.

Yang, Z. W., and J. A. Babitch. 1988. Factors modulating filament formation by bovine glial fibrillary acidic protein, the intermediate filament component of astroglial cells. Biochemistry 27:7038-7045.

Yang, Z. W., F. K. Chung, and J. A. Babitch. 1988. Characterization and location of divalent cation binding sites in bovine glial fibrillary acidic protein. Biochemistry 27:7045-7050.

ACKNOWLEDGEMENTS

I would like to express my sincere appreciation to my major professor, Dr. Marvin Stromer, for his encouragement, advice and understanding during the course of this investigation and the preparation of this dissertation. I know very clearly that Dr. Stromer is behind me all the time whenever or wherever I have problems. "Thanks" are not enough to express my appreciation for him.

I would also like to thank the members of my committee, Dr. Richard Robson, Dr. Ted Huiatt, Dr. Harry Horner and Dr. Homer Walker for their advice and suggestions while serving on my graduate committee. Special thanks to Dr. Robson for his assistance in solving the problems that I encountered either academically or personally during the course of my study.

I would also like to express my gratitude to Mary Sue Mayes, Mary Bremner, Kathy Schneider, Jo Philips, Janet Stephenson, Stephan Bilak, Jean Schmidt, and Kim Ho for their excellent technical assistance. Special thanks to Mary Sue for considerable moral support when I had difficulties in my research.

Most important, I would like to thank my wife, Lingo, and my son, Joseph, for their patience and understanding during my career as a graduate student.